U.S. Residential Decarbonization: Systems Thinking Insights Across Technological, Infrastructural, and Socio-Behavioral Levers

by

Shuhaib Nawawi

A dissertation submitted in partial fulfillment
of the requirements for the degree of
Doctor of Philosophy
(Environment and Sustainability)
in the University of Michigan
2026

Doctoral Committee:

Assistant Professor Parth Vaishnav, Chair
Associate Professor Michael Craig
Professor Carol Menassa
Professor Shelie Miller

Shuhaib Nawawi

shuhaib@umich.edu

ORCID iD: 0000-0002-9394-5104

© Shuhaib Nawawi 2026

Dedication

To those who seek clarity amid complexity
and pursue growth with humility.

Acknowledgements

There are many people without whom this dissertation would not have been possible. I would like to thank my committee chair, Parth Vaishnav, for encouraging deliberate, System-2–style thinking (in the sense of Kahneman's *Thinking, Fast and Slow*) and for pushing me to go deep in my analyses. He was also exceptionally generous with his time and guidance. From him, I learned to assess the premises of questions and arguments and to be cautious about what an analysis can and cannot claim. I also thank my committee members. Michael Craig provided fast, constructive feedback and modeled effective research communication; his three-minute thesis was instrumental in shaping my identity as a young researcher. Shelie Miller introduced me to systems thinking and, through a faculty search committee, taught me to evaluate candidates on their own merits rather than through comparison, a lesson that helped me better manage impostor syndrome and learn to stay in my own lane in academia. Carol Menassa generously lent her expertise in human–built environment interactions throughout this process.

The Ford School felt like my second home on campus, after SEAS. I thank Shobita Parthasarathy and Devin Judge-Lord for pushing me to question my worldview and rigorously engage with counterarguments. Throughout their courses, I was repeatedly reminded—most memorably by Shobita—that *"technical expertise does not equal social wisdom,"* a lesson that pushed me to look beyond models and simulations, engage with insights from the social sciences, and listen more carefully to the people affected by the policies we study. While the readings were demanding and often dense, they sharpened my reading comprehension and fundamentally shaped how I think about the ways scientists inform policy, and how policy, in turn, shapes scientific questions and research priorities. I thank Julie Berson Grand for giving me the opportunity to engage in advocacy efforts related to building code reform in Michigan, including traveling to Lansing to speak with legislators and staffers. I am especially grateful to Beth Chimera; through our meetings, I felt my critical thinking sharpen through the process of writing, learning to use writing not just as a means of communication, but as a tool for thinking.

I gratefully acknowledge financial support from the SEAS Fellowship, the Graham Sustainability Institute, and Rackham for supporting my time at the University of Michigan. I also thank Friends of IIASA, through the Wes and Ankie Foell Fund Grant, which made my participation in the Young Scientists Summer Program (YSSP) at IIASA in Austria possible, and the U-M Office of the Provost for supporting my participation as an observer at COP28 in the UAE. Finally, I am grateful to the SEAS community—including faculty, my PhD cohort, fellow students, and staff, especially Jennifer Taylor and Mark Romanowski—for creating a collegial environment and for making the administrative side of graduate school feel manageable.

I also thank the YSSP community for the rich intellectual exchange and for broadening my perspective on science beyond the U.S. context. I am especially thankful to my mentors at IIASA—Alessio, XiaoYang, and Bas—for seeing my potential and for their guidance.

I would like to thank my tennis family at the Chippewa Club, especially the pros and members of the club, for being a big part of my PhD journey. Whenever I was not working, I was usually on the courts, focusing on the ball. Tennis has been my outlet and my therapy—teaching me to stay present, accept missed shots (even top professionals miss them), and always have fun. I am especially grateful to Randy, my team captain, who consistently reminded me of the importance of respect and good sportsmanship, lessons that extended well beyond the court.

I thank my family, especially my parents, Rahana Ibrahim and Nawawi Ismail for their unwavering love and support. I left home at the age of twelve to attend boarding school, a decision that ultimately changed the trajectory of my life. Even when I did not fully understand it at the time, my parents knew exactly what they were doing, and I am deeply grateful for their trust, guidance, and for never missing me in their daily prayers.

Thank you to my main support system: Frank, for always reminding me not to put so much pressure on myself (as Billy Joel says, *"Slow down, you crazy child"*); Darin, for making me do fun things and for introducing me to the world of art and teaching me how to appreciate it; and Archie, the best canine companion one could ask for. Thank you also to Congyi Dai, for always having my back and for encouraging me to dream big and "manifest" those dreams. Finally, thank you to Ann Arbor for being home for much of my adult life since 2015.

Table of Contents

Dedication ii

Acknowledgements iii

List of Tables ix

List of Figures x

List of Appendices xii

Abstract xiii

Chapter 1 Introduction 1

1.1 Residential decarbonization as a systems problem 3

1.1.1 Interacting technical, human, infrastructural, and climatic systems 3

1.1.2 Multiple objectives across decision scales and stakeholders 4

1.1.3 The need for interdisciplinary perspectives 5

1.2 Why focus on the United States? 5

1.3 Overview of chapters 6

1.3.1 Chapter 2: Household-Power Systems Trade-offs 8

1.3.2 Chapter 3: ASHP Frosting and Thermal Comfort 11

1.3.3 Chapter 4: Structural and Behavioral Sufficiency 14

Chapter 2 Cross-Sectoral Trade-offs in a Changing Climate: Surrogate Models to Balance Home Energy Bills, Occupant Comfort, and Power System Externalities 17

2.1 Introduction 17

2.2 Data and Methods 23

2.2.1 Reduced complexity building energy model 23

2.2.2 Generating EnergyPlus training data 23

2.2.3 Computing hourly heat gains and losses 23
2.2.4 Training RC-BEM with linear regression 24
2.2.5 Validating RC-BEM against EnergyPlus 24
2.2.6 Computing ASHP performance (COP) 25
2.2.7 Electricity demand for all-electric HVAC 25
2.2.8 Monetization approaches 26
2.2.9 Optimization model setup 27
2.2.10 Optimization scenarios 28
2.2.11 Estimating income from home attributes 29
2.2.12 Statistical analysis 29
2.3 Results 30
2.3.1 Maintaining indoor thermal comfort is more energy intensive in colder cities 30
2.3.2 Thermal comfort is more than three times as valuable as the cost of the energy used to provide it 32
2.3.3 Across home sizes, thermal comfort costs and cost disparities are lower for newer homes 34
2.3.4 No consistent correlation between household income and the marginal cost of thermal comfort 36
2.4 Discussion 38
2.5 Limitations of the study 39
Chapter 3 Anti-Frost Coatings Reduce Winter Emissions from Heat Pumps Without Compromising Comfort 41
3.1 Introduction 42
3.2 Data and Methods 44
3.2.1 Climate data and frosting conditions 45
3.2.2 Reduced-Complexity Building Energy Model 46
3.2.3 RC-BEM temporal downscaling 47

3.2.4 Heat pump performance model 47
3.2.5 Emissions computation 48
3.3 Results 49
3.3.1 Emissions across scenarios 49
3.3.2 Indoor temperature impacts 51
3.3.3 Timing of defrost-related cooling 53
3.3.4 Energy–comfort trade-offs 54
3.4 Discussion 56
Chapter 4 Beyond Efficiency: Sufficiency Unlocks Deep Decarbonization of U.S. Residential Sector 58
4.1 Introduction 59
4.2 Policy scenario framework 61
4.3 Data and Methods 63
4.3.1 Stock Turnover Model 63
4.3.2 Reduced-Complexity Building Energy Model 63
4.3.3 Proxies for Missing Efficiency Classes and Multi-family Homes 64
4.3.4 Model Integration & Validation 65
4.3.5 Final Energy Demand 65
4.3.6 Primary Energy Demand and Emissions 66
4.4 Results 67
4.4.1 Residential energy demand can be decoupled from floorspace growth 67
4.4.2 Structural sufficiency and efficiency reshape diurnal load profiles 69
4.4.3 Behavioral sufficiency yields substantial additional reductions in energy demand 71
4.4.4 Housing improvements narrow geographic variation in sufficient-comfort savings 73
4.4.5 Deep residential decarbonization hinges on housing and grid transformations 75
4.5 Discussion 77

4.6 Limitations of the study 78
Chapter 5 Synthesis and Outlook 79
5.1 Contributions of This Dissertation 80
5.2 What Simulation-Based Analysis Reveals and What It Does Not Capture 82
5.3 From Technical Feasibility to Real-World Implementation 84
5.4 Recommendations for Future Research 85
5.5 Outlook for U.S. Residential Decarbonization 87
Appendices 88
Bibliography 117

List of Tables

Table 1.1: Scale and methods of analysis used in each chapter.....7

Table 2.1: Comparison of building energy modeling paradigms. 20

Table 2.2: Monetization methods used in mixed-integer linear programming.....21

Table A.1: Relevant publications on residential HVAC electrification in the U.S. 88

Table A.2: Relevant publications on surrogate building energy models. 89

Table A.3: Performance of RC-BEM for 54 U.S. cities.....90

Table A.4: Residential electricity rates and thermal discomfort slopes. 91

Table A.5: T0 optimization results for 54 U.S. cities. 92

Table A.6: T3.5 optimization results for 54 U.S. cities.....93

Table A.7: 1x optimization results for 54 U.S. cities. 94

Table A.8: 3x optimization results for 54 U.S. cities.....95

Table B.1: Distribution of baseline heating setpoint temperatures (°F).....103

Table C.1: Comparison of key literatures focusing on U.S. residential decarbonization. 106

Table C.2: Shares of rural residential building archetypes in 2020 by state. 107

Table C.3: Shares of suburban residential building archetypes in 2020 by state. 109

Table C.4: Shares of urban residential building archetypes in 2020 by state.....111

Table C.5: 2020 site end-use consumption [trillion BTU] in the U.S. 113

List of Figures

Figure 1.1: U.S. GHG emissions by electricity end-use sector in 2022. 1

Figure 1.2: U.S. direct and indirect GHG emissions from buildings in 1990-2022. 2

Figure 1.3: Interacting levers of building decarbonization. 3

Figure 1.4: Climate diversity of contiguous U.S. 6

Figure 1.5: Graphical abstract of Chapter 2. 8

Figure 1.6: Graphical abstract of Chapter 3. 11

Figure 1.7: Graphical abstract of Chapter 4 14

Figure 2.1: Overview of modeling framework. 22

Figure 2.2: Annual cost-comfort trade-offs. 31

Figure 2.3: Internal temperature extremes. 33

Figure 2.4: Energy costs to improve thermal comfort. 35

Figure 2.5: Income-based disparities in thermal comfort improvement costs. 37

Figure 3.1: Conceptual framework and defrost-management scenarios. 45

Figure 3.2: Median winter emissions across scenarios. 50

Figure 3.3: Indoor temperature impacts of 'No aux heat' and 'No aux heat + 2°C'. 52

Figure 3.4: Diurnal distribution of frost-prone outdoor conditions. 54

Figure 3.5: Winter comfort–energy tradeoffs across ten U.S. cities. 55

Figure 4.1: Scenario framework for the U.S. residential sector. 61

Figure 4.2: U.S. residential floorspace and final energy across housing stock pathways. 68

Figure 4.3: Hourly energy load by Census region for the first three days of January and July. ..70

Figure 4.4: Impact of thermostat setpoints on U.S. residential final energy demand. 72

Figure 4.5: State-level final energy savings from Baseline to Sufficient Comfort in 2050. 74

Figure 4.6: National primary energy demand and emissions 76

Figure 5.1: Integrative framework of dissertation contributions 79

Figure 5.3: Heating setpoint distributions by thermostat management strategy (Claire et al.). ...83

Figure 5.4: Cooling setpoint distributions by thermostat management strategy (Claire et al.). ...83

Figure A.1: Customized thermostat setback on EnergyPlus. 96

Figure A.2: RC-BEM validation against EnergyPlus Simulations. 97

Figure A.3: Comparison of ordinary least squares (OLS) and penalized regressions. 98

Figure A.4: Heating discomfort costs across six representative cities. 99

Figure A.5: Cooling discomfort cost across six representative cities. 100

Figure A.6: Temperature-dependent ASHP coefficient of performance (COP). 101

Figure A.7: Annual cost trade-offs under historical, RCP4.5, and RCP8.5. 102

Figure B.1: City selection based on frosting severity. 104

Figure B.2: Example of internal temperature drop after 15 minutes of defrosting. 105

Figure C.1: National population trajectory under SSP2. 114

Figure C.2: State-level population trajectories under SSP2. 115

Figure C.3: Sensitivity of national final residential energy demand to climate pathways.....116

List of Appendices

Appendix A: Supplementary Information for Chapter 2 88

Appendix B: Supplementary Information for Chapter 3 103

Appendix C: Supplementary Information for Chapter 4 106

Abstract

The U.S. residential sector emits roughly 974 million metric tons of CO_2-equivalent annually, accounting for 15% of national greenhouse gas emissions. Decarbonizing this sector is not merely a technological challenge; it requires addressing dynamic interactions among **building technologies, infrastructure, household behavior, and a changing climate**. Beyond mitigation, homes are central to climate adaptation, shaping indoor thermal safety under increasingly frequent and severe climate extremes. This dissertation develops and applies multi-scale quantitative systems modeling to U.S. residential decarbonization, spanning air source heat pump performance (ASHP), building-level thermal response, and housing stock evolution, as well as the mutual interactions between all three factors.

Challenging the conventional building energy modeling strategy, which treats indoor temperature setpoints as inviolate, the first study **develops a weather-responsive surrogate modeling framework that treats indoor temperature as a decision variable and monetizes thermal comfort**, enabling its integration into large-scale optimization of household and power system costs. Applied to 17,000 statistically representative single-family homes across 54 U.S. cities, the analysis shows that household objectives (cost, comfort) dominate system-level trade-offs, accounting for 54–98% of total system costs. Power systems cost tradeoffs (i.e., peak demand vs externalities) play a smaller role. Climate and building vintage strongly shape the marginal cost of comfort improvements: the cost per degree-hour of additional comfort is 2–4 times higher in cold climates than in warm climates. Newer homes require roughly 50% less energy per unit floor area per degree of increased comfort than pre-1950 homes, an efficiency advantage partially offset by growth in house size over time.

The second study **examines the challenge of operating ASHPs in cold climates, where frost accumulation on the outdoor heat exchanger degrades heating performance and triggers periodic defrost cycles to melt accumulated ice**. During these defrost cycles, ASHPs typically activate auxiliary resistance heating to maintain indoor temperature—a practice that is

energy- and emissions-intensive. Eliminating resistance backup reduces winter emissions substantially but causes indoor temperature drops of 1–5 °C during defrost periods, revealing a comfort–emissions trade-off. To resolve this trade-off, the study evaluates a novel zwitterionic anti-frost coating modeled as eliminating the need for defrost, thereby avoiding resistance heating and reducing emissions by approximately 40% while maintaining preferred indoor temperatures. These findings quantify how materials innovation can translate into system-level emissions reductions without compromising thermal comfort in cold climates.

Extending the analysis to the U.S. housing stock, the third study integrates a dynamic stock turnover model with the previously developed hourly, climate-responsive building energy model to **examine how structural sufficiency (i.e., moderating dwelling size and shifting toward multi-family housing) and behavioral sufficiency (i.e., adopting health-informed thermostat setpoints) reshape residential energy demand over time**. Under business-as-usual housing trends, final residential energy demand increases by 11% between 2020 and 2050. Structural sufficiency reduces mid-century demand by 31%. When combined with efficiency improvements, total final energy demand declines by up to 45%. Adopting behavioral sufficiency yields additional reductions of 31–33% relative to current comfort practices.

Collectively, these studies demonstrate that deep residential decarbonization depends not only on cleaner technologies, including materials-scale innovations and high-efficiency cold climate ASHPs, but also on transforming how homes are built, operated, and experienced. Integrating behavioral, technological, and structural levers within multi-scale quantitative models is essential for designing resilient and equitable pathways under a changing climate. This dissertation develops and demonstrates tools to allow for a more human-centered and demand-focused approach to U.S. residential energy transition.

Chapter 1 Introduction

In the United States (U.S.), residential and commercial buildings accounted for approximately 31% of total greenhouse gas (GHG) emissions in 2022, based on electricity end-use sector accounting (Figure 1.1).[1,2] Total U.S. GHG emissions that year were approximately 6.34 $GtCO_2$-eq (gigatonnes of carbon dioxide equivalent), corresponding to roughly 2.0 $GtCO_2$-eq attributable to the buildings sector.[1] These emissions arise from two main sources—direct on-site fossil fuel combustion and indirect emissions from electricity generation—which have followed markedly different historical trajectories.

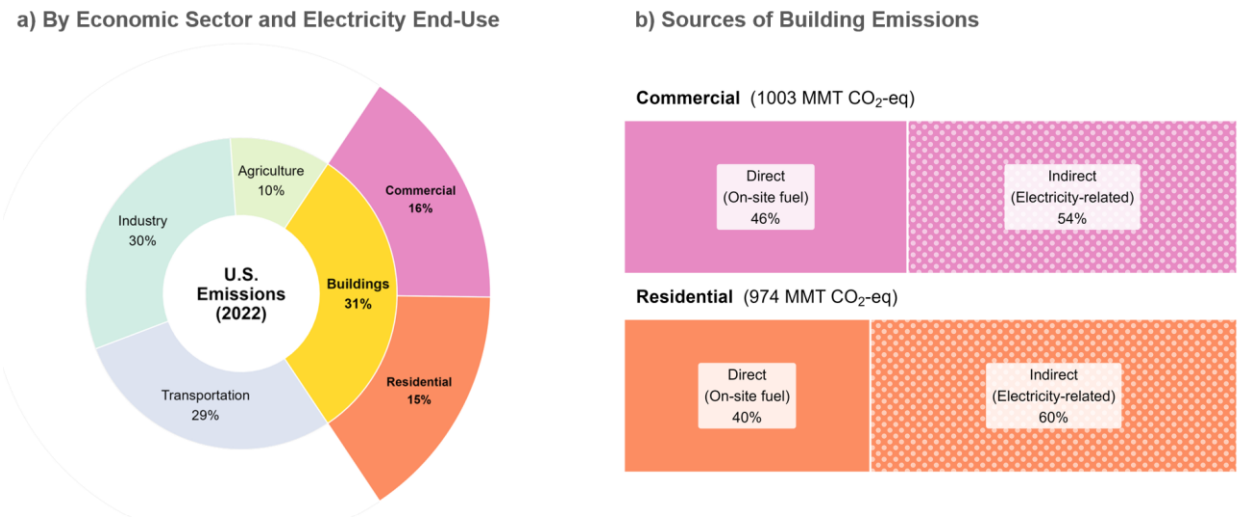


Figure 1.1: U.S. GHG emissions by electricity end-use sector in 2022.

Historically, GHG emissions from the U.S. buildings sector have been shaped primarily by the carbon intensity of the electricity system. This relationship is evident in emissions trends: electricity-related emissions peaked around 2007 and then declined with coal retirements and lower-carbon generation, while direct fossil fuel use in buildings remained relatively stable (Figure 1.2).[1,3] Accordingly, electricity decarbonization alone is insufficient to achieve deep decarbonization of the buildings sector.

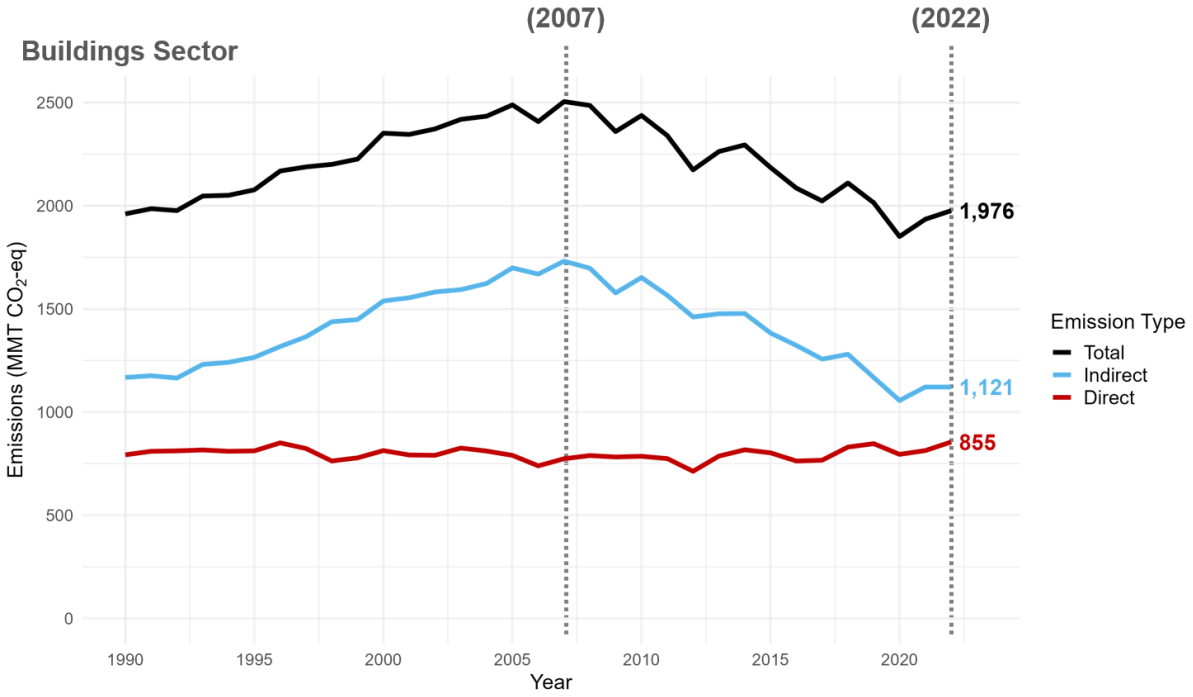


Figure 1.2: U.S. direct and indirect GHG emissions from buildings in 1990-2022.

Within the buildings sector, residential buildings are critical for determining how households are exposed to ambient conditions, because they provide energy services that sustain daily life. In an average U.S. household, roughly 60% of site energy use is devoted to thermal services, including space heating, cooling, and water heating, which are highly sensitive to outdoor temperature.[4,5] As heat waves and cold spells intensify[6], peak heating and cooling demands during extreme events increase, households that cannot maintain safe indoor temperatures because of building performance limits, energy system constraints, or affordability face heightened health and safety risks.

Recent assessments by the Intergovernmental Panel on Climate Change (IPCC) indicate that global mean temperatures are on track to reach or temporarily exceed the 1.5 °C threshold articulated in the Paris Agreement by around 2030, absent rapid and sustained emissions reductions.[7–10] Under this tightening climate constraint, the IPCC emphasizes the need for simultaneous, near-term mitigation and adaptation to address climate risks that are already unavoidable.[11] This convergence heightens the urgency of strategies that jointly reduce emissions and maintain safe indoor conditions in a changing climate.

1.1 Residential decarbonization as a systems problem

1.1.1 Interacting technical, human, infrastructural, and climatic systems

Residential decarbonization is a systems problem in which outcomes—such as energy demand, thermal comfort, costs, and emissions—emerge from the interactions among building technologies, energy infrastructure, household behaviors, and climatic conditions.[12] Changes in any part of this system can propagate across others, altering trade-offs among these outcomes.

Within this system, residential buildings mediate the relationship between outdoor climate and indoor conditions through socio-behavioral (e.g., thermostat settings, occupancy schedules), technological (e.g., gas furnaces, ASHPs), and infrastructural (e.g., insulation, infiltration, thermal mass) elements, as illustrated in Figure 1.3. Working together, these components determine how effectively homes protect occupants from thermal stress and environmental hazards, especially during climate extremes.

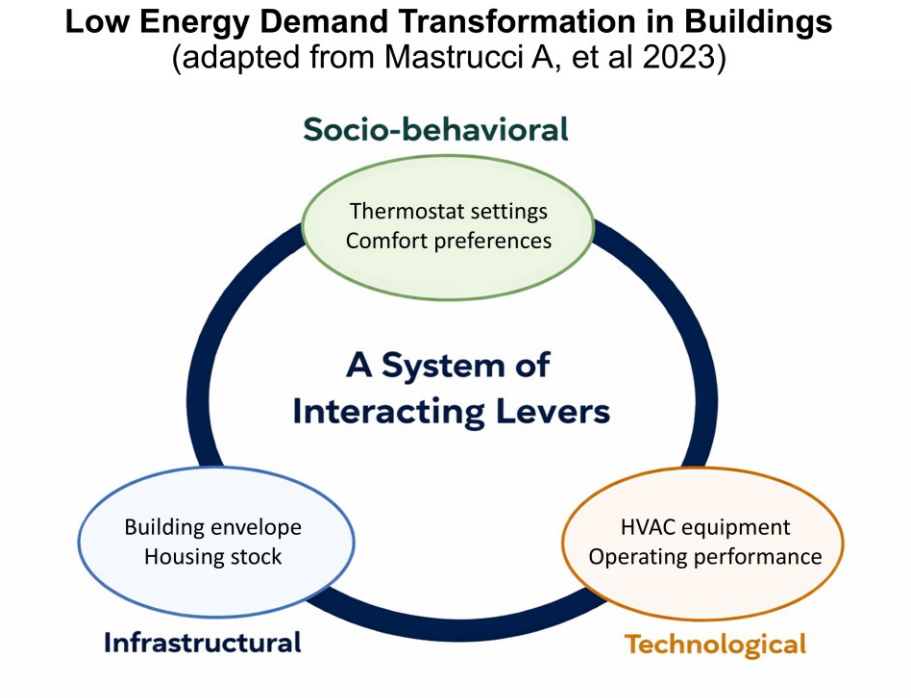


Figure 1.3: Interacting levers of building decarbonization.

This dissertation adopts a systems-oriented approach to evaluate residential decarbonization strategies that account for technical performance, household behavior, infrastructural, and climatic conditions. While the analysis is primarily quantitative and modeling-based, insights from social science and policy research help inform key assumptions, better capture household decision-making, and address distributional implications relevant to residential decarbonization.

1.1.2 Multiple objectives across decision scales and stakeholders

Residential decarbonization involves multiple stakeholders with distinct objectives and uneven decision-making power.[13,14] Households prioritize affordability, thermal comfort, and control over indoor conditions, while utilities focus on grid reliability, peak demand management, and system costs.[15–17] Policymakers and regulators pursue societal goals such as emissions reduction, public health, and equity through instruments like building codes and financial incentives.[18,19] Because these objectives are not always aligned, actions to advance one goal or stakeholder interest can be detrimental to others.

Decision-making authority is uneven: homeowners typically control long-term investments such as equipment replacement and building retrofits, while renters often have little influence despite facing energy and comfort consequences.[20,21] This split incentive limits the effectiveness of many decarbonization strategies.[20] Even among homeowners, disparities in financial resources and information further differentiate who can participate and benefit from decarbonization.[21–23]

Residential energy and planning decisions occur over multiple time horizons, with consequences that can persist for decades. Short-term actions, such as adjusting thermostat settings or responding to price signals, influence daily energy use and comfort. Medium-term investments, including heating system replacements and building upgrades, establish operating costs and emissions for years.[24] Long-term planning and policy decisions, including building energy codes and housing development patterns, shape building forms and aggregate energy demand over decades.[25] Together, these decisions can create structural lock-ins[26] that constrain future decarbonization pathways, particularly given biophysical feedbacks between urban climate and building energy demand that complicate long-term planning.[27]

1.1.3 The need for interdisciplinary perspectives

Residential decarbonization involves multiple interacting systems—technological, economic, policy, and social. Disciplinary approaches, although valuable, have limitations: engineering analysis often overlooks household agency and lived experience, while economic and policy models can miss technical detail and climate responsiveness. Social science brings essential understanding of behavior and equity, yet is rarely included in modeling framework.

Some may argue that specialized models are sufficient or that interdisciplinary approaches are too complex. However, research shows these methods often overlook key interactions and equity gaps, such as financial barriers and split incentives. Integrated frameworks that combine engineering, behavioral, and policy perspectives are needed to develop robust and equitable residential decarbonization strategies.

1.2 Why focus on the United States?

As the world's second-largest emitter and one of the countries with the highest cumulative CO_2 emissions, the U.S. accounts for about 13% of current annual global fossil emissions, making it central to international decarbonization efforts.[28] Its wide variation in climate (see Figure 1.4)[29], building characteristics[30], and electricity generation mix[31] leads to substantial regional differences in technology adoption, energy demand, and emissions outcomes. Amid this heterogeneity, recent decades have seen heat waves in large U.S. cities become more frequent, intense, and longer-lasting, with the average city experiencing 0.6 additional events per decade—thereby increasing public health risks and underscoring the urgency of residential decarbonization.[32] This complexity calls for deep, nuanced analysis to inform effective decarbonization strategies and policy decisions.

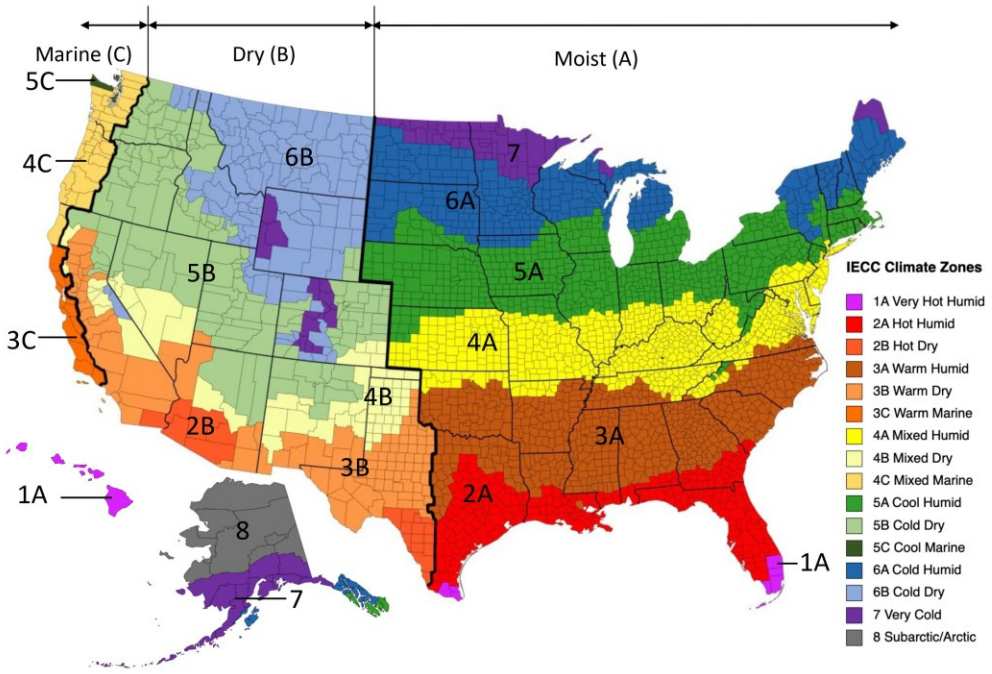


Figure 1.4: Climate diversity of contiguous U.S.

At the same time, socioeconomic diversity and concerns of distributive justice further complicate the residential energy landscape. Variations in income, housing quality, and tenure status influence household vulnerability and access to upgrades, with renters and low-income households often facing higher energy costs and limited control.[33–35] Without intentional focus on these factors, decarbonization policies can reinforce or even widen existing disparities—raising questions of fairness and equity in how benefits and burdens are distributed across the population. Thus, as permitted by available data and modeling capabilities, this dissertation considers how benefits and burdens are distributed across household groups.

1.3 Overview of chapters

Each chapter addresses a distinct but related aspect of U.S. residential decarbonization (Table 1.1). Across the dissertation, the analysis intentionally shifts in scale from detailed building simulations, to component-level heat pump performance, to long-term housing stock dynamics.

Table 1.1: Scale and methods of analysis used in each chapter.

Chapter	Scale of Analysis	Primary Methods
Ch. 2 Household-Power Systems Trade-offs	17,749 representative single-family homes in 54 U.S. cities	Surrogate-based building energy modeling; thermal comfort monetization; emissions and peak demand analysis
Ch. 3 ASHP Frosting and Thermal Comfort	7,806 representative single-family homes in 25 cold-climate U.S. cities	Heat pump performance modeling under frost and defrost conditions; comfort–emissions trade-off analysis
Ch. 4 Structural and Behavioral Sufficiency	U.S. residential housing stock evolution (contiguous U.S.; single-family and multifamily)	Housing stock turnover modeling; comparative analysis of efficiency and sufficiency scenarios

These chapters are based on the following journal articles:

Chapter 2: Household-Power Systems Trade-offs

> Nawawi, S., Yi, M., Craig, M., Deetjen, T., & Vaishnav, P. (2025). Cross-sectoral trade-offs in a changing climate: Surrogate models to balance home energy bills, occupant comfort, and power system externalities. iScience, 28(6). https://doi.org/10.1016/j.isci.2025.112728

Chapter 3: ASHP Frosting and Thermal Comfort

> Nawawi, S., Tuteja, A., & Vaishnav, P., Anti-Frost Coatings Improve Thermal Comfort and Reduce Emissions in Cold-Climate Heat Pumps. *Submitted.*

Chapter 4: Structural and Behavioral Sufficiency

> Nawawi, S., Vaishnav, P., Zhong, X., & Mastrucci, A., Beyond efficiency: Sufficiency unlocks deep decarbonization of U.S. residential sector. *In preparation*

Additionally, the model developed in Chapter 2 has also been used for the following article:

> Ying, M., Nawawi, S., & Vaishnav, P. (2026). Efficient electrification in a warming climate could contribute to keeping energy burdens in check. Communications Sustainability, *Forthcoming*

1.3.1 Chapter 2: Household-Power Systems Trade-offs

Chapter 2 develops a multi-objective modeling framework to quantify trade-offs among household energy bills, indoor thermal comfort, and power system impacts in an increasingly electrified residential sector across diverse U.S. climates.

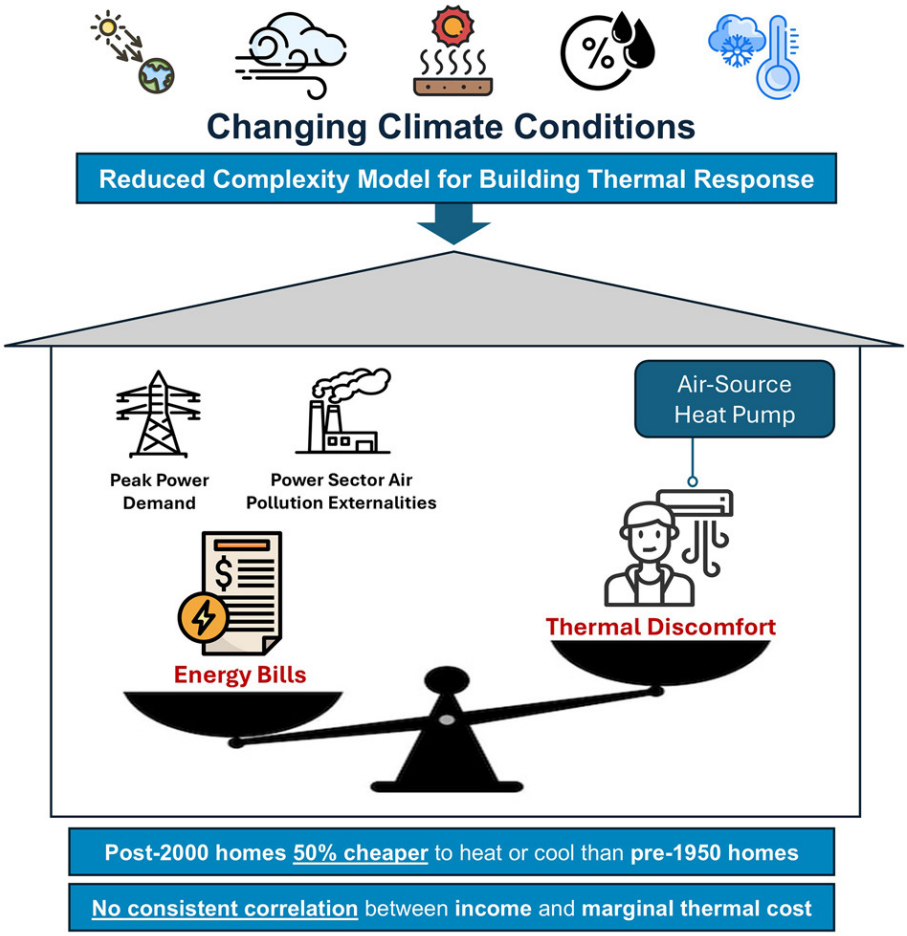


Figure 1.5: Graphical abstract of Chapter 2.

Background and Motivation

Trade-offs are inherent in both residential energy use and power system planning. Households balance energy costs and indoor thermal comfort, while system planners face competing objectives related to emissions reduction, peak demand management, and infrastructure investment. Electrification of residential space heating via air-source heat pumps (ASHPs) tightens the coupling between these domains by shifting heating demand onto the electricity

system, linking household comfort and energy costs more directly to power system conditions. Evaluating these coupled trade-offs requires modeling frameworks that jointly represent buildings and electricity systems, as single-sector approaches can miss critical interactions. However, fully integrated models are often computationally intensive, leading prior work to rely either on high-fidelity case studies with limited scope or on aggregated representations suitable for large-scale analysis. More often, the trade-off between comfort and the potential flexibility offered by electrified space heating demand is ignored. This trade-off constrains the ability of existing frameworks to systematically assess household–power system interactions across diverse climates, motivating the need for scalable approaches that retain essential physical and comfort dynamics.

Research Questions

1. *What are the tradeoffs between thermal comfort, energy cost, peak power, and power sector damages in fully electric residential heating systems under historical and future climates?*
2. *How do these trade-offs vary across climate regions, building vintages, and household income groups?*

Methods

Chapter 2 develops a surrogate building energy model that balances physical realism with computational tractability and embeds it within a framework capable of rapidly co-optimizing multiple objectives. The surrogate model is trained on customized physics-based simulations and applied to a large, statistically representative sample of single-family homes across 54 U.S. cities. Within the co-optimization framework, household energy bills, monetized thermal discomfort, peak electricity demand, and power-sector emissions are evaluated jointly under historical and future climate conditions. Monetizing thermal comfort enables explicit representation of household comfort–cost trade-offs within a linear optimization setting, while the lightweight surrogate structure allows rapid exploration of sensitivities across key assumptions, climates, and building characteristics.

Results

1. Thermal comfort costs dominate household–system trade-offs, especially in cold climates

Across 54 U.S. cities, household-level costs (energy bills plus monetized thermal discomfort) account for 54–98% of total system costs, depending on the comfort scenario, with the highest shares observed when thermal discomfort is explicitly valued. In cold cities such as Duluth and Detroit, maintaining indoor temperatures at fixed setpoints requires 2–4× higher annual heating costs than in warm cities like Orlando and Phoenix, reflecting lower heat pump efficiency, longer heating seasons, and higher electricity prices.

2. Households implicitly value thermal comfort at multiples of its energy cost.

Allowing unrestricted temperature deviation leads to indoor winter temperatures as low as −4 °C in Duluth and summer temperatures exceeding 40 °C in Phoenix, indicating intolerable conditions. Optimization results show that valuing discomfort at the direct energy cost (1x) produces intolerable indoor temperatures. Increasing the valuation to 3x moves temperatures closer to ASHRAE comfort bounds, but in many climates 3x yields only marginally acceptable conditions. This suggests that households implicitly value thermal comfort at multiples of its direct energy cost, potentially exceeding three times the cost of energy in extreme climates.

3. Newer homes require substantially lower costs to improve thermal comfort.

Controlling for home size, the marginal cost of improving thermal comfort in post-2000 homes is approximately 50% lower than in pre-1950 homes. In cold climates, median costs fall from $25–$39 per °C-month in older homes to $13–$19 per °C-month in newer homes, while cost disparities between large and small homes narrow substantially. These patterns are consistent across climate zones and align with the historical introduction of building energy codes.

4. We found no robust, systematic relationship between income and marginal comfort costs.

Across 212 combinations of city, season, home size, and income group, 157 show no statistically significant difference in the marginal cost of thermal comfort between income groups. While lower-income households face higher costs more frequently in raw comparisons, only 39 cases exhibit statistically significant regressive differences, indicating that building characteristics and climate dominate comfort costs more strongly than income alone.

1.3.2 Chapter 3: ASHP Frosting and Thermal Comfort

Chapter 3 quantifies how frost formation and defrost management in air-source heat pumps affect winter energy use, greenhouse gas emissions, and indoor thermal comfort in cold-climate U.S. cities.

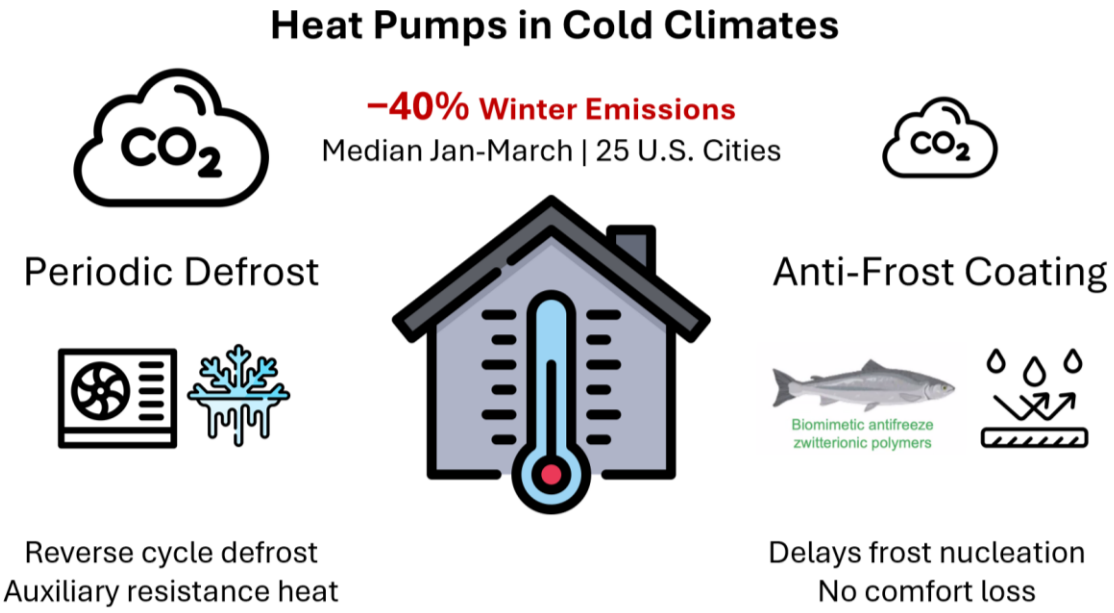


Figure 1.6: Graphical abstract of Chapter 3.

Background and Motivation

In cold and humid conditions, frost formation on air-source heat pump (ASHP) outdoor coils degrades performance and necessitates periodic defrost cycles. During defrost, heat is drawn from the indoor space, often requiring auxiliary electric resistance heating to maintain comfort. Prior laboratory and field studies have documented substantial efficiency losses from frosting and defrost operation, but these analyses are largely limited to component-level performance or short-term field demonstrations at individual sites. As a result, existing work provides limited insight into how defrost-related performance penalties translate into indoor temperature outcomes, winter electricity consumption, and emissions at scale across diverse housing stocks and climates. This gap is particularly important because auxiliary resistance heating—rather than the defrost cycle itself—can dominate winter electricity use and emissions in cold-climate ASHP

systems. A system-level framework that links climate conditions, building thermal response, and heat pump operation is therefore needed to evaluate the comfort–energy–emissions trade-offs associated with alternative defrost-management strategies.

Research Questions

1. *How do different defrost-management strategies affect winter electricity consumption, GHG emissions, and indoor thermal comfort in cold-climate ASHP-heated homes?*
2. *What is the potential system-level impact of frost-suppression strategies, such as anti-frost coatings, on winter emissions and thermal comfort?*

Methods

Chapter 3 builds on the reduced-complexity building energy model developed in Chapter 2 and extends it by explicitly resolving sub-hourly ASHP defrost dynamics. Approximately 7,900 representative single-family homes across 25 frost-prone U.S. cities are simulated using climate data, a surrogate building thermal model, and a 15-minute heat pump performance model calibrated to cold-climate ASHP manufacturer data. Four defrost-management scenarios are evaluated: (i) current practice with auxiliary electric resistance heating, (ii) defrost without auxiliary heating, (iii) defrost without auxiliary heating combined with a +2 °C thermostat setpoint increase, and (iv) idealized anti-frost coatings that suppress frost formation and eliminate defrost operation. Outcomes include indoor temperature deviations during defrost, winter electricity consumption, and consequential emissions computed using short-run marginal emission factors.

Results

1. *Auxiliary resistance heating dominates defrost-related emissions.*

Across the 25 cities, auxiliary resistance heating accounts for roughly one-quarter of winter electricity use in the baseline configuration and drives the majority of defrost-related emissions. Eliminating resistance backfill reduces median winter emissions by 35–46%, depending on the comfort strategy.

2. *Defrost without resistance heating substantially reduces emissions but introduces short-duration comfort losses.*

Removing auxiliary heating lowers median winter emissions by up to 63% in some cities but causes median indoor temperature drops of 1–3 °C during defrost, with first-percentile events reaching 4–5 °C below the setpoint in the coldest locations.

3. *Frost-suppression strategies offer an efficient comfort–energy trade-off.*

Anti-frost coatings reduce median winter emissions by approximately 40% relative to current practice while fully eliminating defrost-related thermal discomfort. Across cities, each 1 °C improvement in worst-case (P1) indoor temperature requires only ~0.5–4% additional winter energy, indicating that frost suppression is a highly energy-efficient pathway for restoring comfort without reliance on resistance heating.

1.3.3 Chapter 4: Structural and Behavioral Sufficiency

Chapter 4 evaluates how long-term changes in housing stock structure and household comfort practices shape U.S. residential energy demand, peak loads, and greenhouse gas emissions under climate change and alternative electricity-sector pathways.

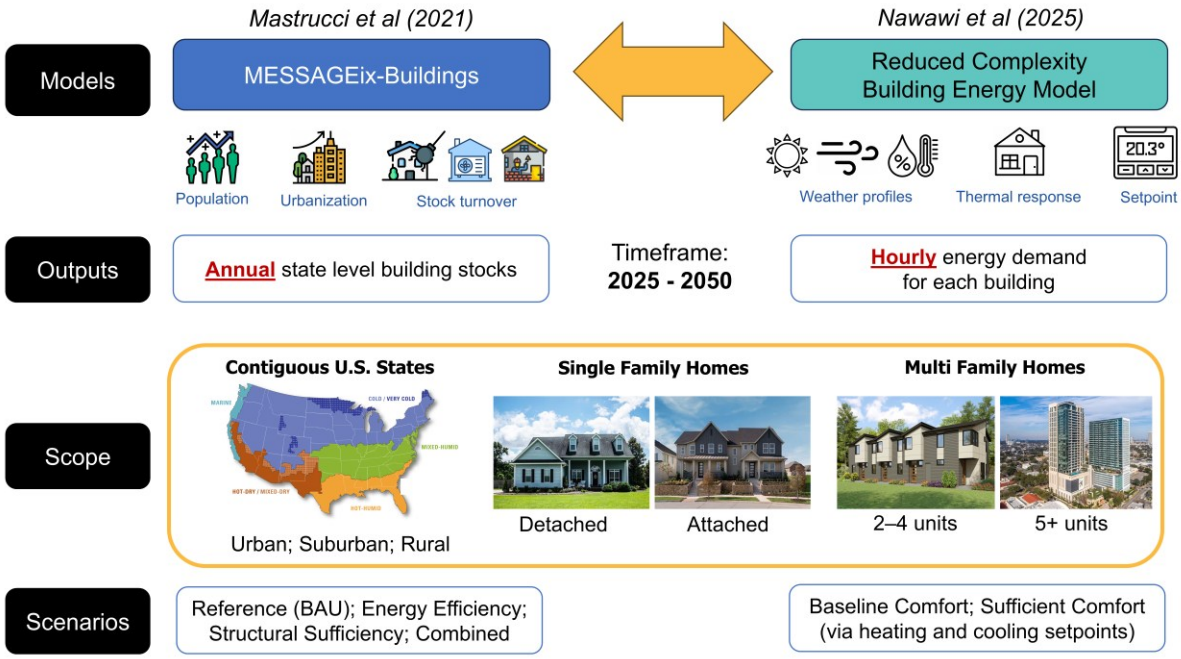


Figure 1.7: Graphical abstract of Chapter 4

Background and Motivation

U.S. residential decarbonization strategies have historically emphasized technological efficiency improvements and electrification, while largely treating energy demand as exogenous. This framing obscures two critical drivers of long-run outcomes: the structural evolution of the housing stock—what we build—and the behavioral practices through which energy services are used—how we live in and condition homes.

Structural factors such as floorspace per capita, housing type (single-family versus multi-family), renovation rates, and electrification create long-lived infrastructural lock-ins that shape energy demand for decades. At the same time, thermostat practices directly determine the level

of heating and cooling services delivered. Although "sufficiency" has been recognized in international climate assessments as a major demand-side mitigation lever, it remains inconsistently represented in U.S.-scale, policy-relevant modeling frameworks and is rarely examined jointly with housing stock evolution, climate change, and grid decarbonization.

Chapter 4 addresses this gap by integrating structural, technological, and behavioral levers within a unified modeling framework.

Research Questions

1. *How do energy efficiency, structural sufficiency (e.g., moderating floorspace growth and shifting toward multi-family housing), and behavioral sufficiency (health-informed thermostat setpoints) individually and jointly shape U.S. residential energy demand through 2050?*
2. *How do these demand-side pathways influence hourly load profiles, seasonal peaks, primary energy demand, and greenhouse gas emissions under alternative climate and electricity-sector decarbonization trajectories?*

Methods

Chapter 4 links a dynamic housing stock–turnover model (STURM within MESSAGEix-Buildings) with the climate-responsive reduced-complexity building energy model (RC-BEM) developed earlier in the dissertation. The stock model projects new construction, renovation, demolition, floorspace growth, and housing type shares at the state level from 2020 to 2050. RC-BEM simulates hourly heating and cooling demand for representative housing prototypes across 54 U.S. cities under historical and future climate trajectories (RCP4.5 and RCP8.5).

Scenarios distinguish between:

- Reference (business-as-usual floorspace growth and technology trends),
- Efficiency (accelerated renovation and electrification),
- Structural Sufficiency (stabilized per-capita floorspace, increased multi-family homes),
- Combined (efficiency + structural sufficiency),

Each housing pathway is evaluated under two thermostat regimes:

- Baseline Comfort (empirically observed setpoints),
- Sufficient Comfort (health-informed setpoints).

Final energy, primary energy, hourly loads, and national CO_2e emissions are computed under alternative electricity-sector decarbonization pathways.

Results

1. *Structural housing transformation decouples energy demand from floorspace growth.*

Under the Reference scenario, residential floorspace expands by 55% between 2020 and 2050, increasing final energy demand by 11%. Efficiency improvements alone reduce 2050 final demand by 18% relative to the Reference case. Structural sufficiency reduces demand by 31%, and when combined with efficiency lowers final energy demand by 45% by mid-century—exceeding the impact of efficiency alone.

2. *Structural sufficiency and efficiency substantially reduce winter peak loads.*

Hourly analysis reveals pronounced winter heating peaks exceeding 200 GW in cold-climate regions. The Combined scenario reduces peak winter loads by approximately 40% relative to the 2050 Reference case, while summer peak reductions are more modest (~25%). These seasonal asymmetries are not visible in annual energy metrics.

3. *Behavioral sufficiency delivers reductions comparable to structural change.*

Adopting health-informed thermostat setpoints reduces final residential energy demand by 31–33% relative to Baseline Comfort across housing pathways. The magnitude of these reductions is comparable to structural sufficiency alone, demonstrating that comfort practices materially shape national energy trajectories.

4. *Deep decarbonization hinges on housing transformation and grid decarbonization.*

Even under aggressive housing and comfort transformations, 2050 emissions outcomes remain sensitive to electricity-sector decarbonization pathways. Sufficiency and efficiency substantially lower demand and emissions, but do not eliminate dependence on grid transformation.

Chapter 2 Cross-Sectoral Trade-offs in a Changing Climate: Surrogate Models to Balance Home Energy Bills, Occupant Comfort, and Power System Externalities

Electrifying buildings using heat pumps may exacerbate the trade-offs between the sometimes-conflicting objectives of building occupants, power systems, and society. To navigate these, we develop a modeling framework that rapidly co-optimizes home energy bills, indoor temperatures, power system air pollution externalities, and peak demand costs. We demonstrate this framework for 17,000 representative single-family homes across 54 U.S. cities under historical and future climates, monetizing thermal discomfort using the travel cost method. Across climates, utility bills and thermal discomfort dominate trade-offs. Other factors play a smaller role. We show that, controlling for home size, the cost of improving thermal comfort is 50% lower in post-2000 homes than in pre-1950 homes. Of the 212 combinations of city, estimated income group pair, house size, and season analyzed, the lower-income household pays more for a marginal increase in thermal comfort in 137 cases, but this difference is significant only in 39 cases.

2.1 Introduction

Electrification is key to the energy transition and will significantly increase interactions among end-use sectors.[14] To effectively navigate this shift, decision-makers must model these increasingly interdependent systems within a unified framework to avoid overlooking crucial cross-sectoral trade-offs. However, such integrated frameworks are often computationally intensive, forcing analysts to either reduce modeling fidelity (i.e., the ability to represent real-world complexity) or limit the scope (e.g., geographical boundary) of their analyses.

For instance, the tools for energy model optimization and analysis (TEMOA) framework models cross-sectoral interactions at high temporal resolution by simulating a few representative days per season and extrapolating the findings to generate annual projections.[36] In another example, to robustly explore the effects of an uncertain and changing climate on power system

operation, Craig et al. focus on the power system in Texas; a nationwide analysis would have been computationally intractable.[37]

Modeling the building sector, which is responsible for 30% of global final energy use and 27% of total energy-related CO_2 emissions, represents a daunting challenge for multi-sectoral Modeling.[38] To inform decarbonization efforts, it is essential to model increased energy efficiency, adoption of low-carbon technologies, and shifts in occupant behavior.[11] Since space heating and cooling account for about 45% of a building's energy consumption in the U.S., targeting heating, ventilation, and air-conditioning (HVAC) systems is crucial for reducing emissions.[4]

Electrifying HVAC systems with air-source heat pumps (ASHPs) plays a critical role in many net-zero strategies.[11,39–44] However, in cold climates, the efficiency and capacity of ASHPs decrease, increasing peak demand on the power system.[15,17,45–49] To address this, utilities implement time-of-use (TOU) electricity rates to incentivize homeowners to shift electricity usage. Controlling a home's electricity use profile may lower stress on the electricity grid, reduce pollution, and lower bills by directing consumption to times when electricity is cleaner and demand is lower. However, such rate structures can disproportionately burden vulnerable populations, who may respond by curtailing their energy use, potentially exposing them to harmful indoor temperatures.[34,50]

These dynamics exacerbate the trade-offs low-income households face between utility bills and thermal comfort, particularly in extreme weather conditions (e.g., the ‘‘heat or eat’’ dilemma).[50] HVAC electrification may accentuate this trade-off further, as heat pumps raise energy burdens in cold climates relative to natural gas heating.[24] This creates even greater incentives for demand reduction during the coldest parts of winter, potentially leading to severe consequences for household comfort and health. As such, a modeling framework that adequately represents the trade-offs inherent in decarbonizing the building sector must account for the interactions between the building's physics, the electricity system, a changing and uncertain climate, and the temperatures experienced by occupants.

Building energy modeling (BEM) includes methods ranging from physics-based simulations to simplified gray-box models, as summarized in (Table 1). Physics-based models

like EnergyPlus offer high fidelity by explicitly incorporating detailed building characteristics and weather conditions to estimate the energy demands for maintaining set-point indoor temperatures. However, they have limited to no invertibility, which we define as the ability to predict how changing energy inputs affects indoor temperatures and thermal comfort. This limitation makes it hard to quantify the interacting effects of occupants balancing thermal comfort with reducing energy consumption on the one hand, and reducing peak electricity demand and air pollution from power production on the other.[16,51,52]

Another drawback of physics-based models is their high computational burden, making them impractical for large-scale or long-term analyses. To meaningfully predict the effects of an increasingly electrified residential sector on power system operation, models must run at high temporal resolutions ($\leq$ 1 h). Additionally, to represent large geographical regions, they need to model a large number of buildings across diverse climate zones. Finally, to capture the uncertain effects of climate change, they need to model an ensemble of potential future climates. Consequently, much of the analysis in this area relies on large simulations run on supercomputers by entities such as the National Renewable Energy Laboratory (NREL), whose ResStock database provides hourly energy end-use profiles for over 900,000 representative buildings across the U.S.[53,54]

Gray-box approaches, such as resistor-capacitor (RC) thermal network models and degree-day methods simplify physical relationships and offer computational efficiency. RC thermal network models employ an analogy with electric circuits, with resistances for heat transfer, capacitances for thermal storage, and buildings simplified into thermal masses. Although suitable for real-time applications like model predictive control, their simplicity limits accuracy for diverse building geometries and complex interactions. In contrast, the degree-day method estimates energy use by calculating the cumulative deviation from a baseline temperature. However, this approach often neglects weather variables beyond ambient temperature, such as humidity and wind speed, which significantly affect building energy demand, limiting their use in power system planning in a changing climate.

Table 2.1: Comparison of building energy modeling paradigms.

Modeling Paradigm	**Physics-based**	**Gray-box**		**Black-box**	**Behavioral Simulation**	**Hybrid**
Example	EnergyPlus	Resistor-Capacitor (RC)	Degree Days	Artificial Neural Network	Agent-Based	RC-BEM (This dissertation chapter)
Functional form	Non-linear ODEs	Non-linear ODEs	Linear	Non-linear	Non- linear	Linear
Temporal resolution	Hourly to subhourly	Daily to minutes	Monthly to daily	Flexible	Hourly	Hourly to subhourly
External validity	High	Low	Low	Depends	Low	Medium
Invertibility	Very difficult	Moderately difficult	Non-invertible	Very difficult	Non-invertible	Easy
Compute burden	Very high	Low	Low	High	High	Low
Weather data input	Multi variable	Primarily ambient T	Only ambient T	Depends	Depends	Multi variable
Main applications	Detailed building design; code compliance	Real-time control; large scale simulation	High-level energy estimations; Energy benchmarking	Energy demand prediction with low interpretability	Occupant behavior & interaction modeling	Large-scale simulations; impacts of flexible energy demand or weather on comfort

Our hybrid model, RC-BEM, integrates physics-based simulation outputs with gray-box statistical methods to overcome limitations of existing models. Its invertibility enables both energy and internal temperature prediction, supporting thermal comfort analyses. Its linear structure ensures scalability for large-scale simulations, capturing building heterogeneity and enabling optimization under changing climate conditions.

[a]External validity indicates a model's ability to account for changes in building characteristics (e.g., insulation, infiltration, size) and their impact on energy consumption.
[b]Invertibility indicates a model's ability to easily predict how changing energy inputs affect indoor temperatures and thermal comfort, and vice versa.

Advanced modeling approaches, such as artificial neural networks and agent-based models, offer flexibility and can capture nonlinear relationships between weather, occupancy, and building characteristics. While capable of high temporal resolution prediction, these models are often too complex and computationally intensive for large-scale trade-off analyses and optimization. Additionally, their black-box nature makes them non-invertible, limiting their utility in studies that require understanding the effects of energy inputs on thermal comfort.

In this study, we introduce a modeling framework that integrates a fully electrified residential sector with power grid dynamics across diverse climate conditions (Figure 1). Applied to 17,000+ buildings across 54 U.S. cities under historical and projected climates, it shows how across climates, utility bills and thermal discomfort dominate household trade-offs, while pollution and electricity distribution costs play smaller roles (see Table 2 for monetization approaches). We further quantify how older homes require higher costs to achieve similar comfort improvements. Additionally, we show that lower-income households face disproportionately high costs to maintain thermal comfort, how these costs have evolved over time, and how they vary across different climates. These insights provide a foundation for designing equitable policies that align decarbonization efforts with affordability and well-being.

Table 2.2: Monetization methods used in mixed-integer linear programming.

Minimization Objectives	**Monetization Approach**	**Source**
Energy Consumption [kWh]	Residential Electricity Rate [$/kWh]	U.S. BLS[55]
Air Pollution Externalities from Electricity Generation [kWh]	Electricity Marginal Factor Estimates [$/kWh]	Azevedo et. al[56]
Annual Hourly Peak Demand [kW]	Distribution Avoided Capacity Cost [$/kWh]	CPUC[57]
Thermal Discomfort [C-hr]	Variation of Travel Cost Method [$/C-hr]	Our contribution

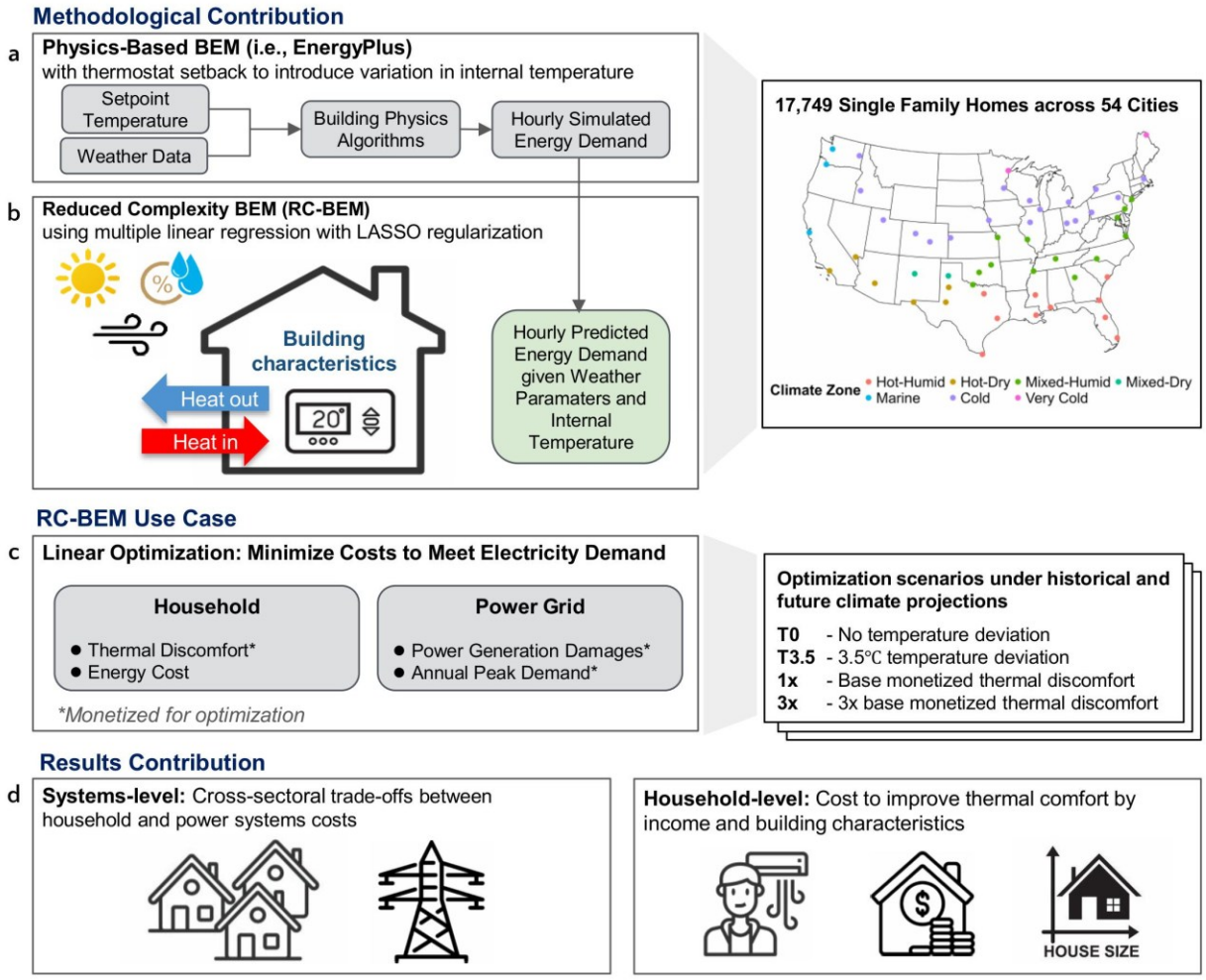


Figure 2.1: Overview of modeling framework.

(A) Training data with internal temperature variations is generated using customized EnergyPlus simulations.
(B) A reduced complexity building energy model (RC-BEM) is developed through penalized multiple linear regression, trained on data from A.
(C) The RC-BEM coefficients are integrated into a mixed-integer linear optimization program to minimize both household- and grid-level costs. Optimization scenarios are analyzed using six annual weather files covering historical (1980–2020) and projected (2020–2060) climates under representative concentration pathways (RCP) 4.5 and RCP 8.5.
(D) We present and discuss the trade-offs at both the systems- and household-levels.

2.2 Data and Methods

2.2.1 Reduced complexity building energy model

We develop RC-BEM, a reduced-complexity building energy model trained on EnergyPlus simulations to predict hourly energy flows in buildings under varying weather conditions and indoor temperatures. We use ResStock to generate a statistically representative housing dataset for 54 U.S. cities, capturing heterogeneity in building characteristics, HVAC efficiency, and climate conditions.[58] We then assume that the heating and cooling demands are provided by efficient ASHPs. We integrate RC-BEM into a linear optimization framework to evaluate the trade-offs between monetized impacts (e.g., utility bills, pollution, grid costs, thermal comfort) under historical and future climate conditions. Finally, we analyze the optimization results for system- and household-level insights. Figure 1 illustrates our modeling framework, from training data generation (panel a) and model training (panel b) to optimization (panel c) and post-optimization analysis (panel d).

2.2.2 Generating EnergyPlus training data

EnergyPlus serves as the high-fidelity physics-based model that generates the training data for RC-BEM. By default, EnergyPlus calculates hourly demand to maintain a constant indoor temperature, limiting its ability to capture occupant-driven variations in heating and cooling patterns. To introduce indoor temperature variability, we implement a twice-a-day thermostat setback, cycling HVAC systems on for six hours and off for six hours (Appendix Figure A.1). This modification allows us to analyze the impact of indoor temperature fluctuations on energy demand and, conversely, the impact of energy demand on internal temperature.

2.2.3 Computing hourly heat gains and losses

We convert appliance-level energy consumption (e.g., natural gas for furnaces, electricity for air conditioners) from customized EnergyPlus simulations into hourly heat flows, accounting for HVAC type and efficiency. For fuel-based heating systems, we calculate hourly heating demand [kWh] by multiplying fuel consumption by a fuel-specific conversion factor and the system's Annual Fuel Utilization Efficiency (AFUE). For electric resistance heating, hourly

heating demand equals the electricity consumption reported in EnergyPlus. For homes with ASHPs, heating demand is calculated as the product of electricity consumption and the heating coefficient of performance (COP). To get the cooling demand [kWh], we multiply the electricity consumption for cooling by the hourly cooling COP, based on the air conditioning SEER rating for that building, which is available in the building metadata.

2.2.4 Training RC-BEM with linear regression

We train RC-BEM using multivariate linear regression on the customized EnergyPlus simulation data to predict the heating and cooling demand for each building with the following equation:

$$Q_t = \beta_0 + \beta_1(T_{i,t} - T_{o,t}) + \beta_2 w_t + \beta_3 s_t + \beta_4 h_t + \beta_5 \varphi_t + \beta_6(T_{i,t} - T_{i,t-1})$$

where t is the hourly time index; Qt is the difference between heating and cooling demands in kWh; β are the regression coefficients unique to each house; TIt and TOt are the internal temperature of each house and external temperature, both in K; w is the wind speed in m/s2, s is the summation of direct normal irradiance, diffuse horizontal irradiance, and global horizontal irradiance in Wh/m2, h is the horizontal infrared radiation intensity in Wh/m2, and ϕ is the relative humidity in %. We used the typical meteorological year dataset, TMY3, which represents the median weather conditions over a multiyear period.[59] This equation captures the interaction of internal temperature and external weather conditions, providing a simplified but robust prediction of heating and cooling demands. To reduce overfitting and improve prediction, we apply a linear Lasso regularization (Figure S3). Once the model is trained and validated, RCBEM acts as a force multiplier, leveraging a single physics-based simulation to assess multiple scenarios.

2.2.5 Validating RC-BEM against EnergyPlus

We assess RC-BEM's predictive accuracy by comparing its hourly heating and cooling demand estimates to separate EnergyPlus simulations with default thermostat settings (i.e., without customized setbacks). For each building, we keep all other inputs unchanged from the training data to ensure a controlled validation (Figure S2A). For each city, we compute the

median normalized root mean square error (NRMSE) of hourly energy demand (Appendix Figure A.2). We further evaluate RC-BEM's peak demand prediction by assessing its annual peak hourly load (i.e., the maximum hourly total demand across all buildings). Lastly, we compare RCBEM's aggregate annual energy demand estimates, summed across all buildings in each city (Figure S2C). See (Table S3) for validation summary.

2.2.6 Computing ASHP performance (COP)

The heat pump COP is calculated in both the heating (superscripted h) and cooling (superscripted c) modes by using a simple linear regression with the following equations.

$$COP_t^h = \beta_a + \beta_b(T_t^I - T_t^O)$$
$$COP_t^c = \beta_c + \beta_d(T_t^I - T_t^O)$$

where *t* is the hourly time index; β are the regression coefficients; T_t^I and T_t^O are the internal temperature of each house and outdoor temperature, both in Kelvin. This regression equation is trained using data from the Cold Climate Air Source Heat Pump (ccASHP) Product List and Specifications compiled by the Northeast Energy Efficiency Partnerships.[60]

2.2.7 Electricity demand for all-electric HVAC

In our analysis, we assume that heating and cooling are provided by efficient electric ASHPs. We convert the heat flows estimated by RC-BEM to ASHP electricity demand using a temperature-dependent COP derived from commercial heat pump data.[60] We constrain COP to a minimum value of 1, accounting for backup resistive heating, following widely used approaches in prior studies.[15,17] The electricity demand for heating is computed by dividing the heating demand by the COP in heating mode. Similarly, the electricity demand for cooling is computed by dividing the cooling demand by the COP in cooling mode.

2.2.8 Monetization approaches

We quantify trade-offs between thermal comfort, energy costs, peak demand, and environmental pollution by assigning monetary values to each factor (Table 2). To compute energy consumption costs, we multiply electricity consumption by the city's annual average residential electricity price or the state average when city-level data is unavailable.[55] To monetize air emissions externalities from power generation, we employ temporally and spatially resolved marginal damage factors, which account for the social cost of carbon (SCC) for climate impacts and the Value of Statistical Life (VSL) for health damages from criteria air pollutants—SO_2, NO_x, and $PM_{2.5}$.[56] These factors are adjusted to reflect a current estimate of the SCC[61] and the latest VSL.[62] We estimate the cost of meeting the hourly peak demand by multiplying the financial benefits of *"...deferring or preventing investments in distribution infrastructure by decreasing distribution peak capacity needs"*[57] by the maximum of the summed hourly electricity demands for all modeled buildings in each city. To our knowledge, no metric within a linear optimization framework adequately monetizes the effects of thermal discomfort. To address this, we adapt the travel cost method from contingent valuation[63] to estimate the value occupants place on thermal comfort. Using RC-BEM, we calculate the change in utility bills caused by a 1◦C change in indoor temperature relative to baseline setpoints for both winter and summer. We repeat this process for three baseline setpoints per building. A linear model correlates utility bills with degree hours of heating or cooling, where the slope represents the cost of purchasing an additional degree-hour of warmth or cooling (Figures S4 and S5). This slope also serves as a proxy for the monetary value occupants attach to enduring or avoiding thermal discomfort for an hour.

2.2.9 Optimization model setup

The optimization model minimizes the annual total cost from peak demand, emissions, energy use, and thermal discomfort.

Objective function

$$\min \qquad f\ P + \sum_{(j,t)} (d_t + e_t) E_{j,t} + \eta \left[\sum_{(j,ht)} \alpha \left| T_{j,t}^{I} - T^{H} \right| + \sum_{(j,ct)} \beta \left| T_{j,t}^{I} - T^{C} \right| \right]$$

where j and t index individual buildings and hourly intervals, respectively; ht and ct are the heating and cooling hours (subsets of t); f is the cost of avoided distribution capacity expansion in \$/kW-yr[57]; P is the annual aggregate hourly peak demand in kW; d_t is the marginal damage factor in \$/kWh[56]; et is the residential electricity price in \$/kWh; $E_{j,t}$ is the electricity demand for ASHP in kWh; η is the thermal comfort cost multiplier; α and β are the cost of thermal discomfort associated with heating and cooling in \$/K-hr, respectively; $T_{j,t}^{I}$, T^{H} and T^{C} are the internal temperature, heating and cooling setpoints in K, respectively. We extract the heating and cooling setpoints from the ResStock database, which utilizes microdata from the Residential Energy Consumption Survey.

Subject to the following constraints

The net heating demand must not exceed ASHP capacity at all hours:
The internal temperature deviation must not exceed ± 3.5K for 300 out of 8760 modeled hours as per ASHRAE 90.1.[64] Key constraints include maintaining internal temperatures within allowable deviations per ASHRAE Standard 55,31 limiting unmet load hours to no more than 300 out of 8760 modeled hours as per ASHRAE Standard 90.1[64], and capping hourly energy use based on the ASHP's capacity.

2.2.10 Optimization scenarios

Our study includes three analyses. First, we compare the cost trade-offs between maintaining internal temperature at building-specific setpoint temperatures (optimization scenario T0) and allowing deviations by up to 3.5 ◦C (T3.5), within ASHRAE's residential comfort recommendations.[65,66] Understanding these trade-offs is crucial, considering scenarios where energy-limiting behaviors are prevalent, especially among low-income occupants who often reside in poorer-quality homes.[34,67] These homes are typically characterized by older structures with inadequate insulation, outdated heating or cooling systems, and high infiltration (i.e., leakier homes).[24] Such households are more vulnerable to energy cost burdens and thermal discomfort.[50]

We recognize that our thermal discomfort monetization approach leaves no room for a consumer surplus (i.e., a situation in which consumers derive more value per unit of good consumed than its price[68]). Therefore, we introduce two scenarios. The first, 1x, does not constrain indoor temperature but values depart from set point temperatures based directly on the cost of energy; that is based on the slopes calculated (Figures S4 and S5). The second, 3x, assumes that the value of discomfort is three times as high as the cost of that discomfort (i.e., the per degree-centigrade-hour value of discomfort is assumed to be three times the slope calculated).

Finally, we assess how climate conditions affect the cost trade-offs in all four optimization scenarios described above, using historical weather data from 1980–2020 and future projected weather data from 2020 to 2060 under the Representative Concentration Pathway (RCP) 4.5 and RCP8.5. We use the Thermodynamic Global Warming (TGW) climate datasets in our analysis.[69] RCP4.5 represents a moderate stabilization scenario, while RCP8.5 represents a high greenhouse gas concentration scenario, allowing us to capture a range of potential climate futures. For each historical and future period, we sample two representative weather years: one ‘‘cold year’’, identified as the year with the highest total heating degree days (HDD) during the winter months (January, February, and December), and one ‘‘hot year’’, identified as the year with the highest total cooling degree days (CDD) during the summer months (June, July, and August). This approach enables targeted analysis of temperature extremes that are most likely to

influence residential energy consumption, occupant comfort, peak power demand, and power sector air pollution externalities.

2.2.11 Estimating income from home attributes

We estimate the probability of a household falling into one of five income categories (<$15k, $15k–$35k, $35k–$75k, $75k–$100k, and >$100k), conditioned on two building characteristics: air conditioning type (window unit, central air, or none) and house size 0–1499 sqft, 1500–2499 sqft, 2500–3499 sqft, >3000 sqft). These conditional probability tables are constructed using Iterative Proportional Fitting with data from the American Housing Survey (AHS) and the American Community Survey (ACS) from the U.S. Census Bureau.[70,71] To account for local variations, we generate a separate table for each city. Once the income distribution is determined, we apply bootstrapping via Kernel Density Estimation, with 1000 bootstrap samples per home, to estimate the income distribution for each household.

2.2.12 Statistical analysis

All statistical analyses were performed in R using base functions and the dplyr package. Statistical testing was limited to income based differences in thermal comfort improvement costs, as presented in Figure 5. For each city, house size, and month, pairwise comparisons between income groups were conducted using the Mann–Whitney U test, with statistical significance defined at $\alpha = 0{:}05$. Results are reported as median values with interquartile ranges. Homes with anomalous or implausible simulation outputs were excluded from the analysis. In Duluth, eleven homes in the $15k–$35k income group and four homes in the $35k–$75k income group with over 3,500 sqft were excluded due to anomalous or implausible results.

2.3 Results

We apply RC-BEM within a mixed-integer linear programming framework to evaluate trade-offs among occupant thermal comfort, household energy cost, peak electricity demand, and air pollution externalities for over 17,000 representative single-family homes across 54 U.S. cities, under both historical and projected climate conditions. We define four optimization scenarios: T0, where indoor temperature is constrained to remain at the setpoint; T3.5, which allows temperature deviations up to 3.5◦C, consistent with the maximum deviation recommended by ASHRAE for maintaining residential thermal comfort[72]; 1x, which places no hard temperature constraints but applies a baseline penalty for discomfort based on energy-equivalent cost; and 3x, which follows the same structure as 1x but triples the discomfort cost. While our modeling covers all 54 cities, we focus our visualizations on six representative locations to illustrate key patterns across diverse climate zones. Complete optimization results for all cities and scenarios are provided in the Appendix Table A.6-A.8.

2.3.1 Maintaining indoor thermal comfort is more energy intensive in colder cities

Figure 2 shows that annual household costs (utility bills and monetized thermal discomfort) consistently exceed non-household costs (monetized peak demand and externalities) in all scenarios except for T0 in Nashville and Duluth. Household costs constitute, on average, 54% (90th percentile range across all homes in all cities: 46%–61%) of total costs in T3.5, 98% (95%–99%) in 1x, and 78% (69%–85%) in 3x. In T0, which is arguably the baseline scenario for most analyses of household energy use, average non-household costs exceed household costs, accounting for 52% (90th percentile range: 47%–58%) of the total. These trends are consistent in 54 cities studied (Tables S5–S8).

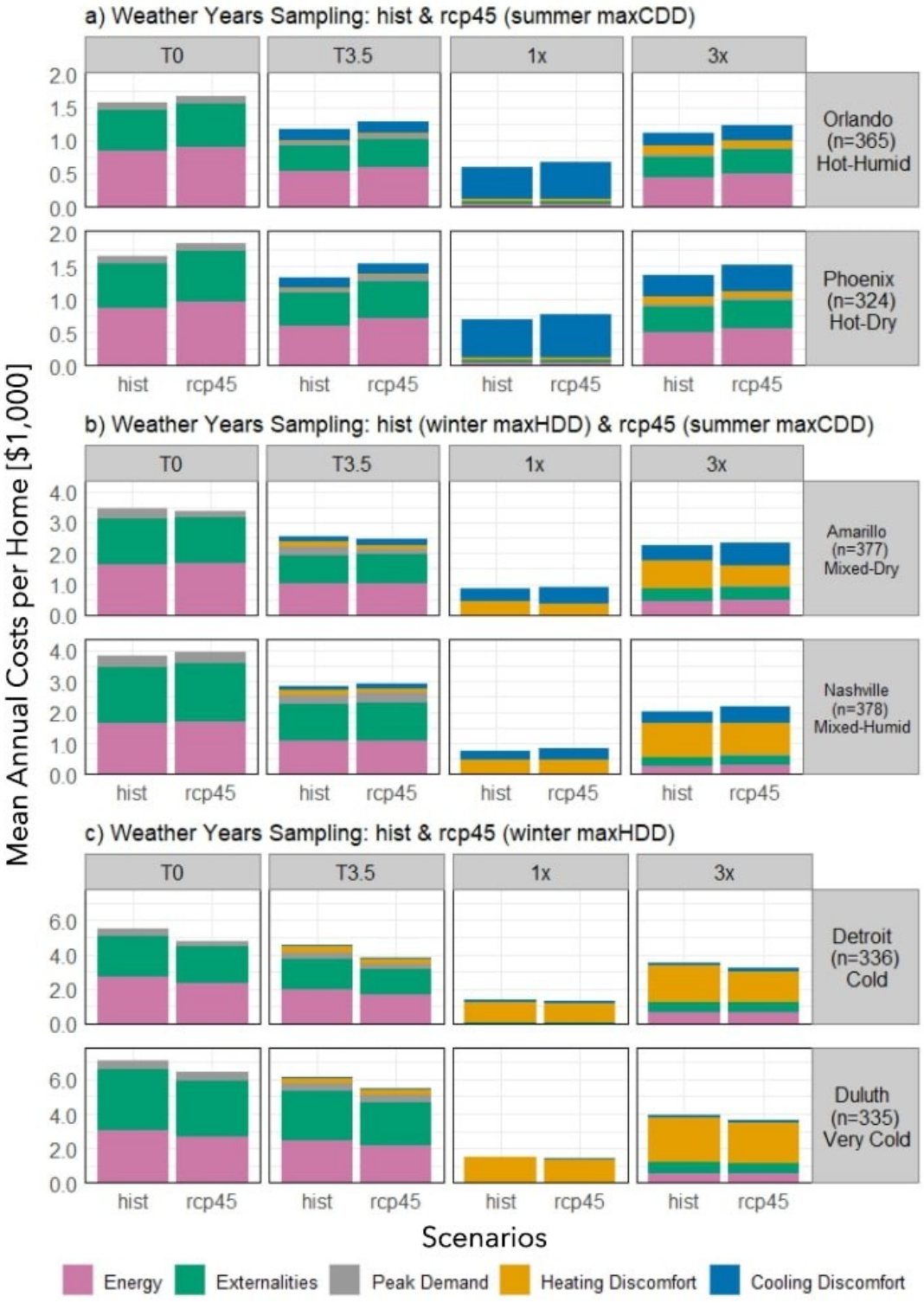


Figure 2.2: Annual cost-comfort trade-offs.

(A–C) Bars show mean annual per-home costs (in $1,000) for energy use, externalities, peak demand, and thermal discomfort, averaged across households in each city (n shown in panels), under four scenarios: T0 (no deviation), T3.5 (±3.5◦C allowed), 1x (no constraint), and 3x (1x with tripled discomfort costs). Cities grouped by (A) Cooling-dominated, (B) Mixed, (C) Heating-dominated.

In colder cities, maintaining thermal comfort is significantly more energy-intensive. For example, in Duluth and Detroit, mean annual energy costs in the T0 scenario range from $2.5k to $2.9k per home, compared to $800 to $950 in Orlando and Phoenix. This disparity is, first, due to the coefficient of performance (COP) of ASHPs, which depends on the temperature differential between the indoor and outdoor air. In cold climates, this difference is large and the COP is low (Figure S6). Second, homes in warmer cities need less total heating and cooling, defined as the sum of heating and cooling degree-days. Lastly, higher residential electricity rates in colder regions compound the financial burden of prolonged heating seasons with lower COPs (Table S4). We also find that peak demand costs respond minimally to increased discomfort, as we define it, across all climate regions. This is because peak demand is driven by short-term energy spikes during extreme weather, rather than cumulative deviations from setpoint temperatures.

2.3.2 Thermal comfort is more than three times as valuable as the cost of the energy used to provide it

Figure 3 shows that under historical winter conditions, 5thpercentile indoor temperatures for a median home would drop from a comfortable 20◦C (68◦F) in T0 to 2◦C (36◦F) in Detroit and -4◦C (25◦F) in Duluth in 1x. Conversely, 95th-percentile temperature for a median home during historical summer conditions are 36◦C (97◦F) in Orlando and a dangerous 42◦C (108◦F) in Phoenix, respectively, in the 1x compared to 24◦C (75◦F) in T0. These indoor temperatures are intolerable and may expose occupants to cold- and heat-related illnesses.[73,74] In 3x, 95thpercentile (summer) internal temperatures come close to meeting the ASHRAE guidelines (T3.5). For instance, in Phoenix's projected future weather, the median 95th-percentile temperature decreases from a dangerous 44◦C (IQR: 43–46) in 1x to 27◦C (IQR: 24–40) in 3x, aligning with the T3.5 range of 27◦C (IQR: 26–29). Most households use enough energy to maintain indoor temperatures within the 3x range, suggesting that they value this thermal comfort at ∼3 times what it costs to obtain it. The RC-BEM thus helps modelers identify a multiplier that, if combined with energy costs, serves as a reasonable proxy for thermal comfort on an individual building basis.

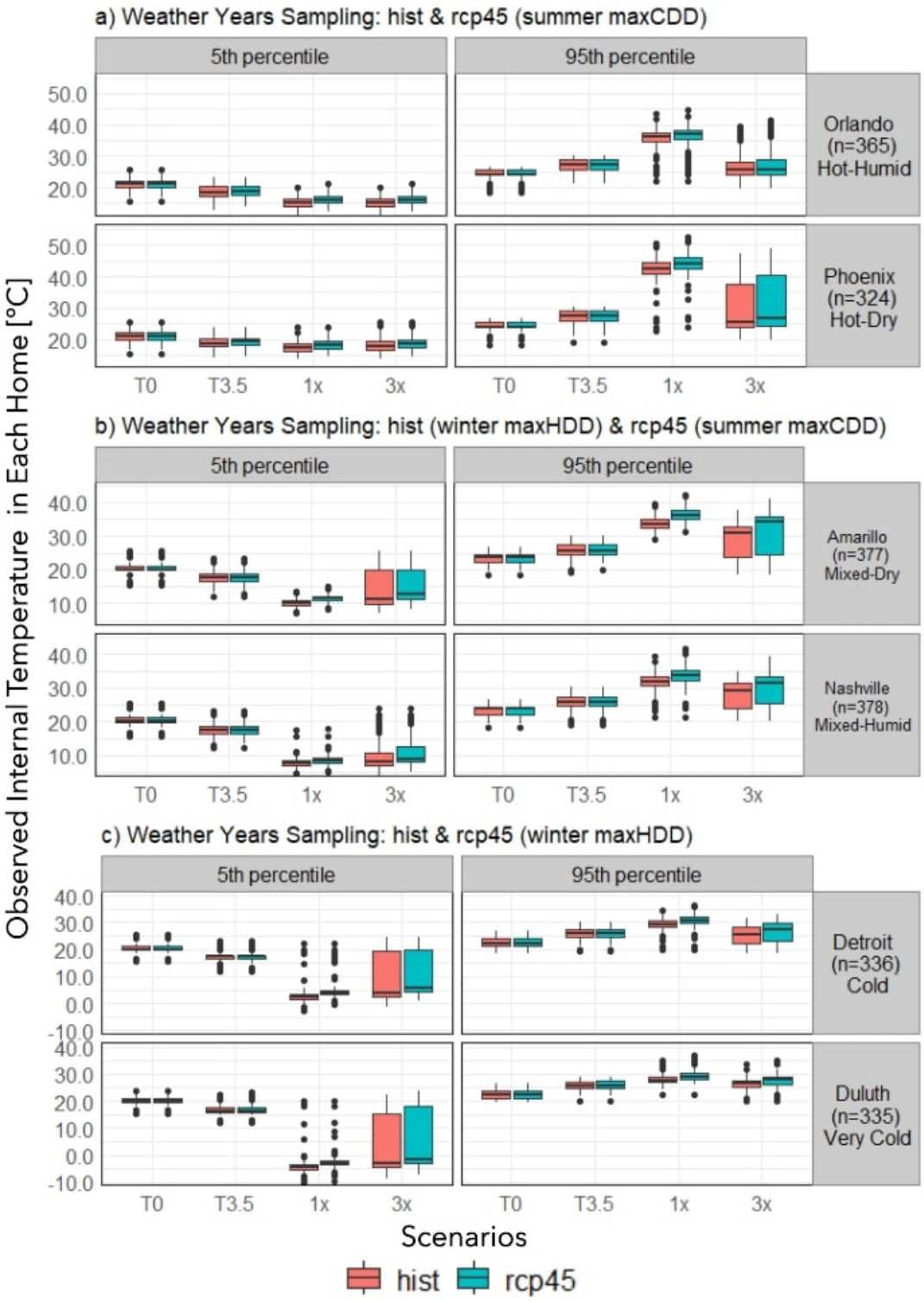


Figure 2.3: Internal temperature extremes.

The 5th-percentile (cold) and 95th-percentile (hot) temperatures represent extremes observed across households (n shown in panels) during the coldest or warmest 144 h of a 2,880-h heating or cooling season (four months). Boxplots show the median (line), interquartile range (box), and 1.5× IQR whiskers; points denote outliers. Cities grouped by (A) Cooling-dominated, (B) Mixed, (C) Heating-dominated.

Despite projected warming under RCP 4.5, internal temperatures show small differences between RCP 4.5 and historical climates across our scenarios (see Figure 3). Our finding—that the 3x and T3.5 scenarios produce nearly similar energy consumption outcomes—is consistent across RCP 4.5 (moderate emissions) and RCP8.5 (high emissions) (see Appendix Figure A.7).

2.3.3 Across home sizes, thermal comfort costs and cost disparities are lower for newer homes

Fig. 4 shows a sharp reduction in the monthly cost of improving thermal comfort across climates. Older homes (built before 1950) have significantly higher costs than newer homes (built in the 2000s), regardless of house size. To better contextualize $/1000◦C-hr, we converted it to $/◦C-month by assuming a continuous temperature adjustment over a standard month (e.g., 30 days × 24 h/day = 720 h), making it equivalent to improving comfort by 1◦C for one month.

Cold regions experienced the largest reductions, with median costs for 2,500–3,500 sqft homes falling by 52% in Detroit (from $39 per ◦C-month in pre-1950 homes to $19 per ◦C-month in 2000s homes) and by 49% in Duluth (from $25 to $13 per ◦C-month). Mixed climates showed intermediate reductions, with costs decreasing by 33% in Amarillo (from $31 to $20 per ◦C-month) and 34% in Nashville (from $23 to $15 per ◦Cmonth). Hot climates had smaller reductions: 19% in Phoenix (from $14 to $11 per ◦C-month) and 13% in Orlando (from $14 to $12 per ◦C-month).

There is also a narrowing of cost disparities between large (>3,500 sqft) and small (<1,500 sqft) homes. In Detroit, among homes constructed in the 1950s, large houses incurred more than five times the thermal comfort cost per ◦C-month of small houses ($59 vs. $12 per ◦C-month). For homes built in the 2000s, the cost of purchasing an additional ◦C-month of comfort was less than twice as high for large homes as for small homes ($22 vs. $12 per ◦C-month).

This implies an increase in energy efficiency that coincides with the introduction of building energy codes in the U.S., which were rolled out in the 1970s. If this increase in efficiency is indeed attributable to building codes,[75] this study offers a novel metric to quantify the benefits of these codes. It also suggests that building codes may have mitigated the increase in residential energy consumption driven by the marked growth in home sizes over the past fifty years.[5]

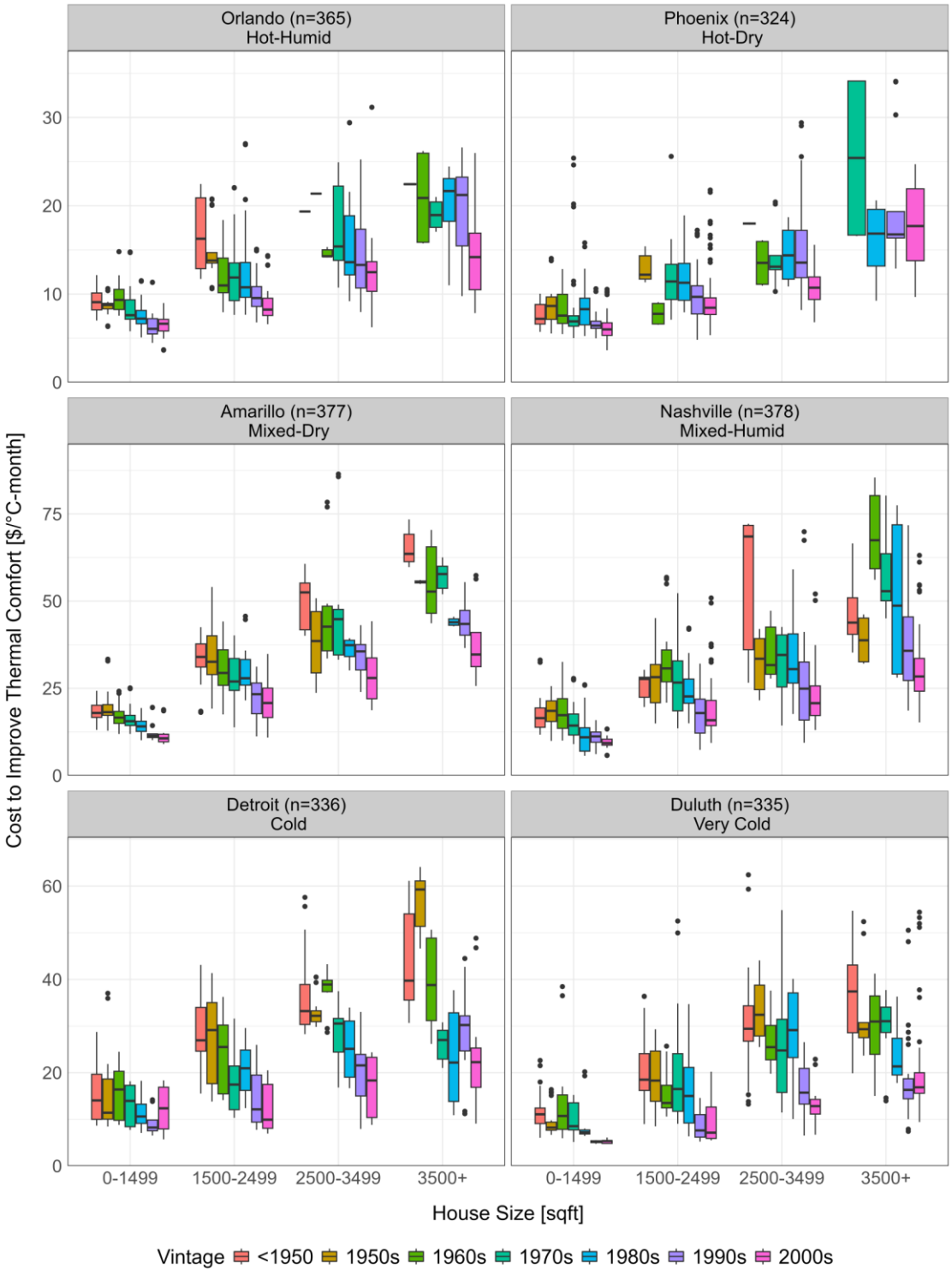


Figure 2.4: Energy costs to improve thermal comfort.

Boxplots show the cost of thermal comfort improvements (in $ per ◦C-month), pooled across households by home size (x axis) and construction decade (legend), segmented by city (n shown). Each boxplot displays the median (line), interquartile range (box), 1.5× IQR whiskers, and outliers (points). Costs are based on the T0 (no deviation) and T3.5 (±3.5◦C allowed) scenarios.

2.3.4 No consistent correlation between household income and the marginal cost of thermal comfort

Prior studies show that lower-income households live in less energy-efficient homes, resulting in higher costs to improve comfort.[24,34,76] However, these findings often rely on limited regional samples. Using RC-BEM, we assess whether these disparities persist across a broad range of homes and climate zones. To estimate household income, we synthesize the U.S. Census and American Housing Survey data to generate a distribution of household incomes conditional on building characteristics for each city (see Methods).

Our results show that income-based disparities in thermal comfort costs persist across most regions, with variations in magnitude and significance by season. Figure 5 shows cases where lower-income households face higher costs (red boxes) more frequently than those with lower costs (blue boxes). In hot-dry regions like Phoenix, significant disparities arise in July, with households in the 1,500–2,499 sqft size range earning $75k–$100k incurring median costs of $19 per ◦C-month compared to $13 per ◦C-month for those earning over $100k. In January, however, these disparities are less pronounced.

In Detroit, significant disparities persist across seasons but vary in magnitude. In January, for homes larger than 1,500 sqft, the cost gap between households earning $75k–$100k and those earning over $100k is approximately $11–$14 per ◦Cmonth. By July, for homes of 1,500–3,499 sqft, the cost gap narrows to about $4–$8 per ◦C-month—two to four times smaller than in January.

In Nashville, none of the income-based disparities are statistically significant, as indicated by the dashed boxes. The results also show a mix of higher and lower costs for lower-income households (red and blue boxes), reflecting inconsistent trends compared to other regions. Additionally, humid regions, such as Orlando, Amarillo, and Detroit, show smaller income-based disparities than their drier counterparts, such as Phoenix, Nashville, and Duluth—a pattern that warrants further investigation.

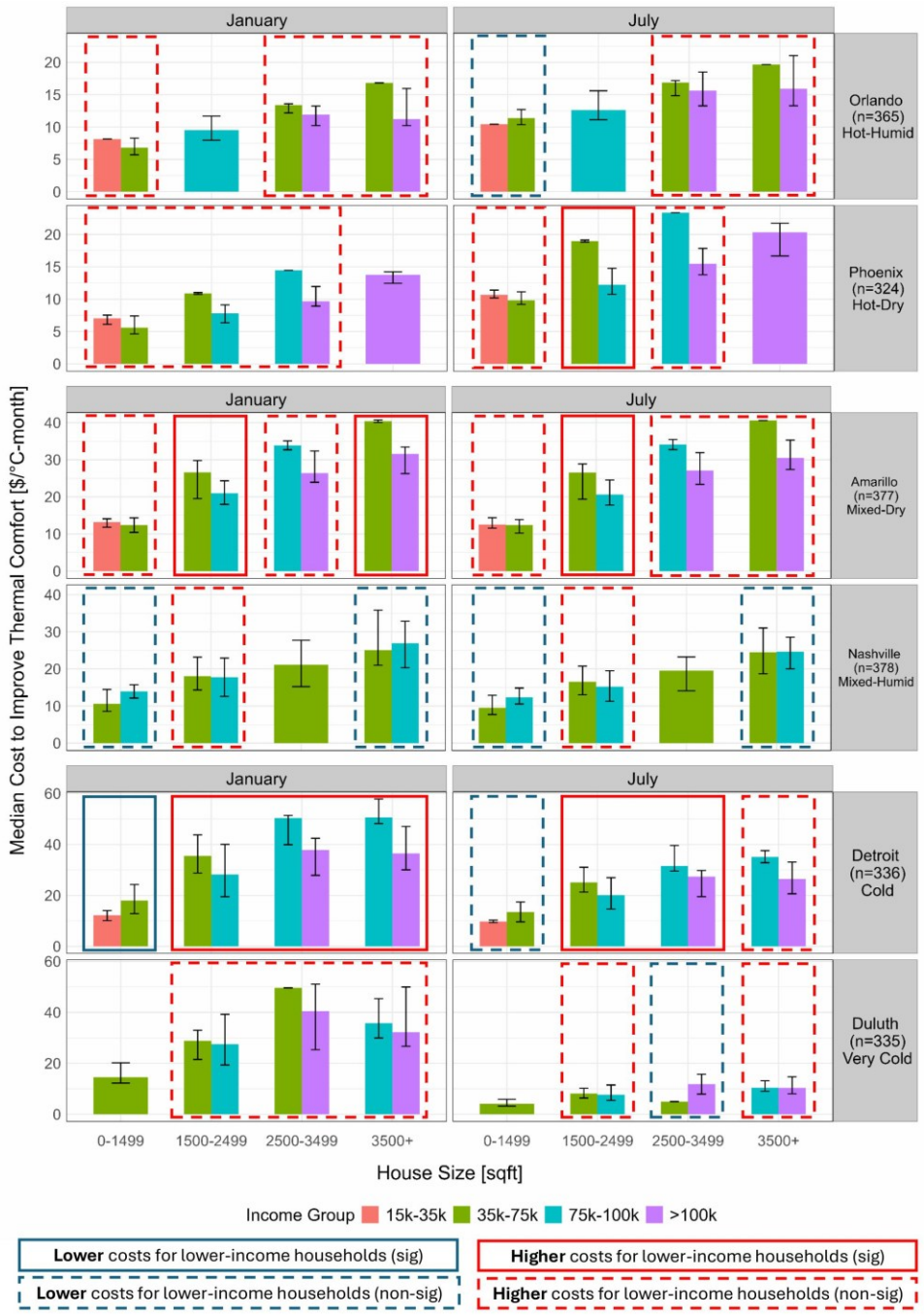


Figure 2.5: Income-based disparities in thermal comfort improvement costs.

Barplots show the median cost of thermal comfort improvements (in $/◦C-month), grouped by house size (x axis) and household income (legend), for January and July under the T0 (no deviation) and T3.5 (±3.5◦C allowed) scenarios. Bars represent the interquartile range (IQR) across households within each group; n per city shown in panel titles. Outlined boxes indicate significant (solid) or non-significant (dashed) cost differences between income groups (Mann–Whitney U test, alpha = 0.05). In Duluth, 11 homes in the $15k–$35k group and 4 homes in the $35k–$75k group (all >3,500 sqft) were excluded due to anomalous values (see SI for details).

Overall, of the 212 combinations of city, estimated income group pair, house size, and season analyzed, 157 show no significant difference in the cost of purchasing an additional unit of thermal comfort (Table S9). Fifty-five combinations do exhibit significant differences, of which 39 are regressive (i.e., the lower-income households pay more) and 16 are progressive. Based only on estimated means (i.e., ignoring statistical significance), 137 combinations are regressive (i.e., the lower income households pay more).

2.4 Discussion

We develop a RC-BEM using penalized linear regression to emulate EnergyPlus simulations with internal temperatures and weather variables as inputs. RC-BEM simulates hourly energy demand of over 17k single-family buildings across 54 U.S. cities, covering seven climate zones. We apply RCBEM in co-optimizing utility bills, thermal comfort, peak demand, and air pollution externalities from power generation under historical and future climate scenarios. RC-BEM runs in milliseconds per building on a laptop; physics-based models take seconds on a supercomputer. Models that can rapidly assess the trade-offs between indoor comfort and other energy-related costs have significant applications in urban energy planning. When combined with high-resolution housing characteristics and census demographic data, these models can help planners pinpoint areas where vulnerable residents (e.g., elderly) are likely at risk of extreme indoor temperatures during extreme weather events or power failures. Utilities or third parties operating demand response programs can build similar surrogate models using thermostat data to optimize community-level signals, ensuring grid stability while minimizing the risk of exposing occupants to unhealthy temperatures. By tailoring demand response at the household level and coordinating load control across multiple buildings, these programs can more effectively balance grid demand while minimizing occupant overrides that could negate their benefits.[16]

Our findings reveal critical disparities in thermal comfort costs, presenting opportunities for equitable policy interventions. In colder climates, older and less energy-efficient homes face disproportionately higher heating costs, underscoring the need for targeted retrofitting programs such as weatherization assistance and insulation upgrades. In warmer climates, lower-income households bear a greater burden of summer cooling costs, highlighting the importance of

income based incentives for energy-efficient ASHPs. Furthermore, our results provide a quantitative evidence highlighting building codes' effectiveness in improving efficiency and reducing disparities of improving comfort, which can be integrated into city-level planning efforts to promote equitable energy policies. The RC-BEM framework advances building energy modeling by enabling the simultaneous optimization of thermal comfort and other costs, addressing limitations in existing methods. As energy transitions reshape interactions across buildings and sectors, modelers must respond with flexible approaches that capture these new dynamics. For example, power sector modelers have generally viewed buildings as a load. Increasingly, it will be important to develop strategies to control the increasingly electrified, and increasingly flexible, building loads as resources and to do so in a way that does no harm. This work is a crucial first step in giving modelers that ability. By identifying key tradeoffs and disparities in comfort improvement costs across regions, this study lays the groundwork for future research on equitable energy transition strategies.

2.5 Limitations of the study

We identify future work areas stemming from our approach's limitations. First, the approach described here brings thermal discomfort into the optimization framework by working backwards from the observation that most people use enough energy to maintain reasonable indoor temperatures. Nonetheless, our work here demonstrates the need for an estimate, rooted in epidemiological data, for monetized harms from unhealthy temperatures to refine this approach.[77,78] Ideally, such proxies would reflect the non-linear relationship between temperature and health damages, which our approach fails to capture. The monetized damages from air pollution, which are widely used in the energy modeling literature, illustrate how valuable such estimates can be in policymaking.[79–81]

Second, RCBEM requires an initial EnergyPlus model for each building, and each model generated is only valid for that building. The building's thermal behavior is codified in the coefficients of the model and there is no transparent connection between its coefficients and thermal characteristics (e.g., leakage rate or insulation). Future work should leverage NREL's large database of simulations to build surrogate models that predict energy use as a function of building characteristics.

Lastly, our simplified ASHP model omits advanced control strategies and subhourly phenomena, such as resistive heating during defrost cycles. However, these effects are leveled out at the aggregate level, as simultaneous operation in resistance heating mode is unlikely. Moreover, because defrost cycles are brief, their impact on household energy costs is minimal. Future work should incorporate dynamic ASHP models to capture these behaviors without compromising scalability for large-scale analyses.

Chapter 3 Anti-Frost Coatings Reduce Winter Emissions from Heat Pumps Without Compromising Comfort

Air-source heat pumps (ASHPs) provide high-efficiency electric space heating and play an important role in residential decarbonization. In cold climates, low outdoor temperatures reduce ASHP efficiency, while frost formation necessitates periodic defrosting, which lowers indoor temperatures and is typically offset by energy-intensive auxiliary electric resistance heating. Anti-frost coatings offer a pathway to suppress frost formation and mitigate these comfort and energy penalties, but their system-level implications for residential ASHP applications have not been quantified. Here, we simulate ASHP operation in ~7,900 single-family homes across 25 U.S. cold-climate cities, comparing current practice, i.e., defrosting with auxiliary electric resistance heating, to defrosting operation without auxiliary heating, and to anti-frost coatings assumed to suppress frost formation and thereby avoid defrost operations. Our calculations show that relative to current practice, anti-frost coatings can reduce median winter emissions by ~40%. Disabling electric resistance heating yields the largest emissions reductions but causes 1–5 °C indoor cooling during defrost, while a +2 °C increase in temperature setpoint halves under-heating. At scale, widespread adoption of anti-frost coatings could yield winter emissions reductions comparable to roughly 30% of U.S. commercial aviation emissions in 2022, while eliminating defrost-related thermal discomfort.

3.1 Introduction

Residential space heating accounts for roughly one-third of U.S. residential direct CO_2 emissions, driven by the widespread use of fossil-fuel furnaces and boilers.[42,82] By replacing fossil-fuel heating with high-efficiency air-source heat pumps (ASHPs), direct on-site GHG emissions can be eliminated, with indirect emissions declining as electricity supplies decarbonize.[39,41,83] In cold climates, however, large temperature differentials between indoor and outdoor air reduce heating output and the coefficient of performance (COP).[15,60] Under frost-prone conditions (−15 °C to 5 °C; relative humidity > 60%), moisture condenses and freezes on the outdoor heat exchanger, forming a frost layer that raises thermal resistance, restricts airflow, and further degrades COP.[84–88] To restore heat transfer performance, ASHPs periodically enter reverse-cycle defrost mode, during which heat is drawn from the indoor space to melt accumulated frost, temporarily lowering indoor temperature and compromising comfort.[86–89]

In cold climates, ASHPs are often paired with auxiliary electric resistance heating to maintain indoor comfort during periods of insufficient heat-pump capacity and defrost operation, which substantially increases electricity consumption.[89–91] Without auxiliary heating, defrost operation results in unmet heating demand, leading to indoor temperature drops and thermal discomfort. To partially offset these comfort losses, occupants may raise thermostat setpoints, trading additional energy use for improved comfort. Despite these alternative approaches to managing defrost-related comfort loss, their relative impacts on indoor comfort, winter electricity consumption, and associated greenhouse-gas emissions remain poorly quantified across climates and housing stocks.

Laboratory and field studies have quantified the performance penalties associated with frost accumulation and defrost operation in ASHPs.[92–98] Controlled laboratory experiments show that frosting progresses through distinct stages: a brief initial period in which wet-coil conditions can temporarily increase heating capacity and COP, followed by mild degradation as frost accumulates, and then a sharp reduction once heavy frost develops.[93] In the final stage, laboratory measurements show that heating capacity can fall by roughly 30–40% within 20–30

minutes and COP typically declines by 15–20%.[93,95,96,98] Field measurements indicate larger penalties, with heating-capacity reductions of 30–50% and COP penalties of 20–40%.[92,94,97]

U.S.-based studies of frosting and defrost operation do not assess impacts on indoor comfort, winter electricity use, or emissions at scale, as existing work is largely limited to short-term field demonstrations at individual buildings and locations.[99–101] Consequently, prior studies provide limited insight into how defrost-related performance penalties translate into system-level outcomes across diverse housing stocks and climate conditions. Although DOE's Cold Climate Heat Pump Challenge has advanced compressor efficiency, refrigerant-cycle design, and low-temperature capacity, it does not explicitly evaluate frosting and defrost-related impacts on indoor comfort, electricity consumption, or emissions.[102]

As an alternative periodic defrost operation, several strategies have been explored to suppress frost formation on ASHP outdoor heat exchangers, including ultrasonic vibration, fin-geometry modifications, and engineered surface treatments.[86] Among these, surface treatments are especially promising because they operate passively and require no mechanical redesign. For example, zwitterionic polymer coatings suppress ice nucleation by forming a strongly hydrated interfacial layer that reduces water mobility and delays freezing, a mechanism inspired by antifreeze strategies observed in cold-adapted organisms such as Arctic fish.[103–105] Laboratory studies report anti-frost times between a few minutes to several hours, under controlled conditions—five to six times longer than those achieved by conventional hydrophilic or hydrophobic coatings.[105–107] However, these advances have been evaluated almost exclusively at the material or component level, with implications for performance, energy use, and comfort remaining uncertain.

This study estimates the "size of the prize" of widespread adoption of frost-inhibiting coatings through an integrated modeling framework that connects ASHP performance, building energy dynamics, and regional climate data. We simulate approximately 7,900 representative single-family homes across twenty-five U.S. cold-climate cities to evaluate how alternative

defrost-management strategies influence household comfort, electricity use, and associated greenhouse gas emissions. The framework compares four defrost-management configurations: defrost operation with auxiliary electric resistance heating (current practice), defrost operation without auxiliary resistance heating, defrost operation without auxiliary resistance heating (with elevated thermostat setpoints), and passive anti-frost polymer coatings that suppress frost formation and avoid defrost operation. This study provides the first system-level quantitative assessment of how defrost-management choices translate into indoor temperature impacts, winter electricity use, and associated GHG emissions across diverse U.S. housing stocks and cold-climate conditions.

3.2 Data and Methods

This study uses an integrated modeling framework that links climate data, a reduced-complexity building energy model, and sub-hourly heat-pump performance models to quantify how defrost-management strategies affect indoor temperature, electricity use, and greenhouse-gas emissions in cold climates (Figure 1). The analysis covers approximately 7,900 representative single-family homes across 25 frost-prone U.S. cities. Housing samples are drawn from NREL's ResStock database, which leverages Residential Energy Consumption Survey (RECS) microdata to represent regional variation in building characteristics and climate conditions.

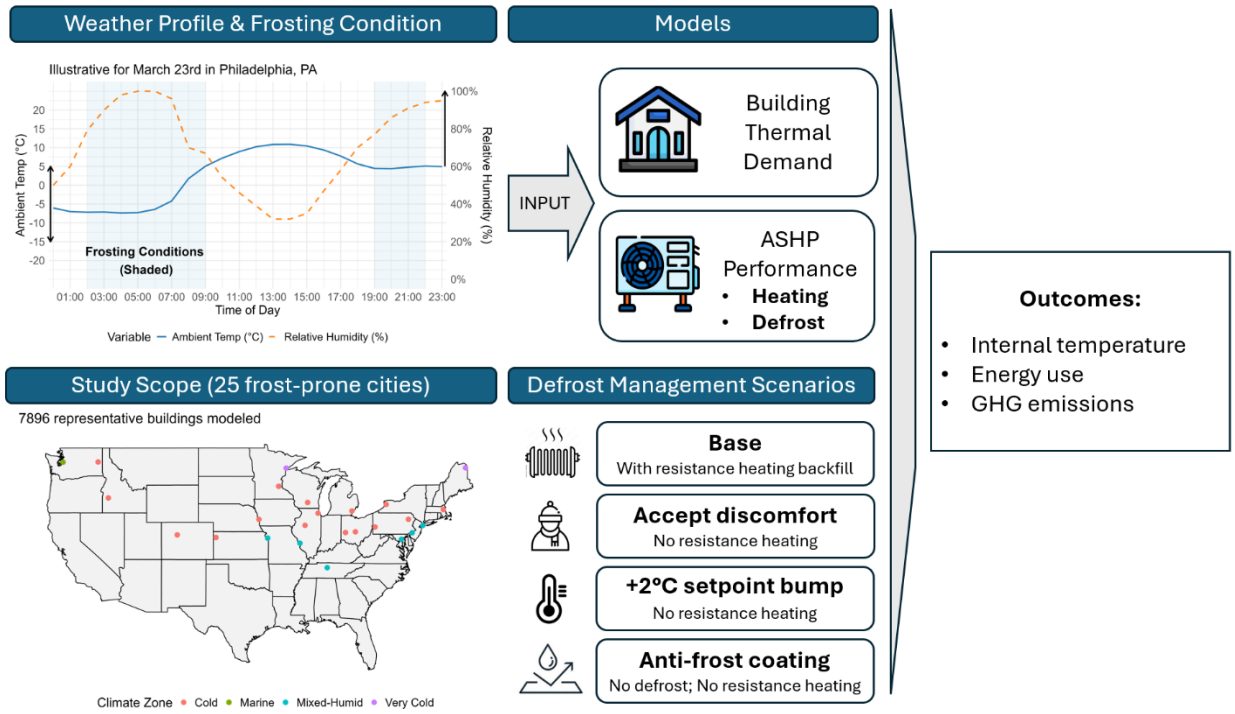


Figure 3.1: Conceptual framework and defrost-management scenarios.

We evaluate four defrost-management configurations, labeled Base, Accept Discomfort, +2 °C Setpoint Bump, and Anti-frost Coating. Only the Base configuration uses auxiliary electric resistance heating backfill. The Base, Accept Discomfort, and +2 °C Setpoint Bump configurations include periodic defrost operation, whereas Anti-frost Coating assumes suppressed frost formation, eliminating the need for defrost and thus resistance heating. The +2 °C Setpoint Bump configuration increases the thermostat setpoint at all hours to partially offset defrost-related indoor temperature reductions.

3.2.1 Climate data and frosting conditions

Hourly meteorological data were obtained from the Typical Meteorological Year (TMY3) dataset.[108] Weather conditions jointly determine building heating demand, heat-pump performance, and the likelihood of frost formation on outdoor coils. The analysis builds on a database of 54 U.S. cities with single-family building models previously developed in earlier work by Deetjen et al. (2021), which selected cities to span the full range of Building America climate zones (DOE's standardized residential climate classifications) and NERC electric-grid regions.[48] To identify frost-prone locations, hourly records were screened for periods with −15

°C ≤ T_{oa} ≤ 5 °C and RH ≥ 60 %, thresholds associated with coil frost formation.[84–86] Screening was performed at hourly resolution, while sub-hourly modeling resolves defrost events. The 25 cities with the highest cumulative frost-prone hours were selected for detailed simulation (Appendix Figure B.1).

3.2.2 Reduced-Complexity Building Energy Model

Evaluating the comfort and energy impacts of heat-pump defrost cycles requires a building model that captures transient indoor temperature response alongside space-heating demand. Building on the framework of Nawawi et al. (2025), a reduced-complexity building energy model (RC-BEM) was used to simulate hourly thermal response for representative single-family homes.[109] Baseline heating setpoints were taken from NREL's ResStock database for each representative home, where base heating setpoints are constructed using RECS microdata; time-varying thermostat schedules were not considered in the analysis. City-specific baseline heating setpoints are reported in Table S1. RC-BEM emulates EnergyPlus simulations through a linear surrogate trained on customized runs with six-hour thermostat-setback cycles that generated controlled indoor-temperature fluctuations for regression training. Model coefficients were estimated separately for each home using penalized multiple linear regression (LASSO) to mitigate overfitting and improve prediction accuracy. Hourly net space-conditioning load $\mathbf{Q_t}$ (kW) was estimated as:

$$Q_t = \beta_0 + \beta_1(T_{i,t} - T_{o,t}) + \beta_2 w_t + \beta_3 s_t + \beta_4 h_t + \beta_5 \varphi_t + \beta_6(T_{i,t} - T_{i,t-1})$$

where $T_{i,t}$ and $T_{o,t}$ are indoor and outdoor air temperatures (K); w_t wind speed (m s^{-1}); s_t and h_t short- and long-wave radiation (W m^{-2}); and φ_t relative humidity (%). The lag term ($T_{i,t} - T_{i,t-1}$) represents building thermal inertia. β_0–β_6 are regression coefficients unique to each home that quantify the sensitivity of thermal load to each predictor. Positive Q_t values denote heating demand, while negative values denote cooling demand. Details on model training and validation are provided in Nawawi et al. (2025).

3.2.3 RC-BEM temporal downscaling

RC-BEM simulations were performed at an hourly time step consistent with the TMY3 weather data. Because defrost cycles in residential air-source heat pumps generally last on the order of 15 minutes or less under standard defrost control logic, hourly outputs of space-heating load and indoor air temperature were linearly interpolated to 15-minute intervals. This temporal downscaling provides the resolution required for the sub-hourly heat-pump performance model during both heating and defrost operation. The resulting 15-minute profiles were used as inputs to the heat-pump performance model described in the following section.

3.2.4 Heat pump performance model

Heating-mode performance was represented using temperature-dependent correlations for heating capacity and coefficient of performance (COP), derived from manufacturer data for cold-climate variable-speed air-source heat pumps compiled in the NEEP cold-climate ASHP database. The model operated at 15-minute intervals, taking RC-BEM heating loads and outdoor air temperature ($T_{o,t}$) as inputs to compute ASHP capacity, electricity consumption, and defrost status for each simulated home. Heating capacity and COP were represented as linear functions of temperature lift. When the building load (Q_t) exceeded available capacity, unmet demand was met by auxiliary electric resistance heating, and COP was constrained to a minimum of 1. Electricity consumption was computed as:

$$E_t = |Q_t| / COP_t, \quad \text{where} \quad COP_t = \beta_0 + \beta_1(T_{i,t} - T_{o,t})$$

Defrost was simulated as periodic reverse-cycle operation triggered after one hour of continuous frosting conditions ($-15\ °C \le T_{oa} \le 5\ °C$, $RH \ge 60\ \%$). During defrost, the heat pump operated in cooling mode, rejecting heat outdoors and temporarily suspending space heating. Each defrost event was modeled as a fixed 15-minute interruption of normal heating, consistent with manufacturer defrost control logic indicating typical reverse-cycle durations of approximately 5–15 minutes.[110] We adopt the upper bound as a conservative assumption, as time–temperature algorithms cap defrost duration even though sensor-based controls may

terminate earlier. Defrost triggering was determined dynamically from hourly frosting conditions, while event duration was held constant to ensure consistent modeling across units and climates.

3.2.5 Emissions computation

We assume that all space heating is electric and supplied by the ASHP, and—in the baseline scenario—by auxiliary resistance heating. Therefore, CO_2-equivalent emissions were computed directly from electricity use using short-run marginal emission factors from NREL's Cambium dataset. These factors are appropriate for a household-level analysis and enable a consequential analysis[111] of both a departure from the most common mode of heating in most U.S. single-family homes (i.e., natural gas) to electric heating[112], and comparisons between different scenarios. Household emissions were calculated by multiplying 15-minute electricity consumption by the corresponding Cambium emission factor and summing over the January–March period, with city-level results reported as distributions across simulated homes.

3.3 Results

3.3.1 Emissions across scenarios

The use of auxiliary resistance heating to backfill comfort during defrost, rather than the defrost mode itself (i.e., the temporary reversal of the ASHP to cooling mode), drives winter defrost-related emissions. Fig. 2A shows that the ***Base*** scenario produces the highest winter emissions (median 6.07 MT CO_2e per home). In this configuration, the defrost cycle uses only about 5% of electricity, whereas auxiliary resistance accounts for roughly one quarter and therefore dominates the emissions impact of the defrost cycle.

Relative to the ***Base***, all three alternatives substantially reduce winter emissions, but through different mechanisms. ***Anti-frost Coating***, assumed to eliminate defrost operation in our analysis, lowers median emissions from 6.07 to 3.50 MT CO_2e per home (−42.3%). ***Accept Discomfort*** produces the largest emissions reduction, to 3.25 MT CO_2e (−46.4%), but does so by permitting brief indoor temperature drops. The ***+2 °C setpoint bump*** partially offsets these temperature reductions, raising median emissions to 3.92 MT CO_2e (−35.4%).

To illustrate system-wide implications, we scale the median per-home reductions observed across the 25 cities to current and plausible future levels of heat-pump adoption. Under current conditions, RECS 2020 [112] indicates that approximately 3.3 million such homes already use ASHPs, for which applying the median reduction from the Anti-frost Coating scenario (2.57 MT CO_2e per home) implies aggregate winter savings of roughly 8–10 million MT CO_2e. If adoption were to rise to 10–15 million homes—consistent with NREL's Electrification Futures Study[82]—the corresponding reductions would reach 25–40 million MT CO_2e annually under today's grid. As electricity systems decarbonize, absolute emissions from all electric-heating scenarios will decline; the totals reported here therefore represent upper-bound estimates.

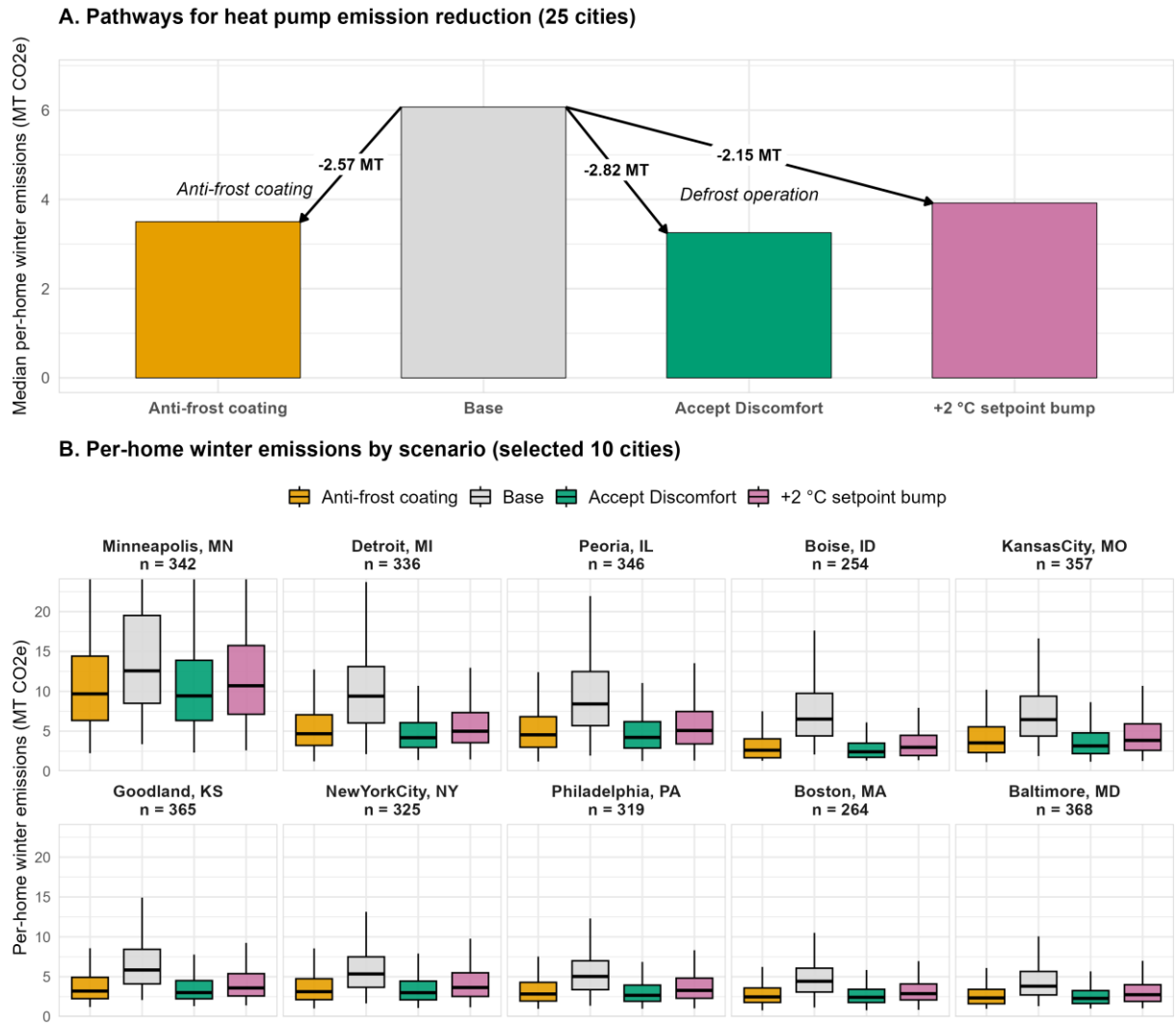


Figure 3.2: Median winter emissions across scenarios.

(A) Median January emissions across 25 frost-prone U.S. cities illustrating two emission-reduction pathways. (B) Emission distributions for 10 representative cities showing regional variation in climate and grid-carbon intensity.

City-level patterns (Fig. 2B) reveal substantial geographic variability. The ten cities shown span a wide range of winter climates, grid emissions intensities, and regional building stocks across the United States. Across these cities, switching from ***Base*** to ***Accept Discomfort*** lowers median winter emissions by 1.53–5.21 MT CO_2e per home (25–63%) by eliminating the need for auxiliary resistance backfill during defrost, at the cost of brief indoor temperature reductions. Detroit, Peoria, and Boise show the largest absolute reductions (4.1–5.2 MT CO_2e per home), while Boston and Baltimore show smaller but still meaningful decreases (1.5–2.0 MT CO_2e per home). Minneapolis experiences a smaller proportional reduction (25%) because many cold hours fall below the frosting threshold, resulting in fewer defrost events and less resistance backfill use in the ***Base*** scenario. ***Anti-frost Coating*** achieves similar emissions reductions by suppressing frost formation and thereby avoiding defrost operation and associated resistance backfill. Removing resistance backfill also narrows cross-city variability: the median interquartile range decreases by 2.40 MT CO_2e when comparing ***Base*** with ***Accept Discomfort*** and by 1.89 MT CO_2e when comparing ***Base*** with ***Anti-frost Coating***.

3.3.2 Indoor temperature impacts

In the ***Base*** scenario, auxiliary resistance backfill maintains the heating setpoint during defrost, whereas the ***Anti-frost Coating*** scenario eliminates defrost entirely. When resistance backfill is removed, defrost operation introduces indoor temperature deviations whose magnitude varies substantially across cities and months (Fig. 3A).

In the ***Accept Discomfort*** scenario, median temperature drops during defrost—averaged across homes—ranged between 1.1 and 3.2 °C below the heating setpoint across the ten cities. The ***+2 °C Setpoint Bump*** scenario partially recovers comfort, bringing eight of the ten cities to within 1 °C of the setpoint, though Boston and Goodland still exhibit median drops of 1.3 °C.

The first percentile (P1) of defrost-period indoor temperature deviations captures the most severe short-duration cooling events, defined by first identifying the coldest 1% of defrost-period indoor temperatures in each home and then averaging these values across homes. Although this corresponds to only ~25–30 winter hours, these events often occur during morning and evening periods of peak heating demand. Under the ***Accept Discomfort*** scenario, P1

deviations ranged from 1.6–4.5 °C below the heating setpoint, corresponding to indoor temperatures of ~16–19 °C), revealing substantially deeper cooling during a small subset of defrost hours than indicated by median values. The ***+2 °C Setpoint Bump*** scenario moderates these extremes, reducing P1 deviations to roughly 0–2.7 °C below the setpoint and keeping P1 indoor temperatures near ~18–21 °C. In most cities, the largest P1 deviations occur in January and diminish toward March, while Minneapolis peaks later, with its largest P1 drops occurring in March due to less frequent defrosting in January and February.

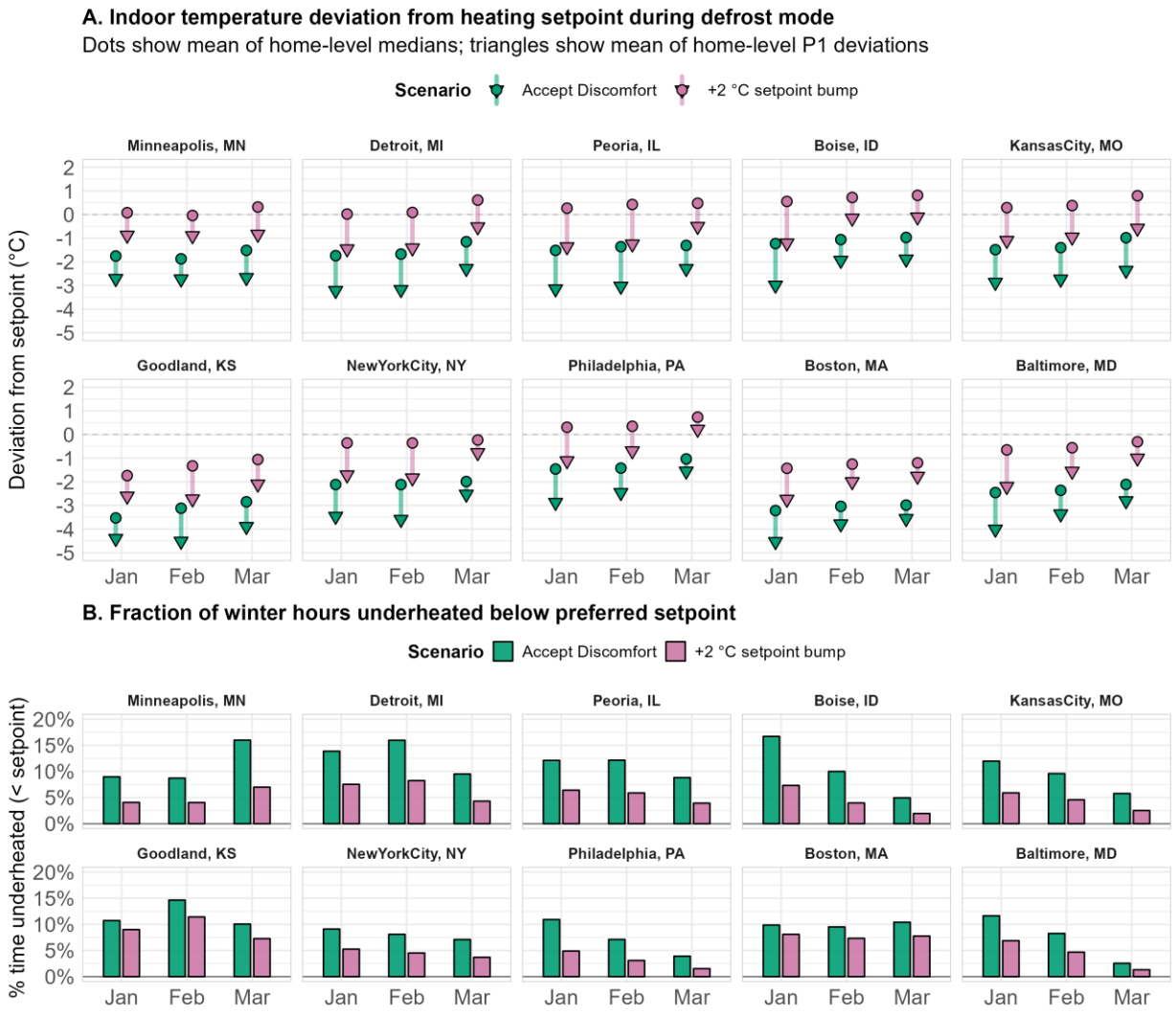


Figure 3.3: Indoor temperature impacts of 'No aux heat' and 'No aux heat + 2°C'.

(A) Deviation from each home's heating setpoint during defrost periods, shown as the mean of home-level median deviations (dots) and the mean of home-level P1 deviations (triangles)
(B) Fraction of winter hours underheated below the preferred setpoint.

In scenarios where auxiliary resistance heating is disabled, the fraction of time spent below the setpoint varies substantially across cities and months (Fig. 3B). In the ***Accept Discomfort*** scenario, under-heating increased by a median +9.7 percentage points (range: +8 to +12 pp). Under the ***+2 °C Setpoint Bump*** scenario, under-heating declines to a median +4.6 pp (range: +1.5 to +8 pp), highlighting its role as a partial comfort-recovery strategy. Most cities showed the highest under-heating in January with declines toward March, although Detroit and Goodland peaked in February, and Minneapolis peaked in March. In cities with limited frosting (Boise, Kansas City, Philadelphia, and Baltimore), March under-heating under the **+2 °C Setpoint Bump** remains below 2.5%.

3.3.3 Timing of defrost-related cooling

When resistance backfill is disabled in the absence of anti-frost coatings, the timing of defrost events becomes critical because associated cooling is no longer actively mitigated. Defrost occurrence reflects the joint variation of ambient temperature and relative humidity, shaped by daytime solar irradiance, producing a pronounced diurnal pattern across cold-climate locations (Fig. 4). City-level mean hourly frost-prone counts during January–March range from 29.7 h (Baltimore) to 64.9 h (Spokane) out of 2,160 total hours. Frost-prone conditions consistently reach a minimum during early afternoon hours (12:00–15:00), while maxima occur during early morning and late evening (03:00–06:00 and 22:00–23:00), overlapping with typical awake and occupied hours.

An exception to the typical diurnal profile of frost-prone conditions is observed in very cold regions, such as Caribou and Minneapolis, where frost-prone conditions are less strongly modulated by time of day and exhibit relatively flat profiles. In these locations, ambient temperatures remain low across much of the day and relative humidity more frequently falls below the frost-prone threshold, limiting the overall frequency of frost-prone hours and dampening distinct morning and evening peaks relative to other cold-climate cities.

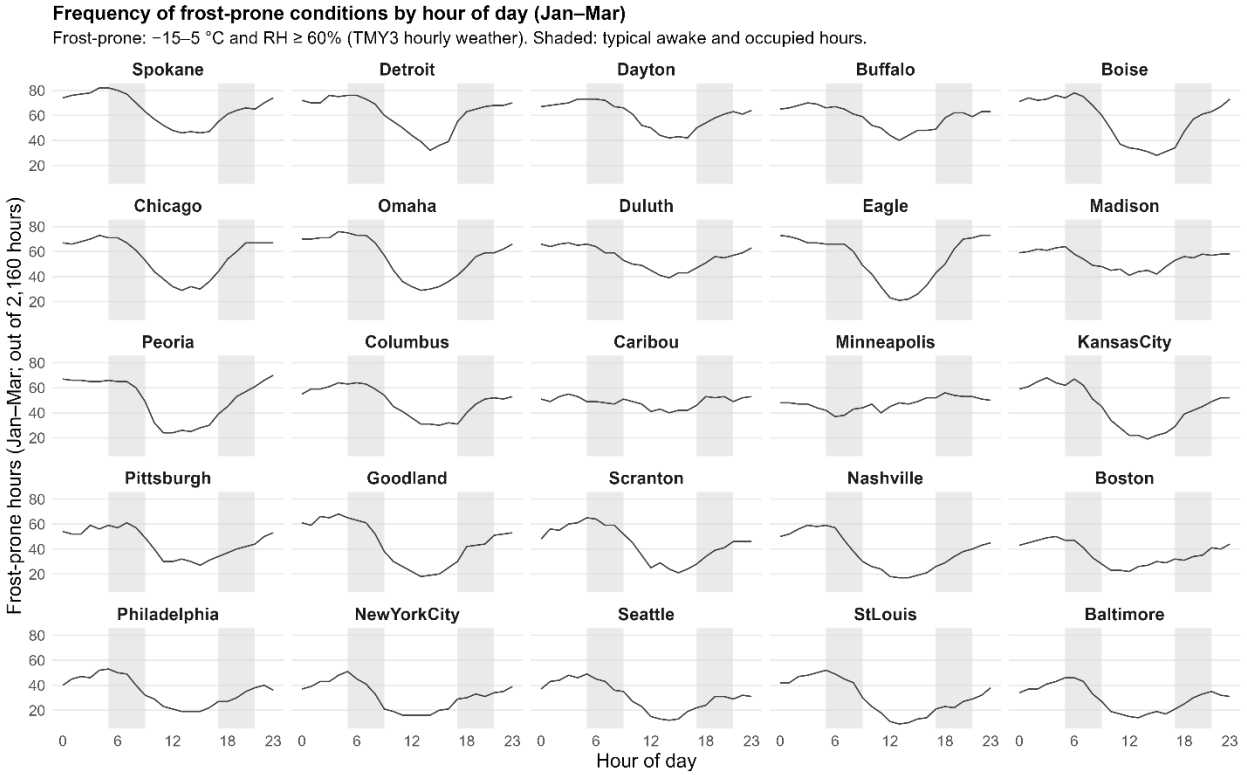


Figure 3.4: Diurnal distribution of frost-prone outdoor conditions.

3.3.4 Energy–comfort trade-offs

Figure 4 summarizes the winter energy–comfort trade-off across the four defrost-management scenarios. The Base scenario is never Pareto-optimal, consistently exhibiting the highest winter energy use. Accept Discomfort minimizes energy use but produces the largest defrost-period temperature drops. The +2 °C Setpoint Bump partially restores comfort, increasing P1 indoor temperatures by ~1.8 °C while still reducing winter energy use by 15–54% relative to the Base. Anti-frost Coating fully restores defrost-period indoor temperatures to those of the Base scenario, increasing P1 indoor temperatures by ~3.0 °C (IQR: 2.7–3.5 °C) relative to Accept Discomfort, while requiring only ~2–12% more winter energy use (median: 6.5%).

The incremental energy required to improve comfort is quantified by the energy–comfort slope between Accept Discomfort and Anti-frost Coating. Across cities, each 1 °C increase in P1 indoor temperature corresponds to approximately 0.5–4% additional winter energy use. Cities

with more frequent or prolonged frosting episodes exhibit steeper slopes (~3–4% per °C), whereas cities with fewer or shorter frosting events require only ~1–2% per °C. Together, these results highlight anti-frost coating as an energetically efficient pathway for eliminating defrost-related discomfort while avoiding the large energy penalties associated with resistance backfill.

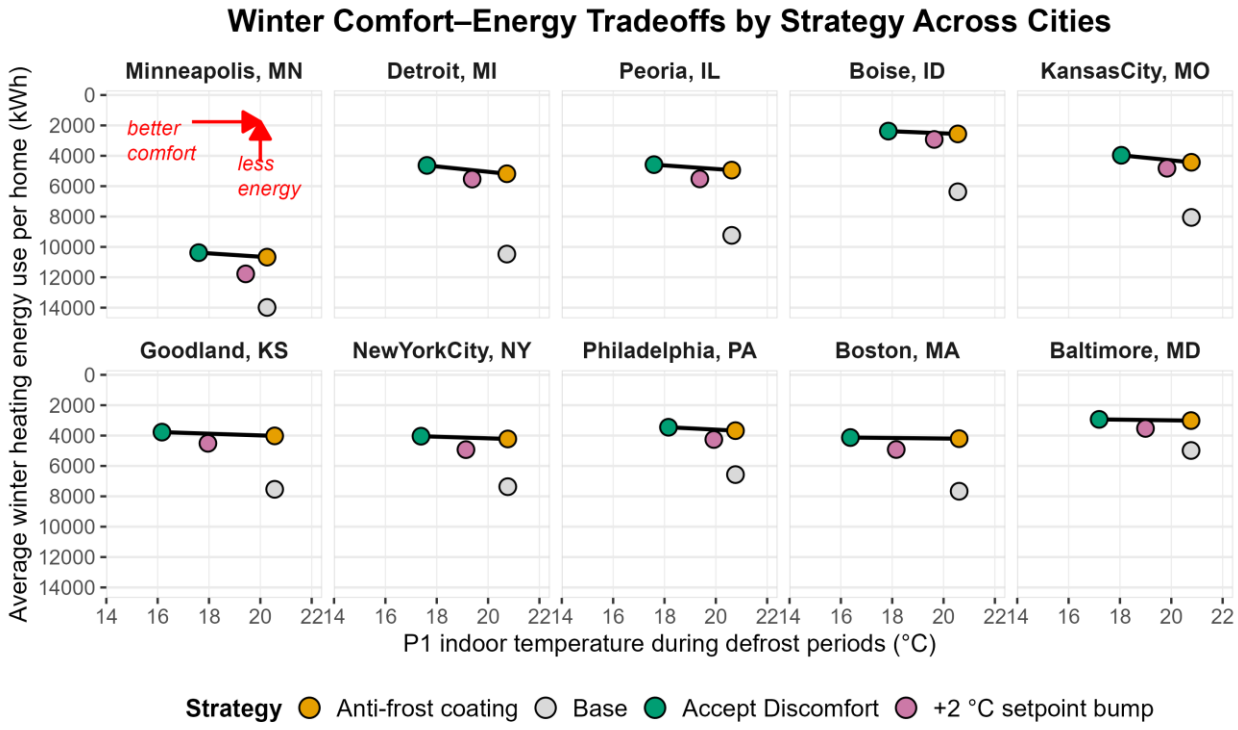


Figure 3.5: Winter comfort–energy tradeoffs across ten U.S. cities.
Points show each strategy's average 1st-percentile indoor temperatures during defrost periods versus average winter heating energy use. Solid lines indicate the Pareto-efficient frontier.

The incremental energy required to improve comfort is quantified by the energy–comfort slope between Accept Discomfort and Anti-frost Coating. Across cities, each 1 °C increase in P1 indoor temperature corresponds to approximately 0.5–4% additional winter energy use. Cities with more frequent or prolonged frosting episodes exhibit steeper slopes (~3–4% per °C), whereas cities with fewer or shorter frosting events require only ~1–2% per °C. Together, these results highlight anti-frost coating as an energetically efficient pathway for eliminating defrost-related discomfort while avoiding the large energy penalties associated with resistance backfill.

3.4 Discussion

Winter heating energy use in cold climates is dominated by auxiliary resistance heating, including resistance backfill during defrost [113]. As a result, defrost-management strategies play a central role in shaping both winter energy use and thermal comfort. Disabling resistance backfill (Accept Discomfort) substantially reduces winter energy consumption but produces the largest indoor temperature drops during defrost events. In contrast, the Anti-frost Coating scenario eliminates frosting altogether, preventing defrost-related cooling and restoring indoor temperatures to Base levels while maintaining low energy use. Because anti-frost coatings are not yet commercially available for air-source heat pumps and Accept Discomfort alone imposes substantial comfort penalties, the +2 °C Setpoint Bump emerges as the most practical near-term strategy: it recovers much of the lost thermal comfort when resistance backfill is disabled while keeping winter energy use far below the Base scenario. At the higher end of the estimated reduction range (25–40 Mt CO_2e), widespread adoption of anti-frost coatings could yield winter emissions reductions comparable to roughly 30% of U.S. commercial aviation emissions in 2022.[114]

These results also highlight important equity considerations. Appendix Figure B.2 illustrates substantial inter-home variability in indoor temperature response during defrost for a representative city, even under identical outdoor conditions and control settings. When auxiliary resistance heating is disabled, some homes experience pronounced short-duration indoor temperature drops during defrost, while others exhibit more moderate responses, reflecting differences in building thermal characteristics. Homes that are more vulnerable to defrost-related cooling would also incur disproportionately higher energy costs if resistance heating were relied on continuously to maintain comfort. Because modest setpoint adjustments require no physical modifications to buildings or equipment, they may be particularly valuable for renters and low-income households who have limited ability to improve building envelopes.

Several limitations in the modeling framework should be considered when interpreting these results. The assumed 15-minute defrost duration does not account for variable termination (i.e., demand defrost controls) in modern ASHPs.[115] The manufacturer-derived performance correlations employed here depend primarily on outdoor temperature and therefore do not

explicitly represent humidity effects or dynamic frost accumulation and shedding. Weather inputs are based on TMY datasets, which smooth interannual variability and may underrepresent the frequency or severity of cold-air outbreaks that strongly influence frosting and defrost behavior.[116] Finally, the Anti-frost Coating scenario is intentionally idealized in that it assumes complete elimination of frosting and defrost events, and is intended to bound potential performance rather than represent a commercially available technology; nonetheless, recent industry efforts are exploring defrost-free heat pump concepts.[117]

Building on these results, defrost management strategies that limit auxiliary heat operation, whether through modest setpoint adjustments or frost suppression approaches such as anti-frost coatings, can meaningfully improve winter comfort while reducing energy demand. By mitigating defrost related comfort penalties and avoiding energy intensive resistance backfill, these approaches strengthen the case for cold climate deployment of ASHPs. Future work should integrate dynamic frost growth and defrost physics with building-scale simulation, explicitly resolve time-of-day effects under realistic occupancy patterns, and evaluate frost-suppression technologies under real-world operating conditions.

Chapter 4 Beyond Efficiency: Sufficiency Unlocks Deep Decarbonization of U.S. Residential Sector

Energy efficiency has dominated U.S. residential energy policy, whereas sufficiency—avoiding energy demand while ensuring wellbeing—has received far less attention. Here, we account for structural sufficiency (i.e., moderating dwelling size and promoting compact, multi-family housing forms) and behavioral sufficiency (i.e., adopting more conservative, health-informed thermostat setpoints), both with and without energy efficiency, using an integrated U.S. housing stock turnover and hourly climate-responsive building energy models. Under business-as-usual housing trends, residential floorspace expands by 55% from 2020 to 2050, increasing final energy demand by 11%. Relative to this 2050 trajectory, efficiency improvements reduce demand by 18%. Structural sufficiency—limiting floorspace growth to 17%—reduces demand by 31%, and when combined with efficiency lowers demand by 45% by mid-century. Adopting Sufficient Comfort setpoints further reduces final energy demand by 31–33% relative to Baseline Comfort across housing stock scenarios. Our findings highlight that both structural and behavioral sufficiency offer considerable untapped potential for deep decarbonization and warrant greater emphasis alongside energy efficiency in shaping residential energy policy centered on climate mitigation and occupant well-being.

4.1 Introduction

The U.S. residential sector accounts for approximately 18% of national energy-related CO_2 emissions[118], with space heating and cooling representing roughly half of household energy use[112]. Addressing residential space-conditioning demand is therefore critical to U.S. decarbonization efforts. Choices about housing infrastructure create long-lived lock-ins[26] by fixing dwelling size and built form (e.g., single-family versus multi-family), constraining the extent to which efficiency measures can reduce energy demand. Mid-20th century policies—most notably the Servicemen's Readjustment Act of 1944[2] (the GI Bill)—accelerated suburban expansion, contributing to a housing stock dominated by single-family homes, which use approximately 30–60% more energy per dwelling than multi-family units[30,112].

Mitigation strategies within the residential sector have largely focused on improving energy efficiency—reducing energy use per unit of service—whereas sufficiency avoids unnecessary energy demand while ensuring wellbeing[11,119,120]. The Intergovernmental Panel on Climate Change (IPCC's) Sixth Assessment report indicates that sufficiency-oriented strategies—particularly those affecting floor area and housing form—can reduce buildings-sector energy demand and associated emissions by roughly 20–45% by mid-century in high-income contexts, including the United States, in some cases approaching the magnitude of reductions achievable through technological efficiency measures[11]. Beyond structural sufficiency, residential energy demand is also shaped by how energy services are used to achieve indoor thermal conditions, underscoring the importance of evaluating sufficiency under alternative comfort assumptions.

Despite this mitigation potential, sufficiency remains inconsistently represented or omitted in quantitative, policy-relevant national decarbonization scenarios, limiting the availability of evidence needed to inform current policy design[121–123]. This underrepresentation reflects, in part, limitations in modeling frameworks commonly used to guide national residential decarbonization policy, which often rely on aggregated or archetype-based representations that limit their ability to capture heterogeneity in housing structure and household practices relevant to sufficiency. Most integrated assessment models (IAMs) capture residential energy use at annual and national scales, aggregating demand and obscuring variation across housing stocks,

households, and subregions[124,125]. These models typically rely on degree-day methods that approximate space-conditioning demand using ambient temperature alone, neglecting important weather factors such as humidity, wind speed, and solar irradiance[6]. Beyond IAMs, much of the building efficiency literature assumes a static building stock, overlooking construction, renovation, and retirement processes that shape long-term residential energy demand[15,17,109]. See Appendix Table A.1 for comparison of key literatures related to U.S. residential decarbonization.

Here, we evaluate how energy efficiency (e.g., electrification via heat pump adoption and building envelope improvements), structural sufficiency, and behavioral sufficiency shape future U.S. residential energy demand and emissions, both individually and in combination. To address limitations of existing modeling approaches, we develop an integrated framework that links a dynamic building stock–turnover model (MESSAGEix-Buildings)[25] with a climate-responsive reduced-form building energy model (RC-BEM)[109]. The integrated framework captures heterogeneity in housing stock evolution—including building types and urban form—while simulating hourly residential thermal demand under future climate trajectories. We conduct simulations for 2020–2050 under Representative Concentration Pathways (RCPs) 4.5 and 8.5, spanning combinations of efficiency and sufficiency pathways, and quantify resulting changes in thermal, site, and primary residential energy demand. We then estimate associated greenhouse gas emissions at the national level under alternative power-sector decarbonization pathways.

This framework enables a comparative assessment of energy efficiency, structural sufficiency, and behavioral sufficiency, revealing how the effectiveness of building-sector policies depends on housing stock evolution and indoor comfort practices, and how incorporating sufficiency alongside efficiency—when resolved across heterogeneous housing stocks and at high temporal resolution—is essential for achieving deep emissions reductions in the U.S. residential sector.

4.2 Policy scenario framework

Our scenario framework distinguishes three demand-side levers: structural sufficiency and energy efficiency in the built environment ("what we build"), and setpoint-based behavioral sufficiency in building operation ("how we use"), as illustrated in Fig. 1. This framing aligns with the IPCC Sixth Assessment Report, which emphasizes infrastructure, technology, and sociocultural practices as key drivers of low-energy demand futures[126,127].

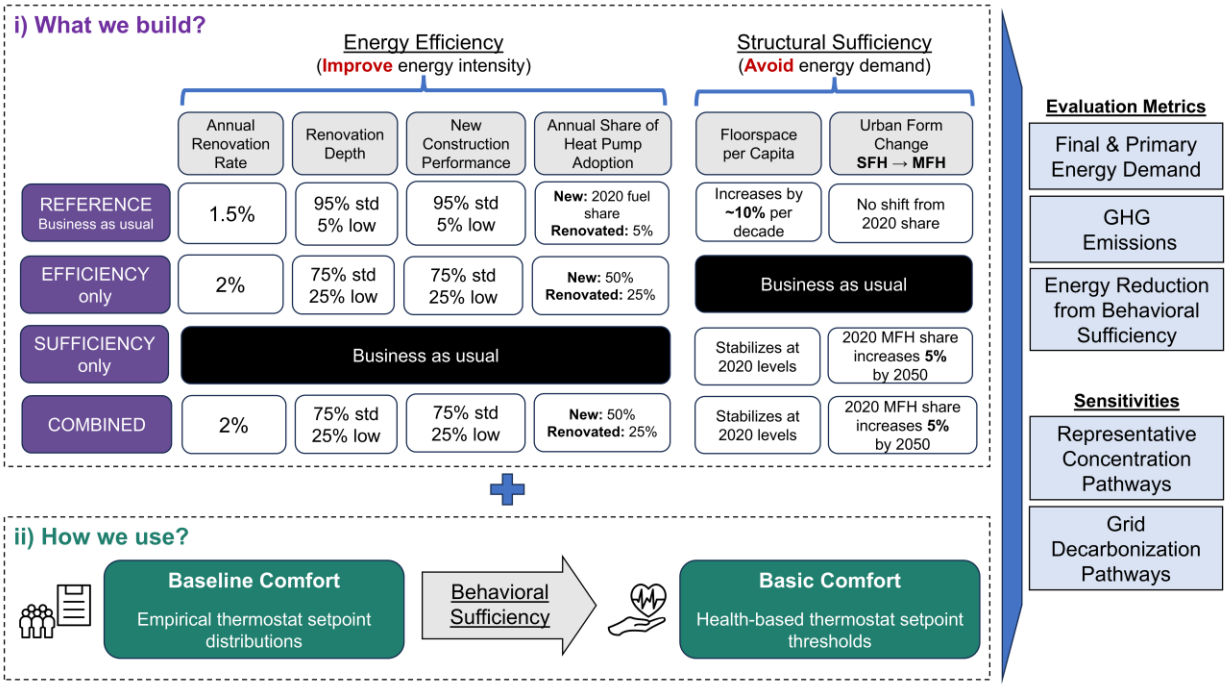


Figure 4.1: Scenario framework for the U.S. residential sector.

Scenarios distinguish between what we build—represented by Reference, Efficiency, Structural Sufficiency, and Combined housing stock pathways—and how we use, represented by thermostat setpoint assumptions spanning Baseline Comfort and Sufficient Comfort. Outcomes are evaluated for residential energy demand and greenhouse gas emissions, with sensitivities to Representative Concentration Pathways (RCPs) and electricity-sector decarbonization pathways.

On the "what we build" dimension, structural sufficiency is represented through changes in per-capita floorspace and housing form, reflected in shifts in the relative shares of single-family and multi-family dwellings. Energy efficiency is represented through assumptions about renovation rates and depth, as well as heating electrification via heat pump adoption.

The **Reference** scenario reflects business-as-usual conditions, characterized by per-capita floorspace growth of 10% per decade in line with recent U.S. housing trends[112], constant housing type shares (Appendix Table A.2-A.4), and recent trajectories for renovation and heat pump adoption. The **Efficiency** scenario accelerates renovation rates (from 1.5% to 2% per year), assumes greater renovation depth represented by larger efficiency gains, and substantially increases heat pump adoption, while holding floorspace growth and housing form constant. The **Sufficiency** scenario stabilizes per-capita floorspace at 2020 levels and modestly shifts the housing stock toward multi-family dwellings, while maintaining Reference efficiency assumptions. The **Combined** scenario integrates the strategies from Efficiency and Sufficiency scenarios. All scenarios use identical state-level population projections from Shared Socioeconomic Pathway 2 (SSP2; "Middle of the Road"; Appendix Table C.1-C.2), ensuring that differences across scenarios reflect only assumptions about housing stock evolution and energy service provision.

On the "how we use" dimension, scenarios represent contrasting heating and cooling practices through different assumptions about thermostat setpoints, which define different levels of space-conditioning energy service. The **Baseline Comfort** scenario samples empirically observed, state-specific distributions of heating and cooling thermostat setpoints, reflecting how U.S. households currently condition their homes[112]. The **Sufficient Comfort** scenario applies health-informed indoor temperature setpoints based on World Health Organization guidance[74,128] and a 2022 California heat protection law[129], representing a lower-bound standard that maintains wellbeing while reducing energy demand.

We evaluate each combination of "what we build" and "how we use" scenarios and assess the sensitivity of outcomes to alternative climate and power-sector pathways. Climate pathways are represented using **RCP4.5**, a moderate-warming trajectory consistent with approximately 2.5–3 °C of global warming by 2100, and **RCP8.5**, a high-emissions trajectory projecting approximately 4–5 °C of warming under limited mitigation[130–132]. Power-sector pathways are represented using three electricity decarbonization cases from the 2024 Cambium dataset[31] produced by NREL (now NLR): a **Mid-case** pathway with central cost assumptions, a **Fossil-leaning** pathway with higher renewable costs and lower natural gas prices, and a **Renewable-leaning** pathway with lower renewable costs and higher natural gas prices.

4.3 Data and Methods

4.3.1 Stock Turnover Model

We use the Stock TURnover Model (STURM), a module of the MESSAGEix-Buildings framework, to project the evolution of the U.S. residential building stock. STURM tracks annual new construction, renovation, and demolition, capturing changes in floorspace, vintage composition, and energy efficiency at regional and national levels. Key parameters—new construction, renovation, and retirement rates—are set exogenously, using parametric variations chosen to span plausible but distinct trajectories (see Fig. 1, What we build? for scenario-specific assumptions).

Household size and urban–rural shares are initialized using the 2020 Residential Energy Consumption Survey (RECS) and assumed constant for all future years. State-level population projections follow the Global Change Analysis Model for the United States (GCAM-USA) under SSP2, which assumes moderate population growth, urbanization, and income with no extreme challenges to mitigation or adaptation. Simulations are conducted at five-year intervals from 2020 through 2050.

4.3.2 Reduced-Complexity Building Energy Model

We use the Reduced-Complexity Building Energy Model (RC-BEM) to estimate hourly heating and cooling demand in U.S. single-family homes under different climates and comfort conditions. RC-BEM is trained on EnergyPlus simulations generated for 54 representative U.S. cities, spanning 16 climate zones across 24 states. To capture building heterogeneity, we use ResStock, a building stock analysis platform developed by the U.S. National Renewable Energy Laboratory (NREL), which synthesizes realistic building prototypes by sampling across distributions of floor area, construction vintage, insulation levels, and HVAC system efficiencies. This procedure yields a sampling pool of ~17,000 unique single-family homes, which forms the basis for scaling results to the national level through integration with STURM building stock projections.

EnergyPlus outputs are converted to heating and cooling demand by accounting for HVAC performance (i.e., Annual Fuel Utilization Efficiency for furnaces and coefficient of performance for heat pumps). RC-BEM is trained using simulations driven by Typical Meteorological Year (TMY3) weather files. For the scenario analyses, however, the model is applied to Thermodynamic Global Warming (TGW)44 climate datasets, which preserve local weather variability while incorporating climate change signals from global models. Indoor temperature states are included as predictors, and multivariate regression with lasso regularization is applied to prevent overfitting. Once trained, RC-BEM produces hourly demand profiles for each prototype across years (2020–2050) and climate scenarios (RCP4.5, RCP8.5). These hourly profiles are subsequently aggregated to annual totals and scaled to the national level using STURM-projected floor areas.

4.3.3 Proxies for Missing Efficiency Classes and Multi-family Homes

RC-BEM represents residential energy performance using nine efficiency classes (s1–s9), which correspond to building construction decades, from pre-1940 stock (s1) through 2010s construction (s9). STURM stock projections include additional classes not directly simulated in RC-BEM (such as new constructions, or renovation-derived classes). To close these gaps, we applied parametric proxy rules derived from RECS median site energy intensity values by construction decade. For example, s1 is represented by s2 adjusted to be 10.4% more energy intensive, and s9 is represented by s8 adjusted to be 7.1% less intensive4. Renovation-derived classes are proxied from their parent vintage, with efficiency improvements of 30% (std) or 60% (low).

Multi-family homes, which are not directly simulated in RC-BEM, are represented using single-family intensity proxies scaled to multi-family floorspace from STURM. When no direct pool was available, we applied donor intensities from the same climate zone, or if still missing, from national averages. This ensures complete coverage of all residential floorspace in STURM.

4.3.4 Model Integration & Validation

To integrate the stock turnover and building energy models, we combine STURM stock projections with RC-BEM intensity estimates in a post-processing framework. For each scenario, STURM provides floor area by region, climate zone, and building vintage, which is matched with RC-BEM heating and cooling intensities (kWh/m²). Total demand is obtained by multiplying intensity by floor area and then aggregating across vintages, zones, and regions.

Where prototype pools were incomplete, we applied a hierarchical fallback procedure: donor intensities were drawn first from the same city, then from the climate zone, and finally from the national average. Monthly demand was distributed using donor shares from the best-available pool. The integrated energy outputs include regional and national totals, per-square-meter intensities, and monthly demand profiles.

Base-year validation compares modeled housing stock and energy demand against observed statistics. Modeled housing units (129.75 million) closely match 2020 U.S. Census housing counts (~126.8 million occupied units). Simulated heating and cooling energy use is calibrated to national residential end-use consumption reported by the U.S. Energy Information Administration (Appendix Table C.5).

4.3.5 Final Energy Demand

We compute site energy demand for heating and cooling by processing the integrated outputs into monthly and annual metrics. Model outputs of "useful" (delivered) energy from RC-BEM are converted to final energy using end-use-specific efficiencies. For heating, we assume 90% efficiency for gas furnaces. For cooling, we apply a year-dependent coefficient of performance (COP), reflecting federal standards and projected improvements (e.g., COP = 3.2 in 2020, rising to 4.4 in 2050).

To ensure consistency with historical statistics, modeled site demand in 2020 is calibrated to the Residential Energy Consumption Survey (RECS 2020). National totals reported in RECS Table CE3.1 are 4,026 trillion Btu (4.25 EJ) for space heating and 866 trillion Btu (0.91 EJ) for space cooling (Appendix Table C.5). Note that we did not include Hawaii and Alaska in out analyses. Calibration factors are computed as the ratio of observed to modeled demand by

Census region and end-use, and applied across all scenario years. This adjustment anchors the model to empirical benchmarks while preserving relative scenario differences.

4.3.6 Primary Energy Demand and Emissions

We translate site energy demand into primary energy by applying region- and year-specific primary energy factors (PEFs) for electricity, derived from NREL's Cambium dataset. For 2020 (historical baseline), we use averages from the 2010s: Northeast 2.63, Midwest 2.92, South 2.62, and West 2.37. For 2050, we use business-as-usual projections: Northeast 2.32, Midwest 2.32, South 2.33, and West 2.17. Non-electric fuels (e.g., natural gas, propane) are assigned a PEF of 1, treating site energy as equal to primary energy.

Each site energy flow is multiplied by its PEF, yielding monthly primary energy demand in exajoules (EJ). Aggregation across fuels and end uses produces regional and national totals. We also compute peak-to-average ratios of monthly demand to characterize temporal demand profiles.

We estimated national CO_2e emissions from the residential sector by combining projected site energy demand with fuel- and grid-specific emission factors. Results are reported as the sum of direct and indirect emissions.

Direct emissions arise from on-site combustion of fossil fuels (e.g., natural gas, fuel oil, propane). State-level residential demand for these fuels was taken from the STURM–ResStock framework under each building stock scenario (REF, MOD, AGG) and comfort behavior (baseline vs. energy-limiting). We applied EPA's emission factors for CO_2, CH_4, and N_2O (converted to CO_2e using 100-year global warming potentials) to compute fuel-specific emissions, which were then aggregated nationally.

Indirect emissions reflect the carbon intensity of electricity supplied to households. For 2020, we used historical average emission rates from EPA's eGRID dataset. For 2025–2050, we applied average emission rates from NREL's Cambium dataset, which provides scenario-specific projections under alternative renewable cost and natural gas price assumptions. Three grid pathways were used: HighRECost_LowNGPrice, MidCase, and LowRECost_HighNGPrice.

Residential electricity demand by state, scenario, and behavior was multiplied by the corresponding Cambium emission rates and aggregated nationally.

4.4 Results

4.4.1 Residential energy demand can be decoupled from floorspace growth

Under the Reference scenario, floorspace expands by 55%, from 27,200 Mm^2 in 2020 to 42,100 Mm^2 in 2050 (Fig. 2A). This expansion is accompanied by an 11% increase in final residential energy demand, from 4.9 EJ to 5.5 EJ by mid-century (Fig. 2B). Nearly all of this increase is driven by space heating, which grows from 4.0 EJ to 4.6 EJ, while cooling demand changes little because efficiency gains offset higher cooling loads from larger dwellings and a warmer climate.

In the Efficiency scenario, floorspace growth mirrors the Reference case; however, final energy demand declines to approximately 4.5 EJ by 2050 (−18% relative to the 2050 Reference value). This reduction is concentrated in space heating: deeper renovations and higher renovation rates reduce useful thermal demand, while heat pump adoption delivers the same heating service with substantially lower final energy requirements than combustion-based systems.

In contrast, the structural sufficiency scenario limits total floorspace growth to 17% by 2050, reducing final energy demand to approximately 3.8 EJ (−31%). This outcome exceeds the reduction achieved through efficiency improvements alone, highlighting the central role of floorspace in shaping residential energy demand. When efficiency improvements are combined with structural sufficiency, final energy demand declines further to approximately 3.0 EJ (−45%) by mid-century, representing the largest absolute reduction across all scenarios.

Across all scenarios, differences between the RCP4.5 and RCP8.5 climate trajectories result in less than a 2% change in total final energy demand in 2050, indicating that mid-century demand outcomes are robust to climate uncertainty (Appendix Figure C.3).

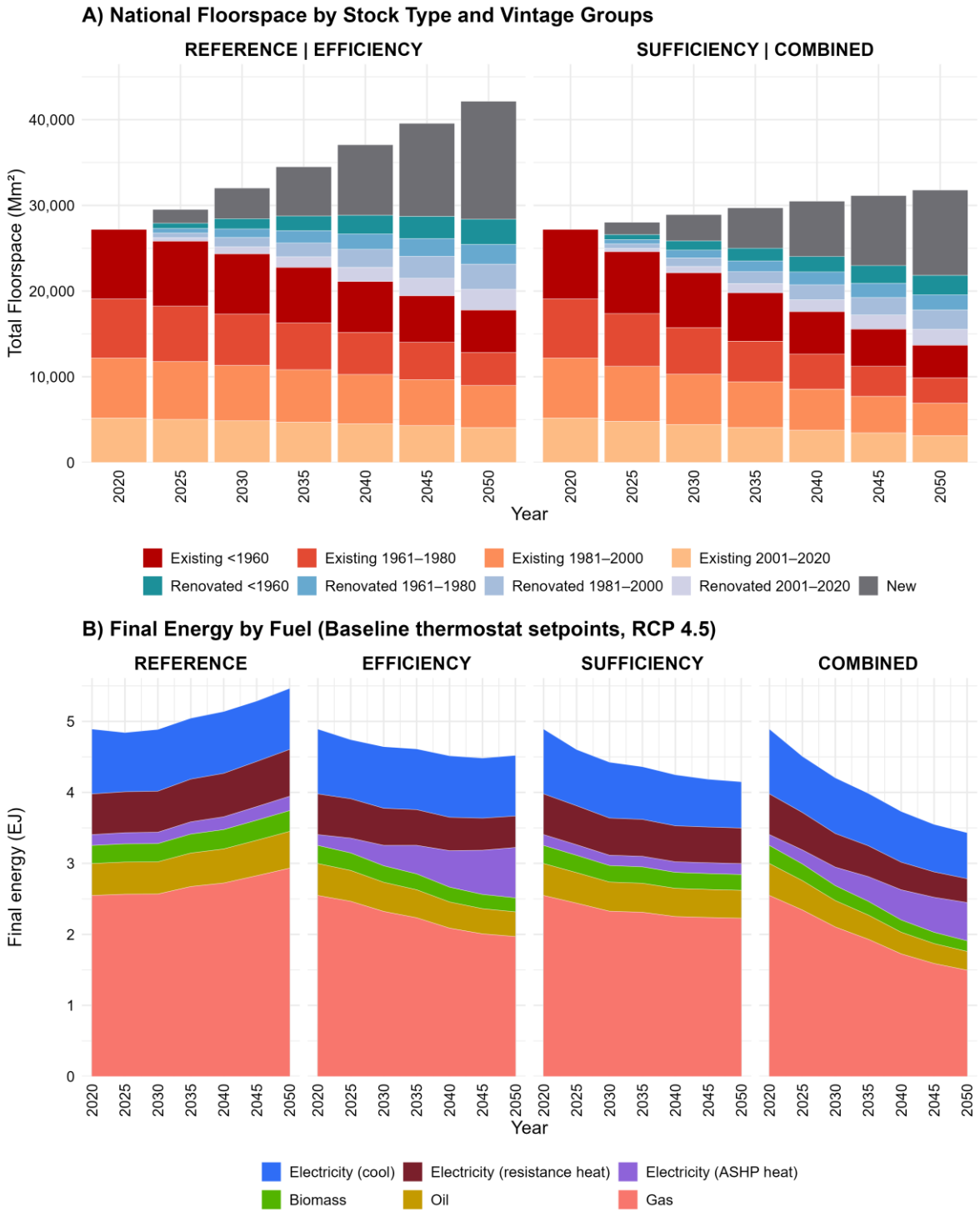


Figure 4.2: U.S. residential floorspace and final energy across housing stock pathways.

(A) National residential floorspace through 2050 by building cohort (existing, renovated, and new construction). (B) Final energy demand by fuel under the same pathways, assuming Baseline Comfort thermostat setpoints and RCP4.5.

4.4.2 Structural sufficiency and efficiency reshape diurnal load profiles

Resolving residential energy demand at hourly resolution reveals how reductions in total energy use are distributed within the day, shaping peak demand and load profiles that are not captured by annual metrics alone (Fig. 3 for illustrative days winter and summer). Such temporal detail is relevant for understanding power-system interactions, including renewable integration and demand-side flexibility, even though these dynamics are not explicitly modeled here.

In January, residential load exhibits a pronounced diurnal structure with morning and evening heating peaks. In the 2050 Reference scenario, peak hourly load is highest in the Midwest, reaching 224 GW, compared with overnight minima of 110 GW. Under the Combined scenario, peak winter load declines by approximately 40% relative to the 2050 Reference case across regions, corresponding to absolute reductions of up to ~88 GW in the Midwest, with little change in diurnal timing.

In July, residential load shifts to afternoon cooling peaks and is much lower in absolute magnitude than in winter, with peak hourly loads reaching ~45 GW in the South and West, compared with winter peaks exceeding 200 GW in cold-climate regions. Under the Combined scenario, peak summer load reductions are more modest at approximately 25%, corresponding to absolute reductions of ~4–11 GW depending on region, with the largest reductions occurring in the South. The timing of afternoon cooling peaks remains unchanged. Together, these results demonstrate a strong seasonal asymmetry, with structural sufficiency and efficiency delivering their largest absolute impacts during winter heating periods—an effect not evident from annual energy metrics alone.

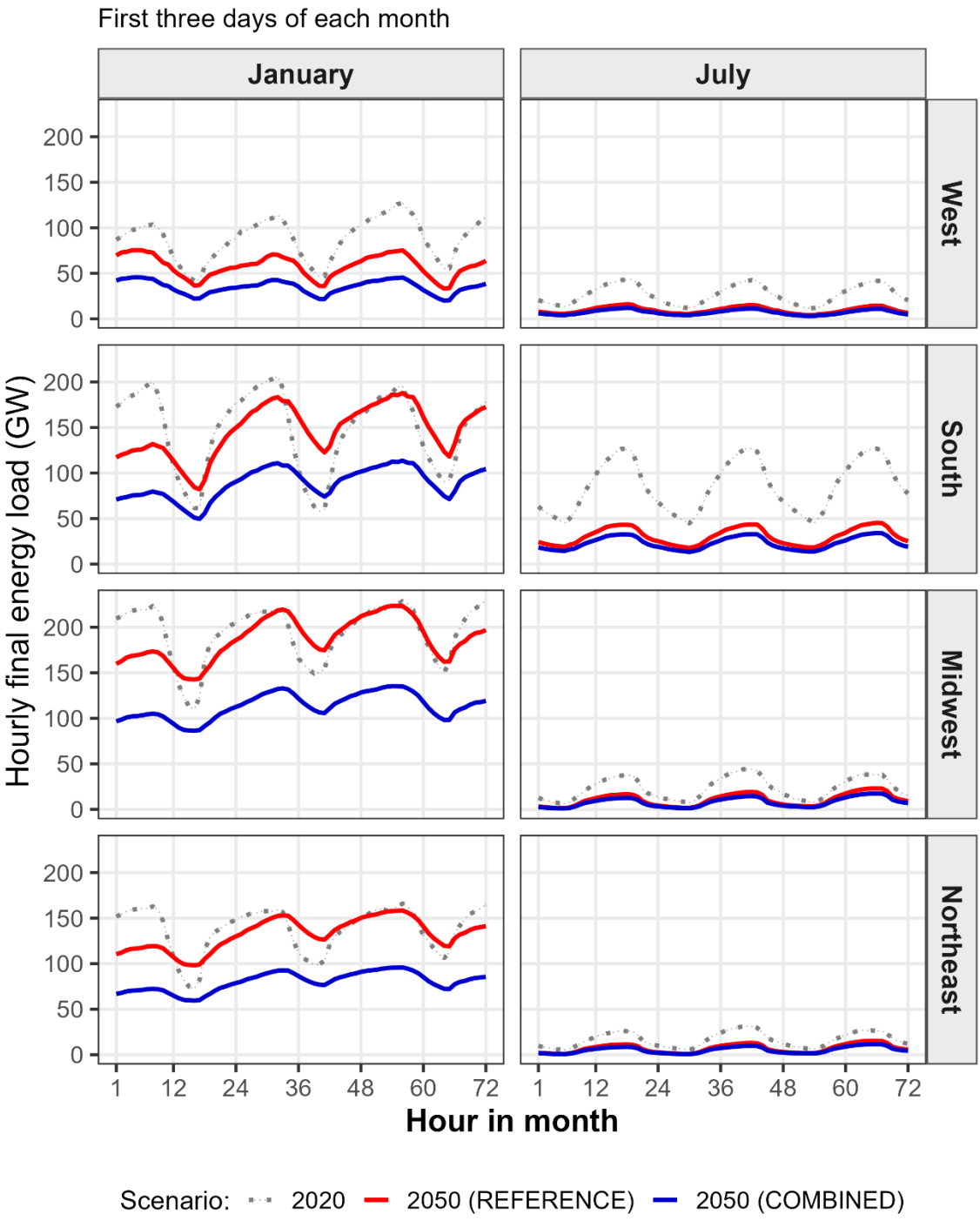


Figure 4.3: Hourly energy load by Census region for the first three days of January and July.

Lines show modeled load in 2020 (dotted grey), 2050 Reference (red), and 2050 Combined efficiency and structural sufficiency (blue) scenarios under Baseline Comfort, assuming RCP4.5.

4.4.3 Behavioral sufficiency yields substantial additional reductions in energy demand

Thermostat setpoints directly determine the level of space-heating and cooling services delivered and therefore represent a key behavioral driver of residential energy demand. According to 2020 Residential Energy Consumption Survey (RECS) data, prevailing thermostat practices in the U.S. result in energy use well beyond levels required to meet health-based comfort guidance. The national median setpoints are 21.1°C and 22.2°C for heating and cooling, respectively (Fig. 4A); fewer than 10% of homes use heating setpoints below 18 °C or cooling setpoints above 26 °C. These distributions define the Baseline Comfort assumption in our model.

By 2050, adopting Sufficient Comfort, assuming household heating and cooling setpoints aligned with health-based temperature thresholds, reduces final residential energy demand by 31–33% (1.6–1.8 EJ) relative to Baseline Comfort across housing stock scenarios (Fig. 4B). The magnitude of this reduction is comparable to that achieved through structural sufficiency alone under Baseline Comfort.

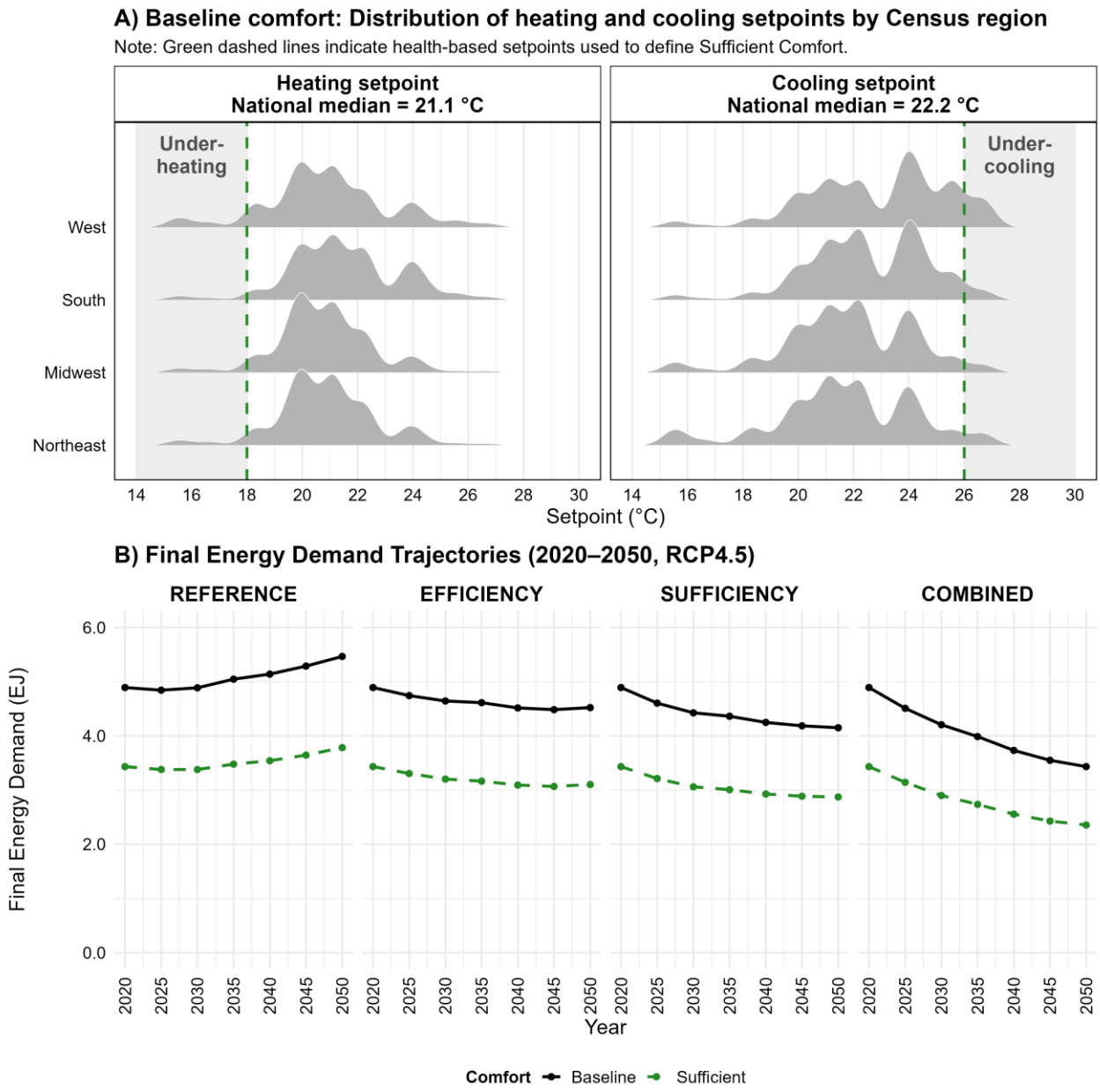


Figure 4.4: Impact of thermostat setpoints on U.S. residential final energy demand.

(A) Distribution of heating and cooling thermostat setpoints by U.S. Census region under Baseline Comfort; dashed lines indicate health-based thermostat setpoints used to define Sufficient Comfort. (B) National final energy demand trajectories from 2020 to 2050 under Baseline Comfort and Sufficient Comfort across housing stock pathways, assuming RCP4.5.

4.4.4 Housing improvements narrow geographic variation in sufficient-comfort savings

We disaggregate state-level energy savings from adopting Sufficient Comfort setpoints to assess geographic variation and distributional impacts (Fig. 5). Across all U.S. states, adopting Sufficient Comfort reduces final energy demand, with absolute savings dominated by population size. Under the Reference scenario, the median state reduces energy use by 33 PJ/year (IQR: 16–66), with the largest contributions from highly populous states such as California and Texas (Fig. 5A). In the Combined scenario, absolute savings fall to a median of 21 PJ/year (IQR: 11–44) due to lower baseline demand, while the interquartile range narrows relative to the Reference case.

Expressed on a per-capita basis, energy savings from Sufficient Comfort are largest in colder regions of the United States, particularly across the Midwest and northern states (Fig. 5B). Under the Reference scenario, per-person savings reach up to 6.1 GJ/person-yr, with a national median of 4.6 GJ/person-yr (IQR: 4.0–5.2). These patterns reflect the dominance of space-heating demand in colder climates, where heating loads are both larger and more energy-intensive than cooling, making energy use more responsive to heating setpoints. In the Combined scenario, both the magnitude and the spread of per-capita savings are reduced, lowering the national median to 2.9 GJ/person-yr (2.7–3.2) and substantially narrowing geographic variation across states.

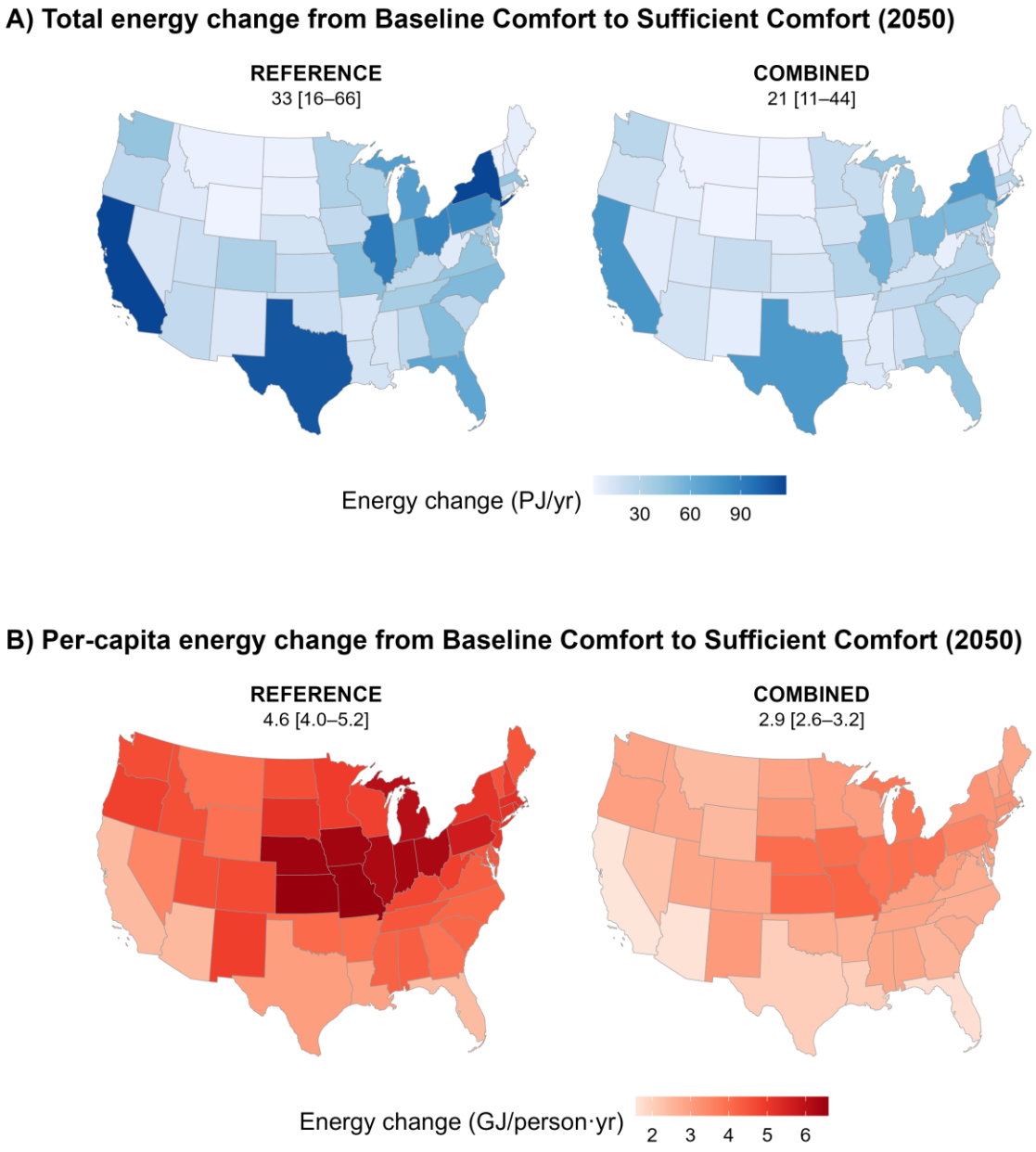


Figure 4.5: State-level final energy savings from Baseline to Sufficient Comfort in 2050.

(A) Absolute annual residential final energy savings by state under the Reference and Combined housing stock pathways.
(B) Corresponding per-capita energy savings. Color indicates savings magnitude relative to Baseline comfort; national values above each map indicate the median [IQR] across states.

4.4.5 Deep residential decarbonization hinges on housing and grid transformations

National primary energy demand in 2050 exhibits strong seasonal variation, with January representing the maximum month across all housing stock scenarios (Fig. 6A). Structural sufficiency and efficiency reduce demand across all months, with the largest absolute reductions occurring in winter. Under Baseline Comfort, structural sufficiency lowers the January peak by 24% relative to the Reference case, while combining efficiency and structural sufficiency reduces the peak by 32% (from 1,281 to 878 PJ). Adopting Sufficient Comfort further reduces the January peak by 24% in both the Reference and Combined scenarios (to 974 and 667 PJ, respectively).

These reductions in primary energy demand correspond to substantial declines in residential GHG emissions across housing stock and grid scenarios (Fig. 6B). Emissions fall rapidly through 2030 as space-heating electrification expands and the electricity sector decarbonizes, declining from 328 $MtCO_2e$ in 2020 to 250 $MtCO_2e$ (−24%) in the Reference scenario and 211 $MtCO_2e$ (−36%) in the Combined scenario under Baseline Comfort.

After 2030, emissions trajectories increasingly reflect electricity-sector assumptions. By 2050, emissions range from 203–231 $MtCO_2e$ in the Reference scenario to 108–133 $MtCO_2e$ in the Combined scenario, depending on grid pathway. Fossil-leaning grids yield persistently higher emissions, while renewable-leaning pathways produce lower outcomes, introducing a 22–33 $MtCO_2e$ (10–25%) spread within each housing stock scenario. Shifting from Baseline to Sufficient Comfort further reduces 2050 emissions by 23–33%, but does not eliminate dependence on electricity-sector decarbonization.

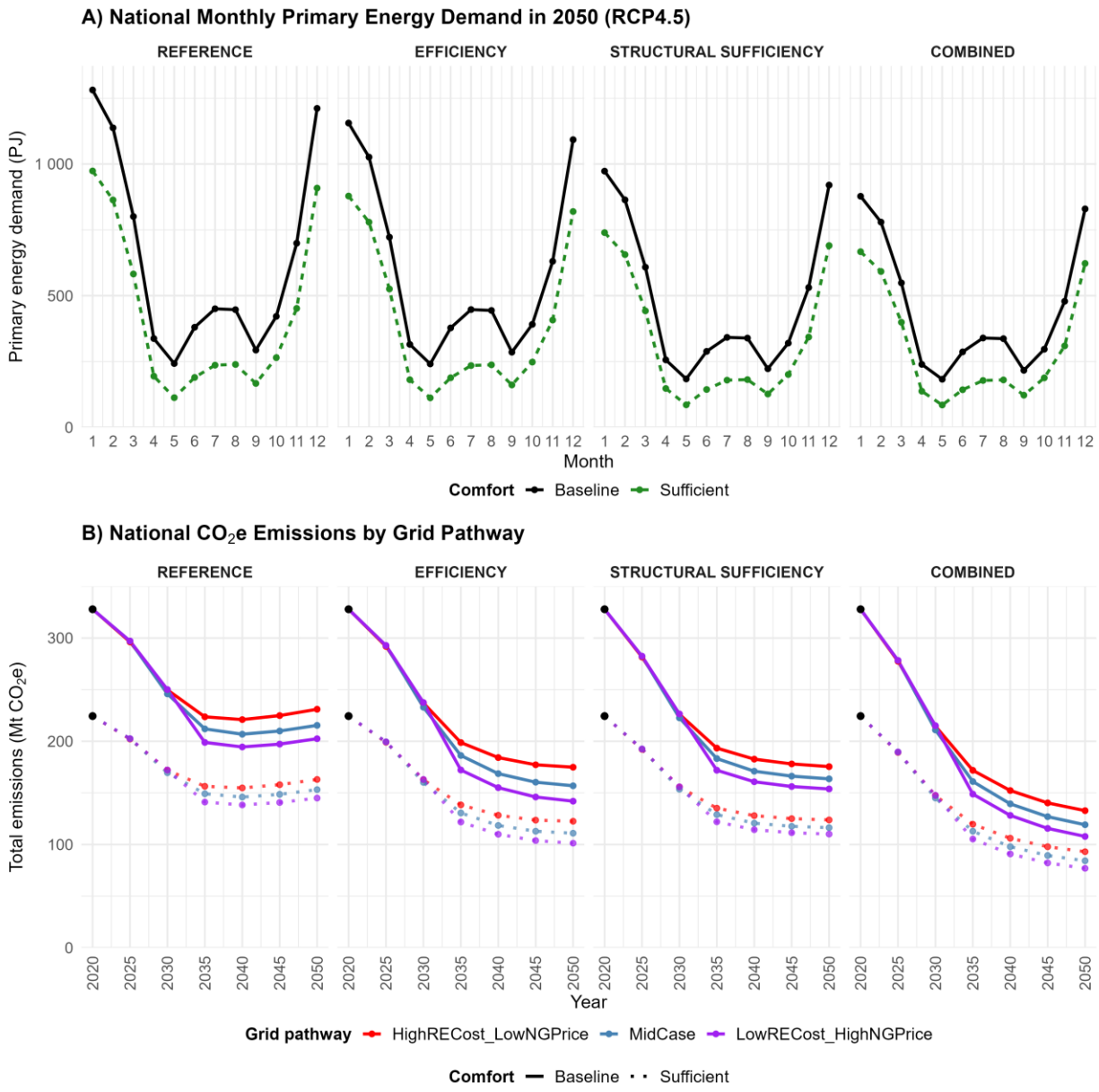


Figure 4.6: National primary energy demand and emissions

(A) Monthly national primary energy demand in 2050 under Baseline and Sufficient Comfort across housing stock pathways, assuming RCP4.5. (B) Annual residential CO_2e emissions (Scope 1 + 2) under alternative housing stock pathways (facets) and electricity-sector decarbonization pathways (colors), comparing Baseline and Sufficient Comfort thermostat setpoints (line types), assuming RCP4.5.

4.5 Discussion

This study presents an integrated U.S. assessment of residential decarbonization pathways, jointly examining structural sufficiency and energy efficiency in the built environment ("what we build") alongside behavioral sufficiency in household operation ("how we use"). By linking a state-level housing stock turnover model with a climate-responsive building energy model, we capture geographic and climatic variation that national assessments often obscure, and can evaluate the potential impacts of sufficiency-based interventions. Here, sufficiency pathways are used as illustrative policy bounds for potential demand reduction, rather than forecasts.

The analysis underscores the long-term consequences of today's housing decisions for avoiding infrastructural lock-in. Our Reference scenario mirrors historic patterns: since the 1970s, average single-family home size has grown by over 20% while household size has declined, resulting in roughly a 40% increase in floorspace per person[112,133]. If these patterns persist, the resulting structural lock-in will offset efficiency gains.

Translating these modeled pathways into practice depends heavily on local context and governance structures. In some states, building codes are set at the state level, which can limit municipal ambition, as in Michigan where local governments are barred from exceeding state standards[134]. Elsewhere, cities have greater autonomy but face zoning restrictions that constrain denser urban form[135,136]. Financial incentives such as the Inflation Reduction Act's rebates for retrofits and electrification (now abrogated) can help overcome these barriers, though recent political efforts to weaken or reverse them threaten long-term decarbonization efforts[18,137]. Because housing form and dwelling size are shaped primarily by long-term planning and regulatory decisions rather than individual consumer choice, advancing structural sufficiency requires reform through zoning, building codes, and coordinated housing supply regulation. Effective policy will depend on multi-level governance, durable financial support, and local planning tailored to regional needs.

Ambitious housing transformation is essential for aligning U.S. climate goals with equitable access to thermal comfort and resilience. Upgrading building infrastructure can reduce energy demand and flatten seasonal energy peaks, easing strain on the grid. Population growth and climate intensity further shape regional disparities in energy use and thermal vulnerability.

As these challenges evolve, policymakers must prioritize designs and practices that ensure safe, efficient, and comfortable housing for all—moving beyond square footage to measure success by equity and well-being. Integrating sufficiency-oriented practices into codes, incentives, and planning frameworks is key for achieving deep decarbonization with fairness and adaptability across communities.

4.6 Limitations of the study

Our analysis has four main limitations. First, our model parameters for new construction, renovation, and retirement are specified exogenously. This prevents life-cycle processes at the household level—such as decisions to renovate versus rebuild or the timing of retirements—from emerging endogenously, and limits insight into how affordability or market dynamics shape stock turnover. Second, we restrict attention to space heating and cooling. While these loads dominate climate-sensitive demand, omitting other end uses understates the residential sector's total footprint and constrains comparability with whole-sector assessments. Third, household income distributions and affordability constraints are not represented, precluding explicit analysis of equity, energy insecurity, or heterogeneous adoption pathways. Fourth, occupant behavior is represented through fixed thermostat setpoint regimes rather than dynamic responses to energy prices, technologies, or extreme events, meaning behavioral conclusions should be interpreted as bounding cases rather than forecasts.

Future work should address these gaps by embedding endogenous household and market decision-making into our modelling framework, extending coverage to non-HVAC end uses, and integrating socioeconomic heterogeneity. Coupling behavioral models of adaptive comfort management with physical energy demand would further capture real-world feedbacks. Together, these steps would enable a more comprehensive, policy-relevant assessment of how residential transformation interacts with equity, affordability, and resilience in the U.S. energy transition.

Chapter 5 Synthesis and Outlook

Residential decarbonization is not constrained by thermodynamics alone. It is shaped by behavioral norms, institutional design, workforce capacity, and long-lived capital investments. The preceding chapters show that while electrification can reduce emissions, outcomes depend critically on comfort valuation, system operation, housing stock characteristics, and governance structures. Technical feasibility defines what is possible; realization depends on how households, markets, and institutions respond. This chapter synthesizes these insights, identifies key limitations of the analysis, and outlines the conditions required for durable U.S. residential decarbonization.

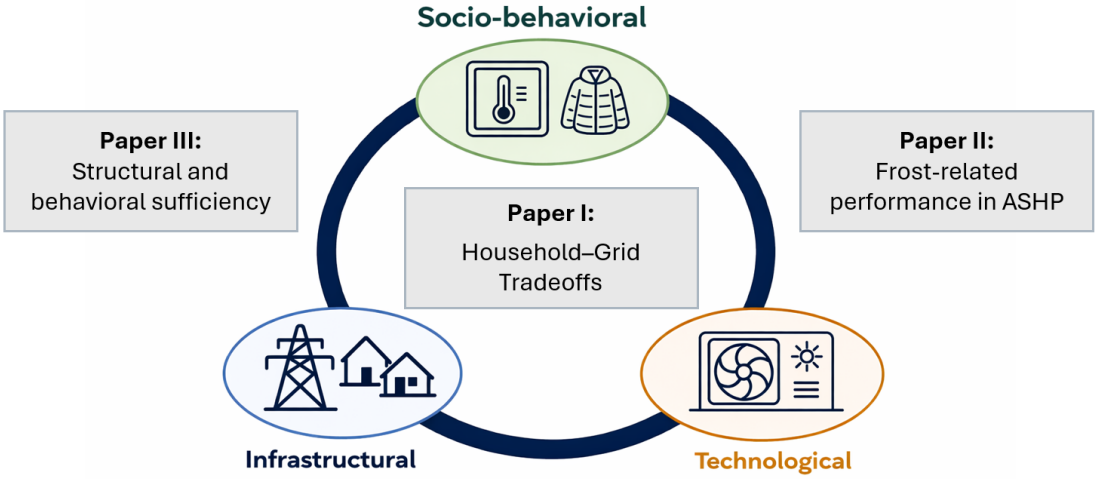


Figure 5.1: Integrative framework of dissertation contributions

Figure 5.1 synthesizes the core contributions of this dissertation. The three papers collectively examine residential decarbonization across socio-behavioral, technological, and infrastructural dimensions. Paper I provides the central analytical framework linking household decision-making to grid-level outcomes. Paper II isolates technological constraints by quantifying performance limitations of air-source heat pumps under frost conditions. Paper III extends the analysis to sufficiency, highlighting how structural and behavioral changes jointly shape energy demand and comfort. Taken together, these components demonstrate that

residential decarbonization is not a single-technology problem, but a system-level challenge requiring coordinated changes across households, buildings, and energy infrastructure.

5.1 Contributions of This Dissertation

This dissertation advances the study of residential decarbonization by developing an integrated framework that links household behavior, building technologies, and energy infrastructure to jointly evaluate energy, comfort, costs, and emissions.

It develops a novel modeling framework that treats thermal comfort as an endogenous component of household decision-making and explicitly monetizes discomfort, enabling direct comparison between energy costs and welfare impacts. Rather than assuming that households consume as much energy as needed to maintain comfort, the framework captures energy-limiting behaviors, allowing comfort to vary in response to costs, preferences, and constraints. In doing so, it shifts building energy modeling from engineering-optimal operation toward behaviorally and economically constrained outcomes, providing a more realistic and human-centered basis for evaluating policies where comfort, health, and equity considerations are central.

At the broader system level, the dissertation improves the representation of residential energy demand in the United States by explicitly capturing heterogeneity across time, geography, and the housing stock. Using the NREL ResStock database to simulate diverse buildings across urban, suburban, and rural contexts, the analysis moves beyond representative-agent approaches and reveals how variation in building characteristics and household behavior shapes the distribution of energy use and comfort outcomes. The framework operates at high temporal resolution, enabling analysis of short-duration peaks and operational dynamics that are increasingly important in electrified systems, and accounts for the evolution of the building stock over time. These features enable system-level insights that cannot be obtained from aggregate or representative models.

At the component level, the dissertation quantifies how performance constraints in air-source heat pumps, a central technology for residential electrification, shape both energy use and indoor comfort. By explicitly modeling frost formation and defrost operation, the analysis demonstrates how cold-climate performance limitations affect energy–comfort trade-offs and

reveals that standard energy-focused assessments can underestimate the full costs and distributional impacts of electrification. This work shows how device-level physical processes, and their mitigation through technological innovation, propagate to system-level emissions and welfare outcomes.

Finally, the dissertation operationalizes the concept of energy sufficiency within a unified modeling framework by quantifying both structural and behavioral pathways. Sufficiency is identified by the IPCC as a key mitigation strategy, yet it remains underrepresented in most U.S. national-scale energy assessments. This work addresses that gap by demonstrating how changes in housing form and floor area, together with thermostat practices, jointly determine energy demand and comfort outcomes. By integrating sufficiency alongside efficiency and electrification, the analysis shows that avoiding unnecessary energy demand can substantially reduce emissions while maintaining well-being.

This portfolio of research establishes that residential decarbonization is not a single-technology challenge but a multi-scale systems problem. At the component level, improvements in device performance shape efficiency and emissions. At the household level, behavioral and digital interventions influence how energy is used. At the building stock level, structural and policy changes determine long-term demand trajectories. Achieving durable decarbonization therefore requires aligned changes across technologies, behaviors, and institutions.

5.2 What Simulation-Based Analysis Reveals and What It Does Not Capture

Simulation-based analysis is effective in identifying structural relationships that are difficult to observe directly and in evaluating counterfactual technologies and operational strategies by varying specific parameters while holding others fixed. This is especially important in the context of a changing climate, where future temperature regimes, extreme events, and weather-dependent technology performance cannot be observed in advance. In this dissertation, the modeling frameworks represent stylized interactions among building physics, heat pump performance, climate conditions, and simplified representations of household behavior. Allowing indoor temperature to vary within thermodynamic constraints clarifies how thermal comfort, energy demand, peak loads, and emissions interact, and makes explicit how modeled outcomes depend jointly on physical limits and behavioral parameters.

However, modeled flexibility does not automatically translate into real-world behavior. Empirical studies of thermostat use demonstrate substantial heterogeneity across households in both heating and cooling seasons. High-resolution data from residential smart thermostats reveal distinct management strategies ranging from stable "set-and-forget" patterns to frequent manual adjustments, with considerable variation even within each category. Observed temperature settings are patterned by demographic characteristics, housing tenure, and technology access. Residential temperature management is therefore embedded in routines, norms, and unequal control over thermal infrastructure—not determined solely by marginal energy costs. Modeling frameworks that approximate household decisions through least-cost logic illuminate structural trade-offs between comfort and energy use, but they abstract from behavioral frictions and non-monetary preferences that shape everyday practice.

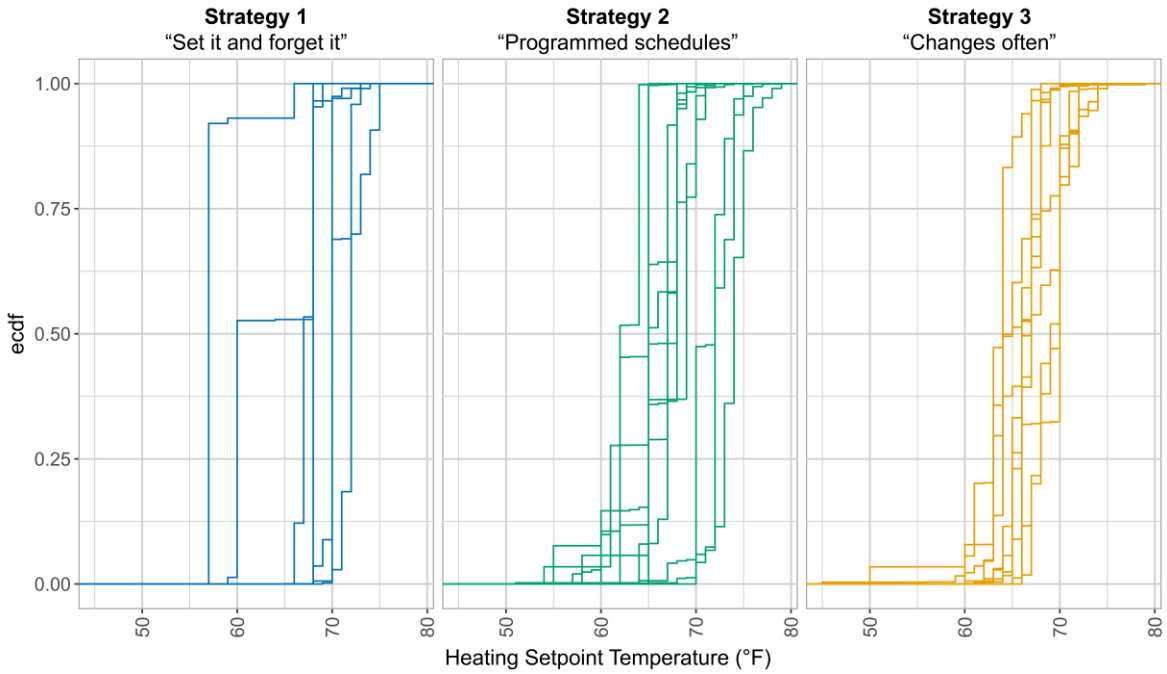


Figure 5.2: Heating setpoint distributions by thermostat management strategy (Claire et al.).

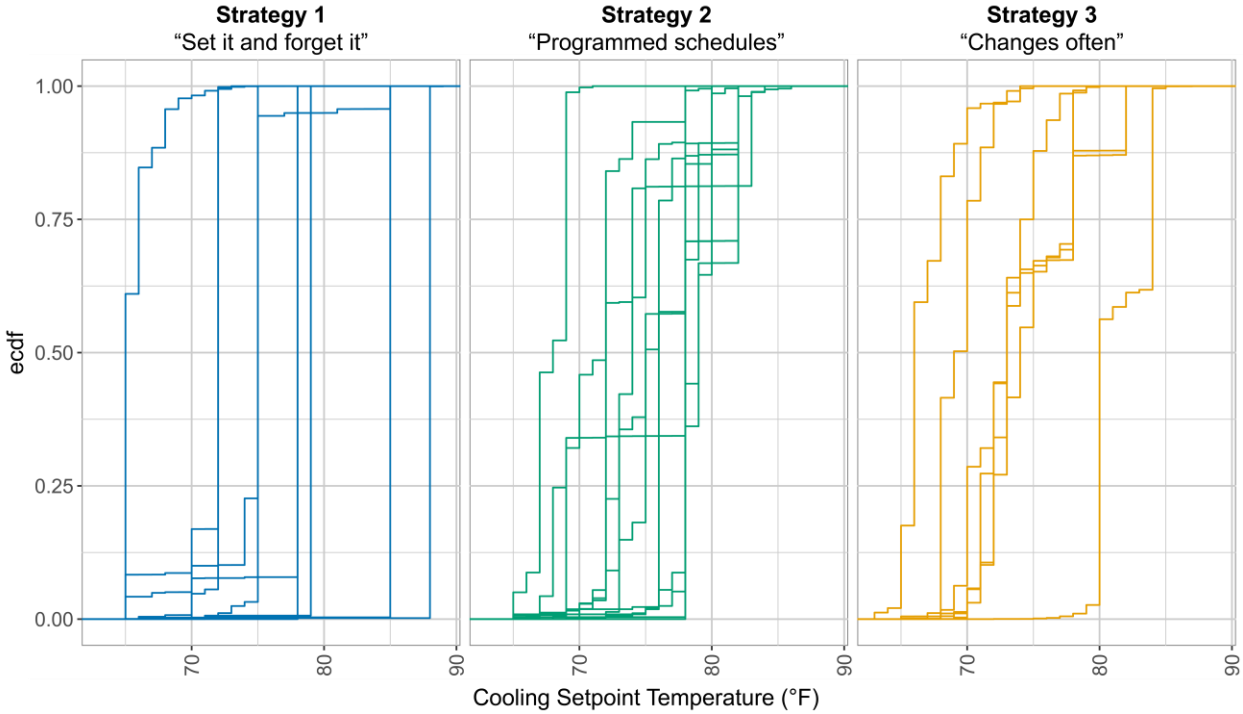


Figure 5.3: Cooling setpoint distributions by thermostat management strategy (Claire et al.).

Behavioral economics further suggests that households may weigh perceived comfort losses more heavily than equivalent energy savings, reinforcing the stickiness of established setpoints. Efficiency improvements or lower operating costs may also induce rebound effects, offsetting a portion of anticipated emissions reductions. Operational flexibility is similarly contingent. Evidence from demand response programs shows that participant overrides can substantially reduce energy savings and diminish reliability contributions during prolonged events. Device-level capability does not guarantee sustained system-level performance. Modeled flexibility should therefore be interpreted as potential responsiveness under defined assumptions rather than guaranteed outcomes.

These observations do not diminish the value of simulation-based analysis. Rather, they clarify its scope. Engineering-economic models reveal structural margins and technical possibilities. The realization of those possibilities depends on behavioral, institutional, and operational dynamics beyond the model boundary. Simulation defines what is feasible under specified assumptions; it does not determine how households or systems will behave in practice.

5.3 From Technical Feasibility to Real-World Implementation

Demonstrating that a decarbonization pathway is technically feasible does not ensure that it can be implemented. Residential energy transitions unfold within legal, political, and administrative institutions that structure which technologies may be deployed, who bears upfront costs, and how standards are enforced.

Building code governance illustrates this dynamic. Statutory frameworks that centralize authority at the state level can limit local experimentation with higher-performance standards, even when technical analysis supports them. Legal preemption defines the permissible space of action. Technical feasibility cannot override institutional design.

Implementation constraints are also distributive. Electrification and efficiency measures frequently increase upfront construction costs while reducing operating expenses over time. Builders, homeowners, renters, utilities, and regulators face different time horizons and risk exposures. Political feasibility depends not only on lifecycle cost-effectiveness but on the

distribution of costs and benefits across actors. Residential decarbonization debates are therefore as much about allocation and risk as about engineering.

Administrative capacity and workforce readiness further condition outcomes. Building codes are not self-executing; they depend on inspection systems, enforcement infrastructure, and professional training. Electrification requires contractors capable of proper sizing, installation, and commissioning of advanced systems. Improper installation can increase auxiliary resistance use, reduce efficiency, elevate peak demand, and undermine modeled emissions reductions. Workforce development and contractor upskilling are therefore central to durable decarbonization. Technical feasibility does not guarantee implementation quality.

Institutional innovation—such as voluntary stretch codes, phased standards, and pilot programs—may help reconcile technical possibility with political constraint. Durable transformation requires governance structures capable of sustaining change across diverse climates, housing markets, and income groups. Technical systems create opportunity; institutions determine whether that opportunity is realized.

5.4 Recommendations for Future Research

This dissertation demonstrates that deep residential decarbonization is simultaneously a technical, behavioral, institutional, and infrastructural challenge. Future research must extend beyond isolated technical optimization and engage more deeply with social science perspectives on behavior, governance, and political economy, while also expanding analytical scope to encompass cross-sectoral and material systems.

First, stronger empirical foundations are needed to understand how households manage thermal comfort and respond to electrification. Large-scale, privacy-preserving analyses of high-resolution thermostat data could refine estimates of temperature elasticity, rebound effects, and comfort adaptation. Living laboratory environments—district-scale developments integrating electrified heating, renewable generation, and coordinated governance—offer opportunities to observe behavioral and institutional dynamics in real time. Such environments can bridge the gap between stylized modeling and lived experience.

Second, institutional and workforce capacity merit deeper investigation. Comparative analysis of building code governance, financing mechanisms, and training systems could clarify how legal and labor market structures shape implementation quality. Integrating public policy, labor economics, and energy modeling would strengthen understanding of how technical feasibility becomes sustained practice.

Third, cross-sectoral integration is increasingly critical. As residential heating electrifies, building demand becomes more tightly coupled to grid decarbonization, storage deployment, and transportation electrification. Integrated modeling frameworks that combine building thermodynamics, power system reliability, and climate stress testing are necessary to assess resilience under compound extreme events.

Finally, future research should expand beyond operational energy to address embodied carbon and material systems. As electricity grids decarbonize, lifecycle emissions from building materials will represent a growing share of total impact. Integrating embodied carbon, bio-based construction, and circular economy principles into residential decarbonization analysis would provide a more comprehensive climate assessment.

Advancing this agenda will require interdisciplinary collaboration across engineering, economics, public policy, and the social sciences. Durable residential decarbonization depends not only on better technologies, but on improved understanding of human behavior, institutional design, workforce capacity, and material transformation.

.

5.5 Outlook for U.S. Residential Decarbonization

The U.S. residential sector sits at the intersection of climate mitigation, human comfort, and social equity. Homes account for a significant share of direct fossil fuel use and are increasingly intertwined with the electricity system as electrification expands. Climate change is intensifying both heating and cooling demands, raising the stakes of thermal resilience. The long-lived nature of housing capital stock creates both opportunity and risk: investments made in the coming decade may shape emissions trajectories for generations.

Electrification provides a viable pathway to substantial emissions reductions, particularly as the electricity grid continues to decarbonize. Yet electrification reshapes trade-offs rather than eliminating them. Comfort valuation, defrost management, auxiliary resistance use, and peak demand interactions influence realized emissions outcomes. Structural characteristics of the housing stock—vintage, envelope quality, and turnover rates—shape both cost and feasibility. Behavioral norms, rebound effects, and override behavior condition realized flexibility. Institutional design and workforce capacity determine implementation quality.

Equity considerations are central. Older and less efficient housing is disproportionately occupied by lower-income households, who also face higher energy burdens and greater exposure to climate extremes. Decarbonization strategies that ignore distributional effects risk exacerbating inequality. Policies must therefore align emissions reduction with affordability, resilience, and fair allocation of costs.

The outlook for U.S. residential decarbonization is conditional but not pessimistic. The technological tools required for substantial emissions reductions exist. The challenge lies in aligning comfort norms, institutional frameworks, workforce development, housing policy, and grid transformation at sufficient pace and scale. Residential decarbonization ultimately represents a human-centered systems transition. Technical systems create the possibility of emissions reduction, but their realization depends on collective decisions about comfort, investment, governance, and professional practice. Buildings do not decarbonize themselves; people—through their choices, institutions, and everyday actions—determine whether technical potential becomes durable reality.

Appendices

Appendix A: Supplementary Information for Chapter 2

Table A.1: Relevant publications on residential HVAC electrification in the U.S.

Publication	*Energy*	*Peak Demand*	*Emissions*	*Thermal Comfort*	*Climate Change*
White et. al (2021)	Yes	Yes	Yes		
Vaishnav & Fatimah (2020)	Yes	Yes	Yes		
Waite & Modi (2020)	Yes	Yes			
Deetjen et. al (2021)	Yes	Yes	Yes		
Doak et al (2022)	Yes		Yes		Yes*
This paper	**Yes**	**Yes**	**Yes**	**Yes**	**Yes**

Existing HVAC electrification literature often neglects thermal comfort, while residential thermal comfort studies typically focus on buildings using conventional heating fuels, with minimal power grid interaction. Furthermore, many studies do not consider the impact of climate change on heating/cooling demands and ASHP efficiency.
*Doak et. al assume constant thermal load from historical climate conditions for future analysis. In contrast, our RCBEM allows analysis of flexible heating demand accounting for variable weather conditions.

Table A.2: Relevant publications on surrogate building energy models.

Publication	*Building Types*	*Location*	*Method*	*Temporal Resolution*
Ascione et. al (2017)	Office	South Italy	ANN	Annual
Hygh et. al (2012)	Office	4 U.S. cities	MLR	Annual
Lam et. al (2010)	Office	5 climates in China	MLR	Annual
Shikatani & Richman (2024)	Single-family	Toronto, Canada	ANN	Annual
Bhavsar et. al (2022)	Single-family	Illinois, U.S.	LGB	Hourly
Staffel et. al (2023)	Residential & Commercial	43 regions (27 countries)	MLR	Daily*
This paper (RC-BEM)	**Single-family**	**54 U.S. cities**	**MLR**	**Hourly**

Many existing building surrogate models lack the temporal resolution required for seamless integration of building and power grid analyses. Methods like Artificial Neural Networks (ANN), Multiple Linear Regression (MLR), and Light Gradient Boosting (LGB) have been used.

Our RC-BEM uses a penalized linear regression to predict hourly heating and cooling demands for over 17,000 single-family homes across 54 U.S. cities and allows rapid optimization of multiple objectives via mixed-integer linear programming.

* Staffel et al. use a representative diurnal profile to get hourly energy consumption from the daily energy consumption.

Table A.3: Performance of RC-BEM for 54 U.S. cities.

Climate	City	State	n	NRMSE	Heating Overpred.	Cooling Overpred.
Cold	Boise	ID	254	27%	15%	1%
Cold	Boston	MA	264	20%	5%	-2%
Cold	Buffalo	NY	326	25%	19%	1%
Cold	Chicago	IL	350	20%	10%	1%
Cold	Colorado Springs	CO	244	27%	5%	-3%
Cold	Columbus	OH	349	22%	10%	1%
Cold	Dayton	OH	345	20%	10%	3%
Cold	Detroit	MI	336	17%	7%	5%
Cold	Eagle	CO	239	23%	10%	2%
Cold	Goodland	KS	365	21%	9%	0%
Cold	Madison	WI	328	18%	8%	1%
Cold	Minneapolis	MN	342	18%	9%	5%
Cold	Omaha	NE	373	19%	9%	4%
Cold	Peoria	IL	346	21%	13%	0%
Cold	Pittsburgh	PA	317	19%	9%	1%
Cold	Salt Lake City	UT	250	33%	20%	1%
Cold	Scranton	PA	317	19%	9%	5%
Cold	Spokane	WA	186	24%	20%	10%
Hot-Dry	El Paso	TX	380	25%	1%	-1%
Hot-Dry	Las Vegas	NV	312	22%	1%	-2%
Hot-Dry	Los Angeles	CA	204	49%	-33%	-7%
Hot-Dry	Lubbock	TX	379	26%	16%	1%
Hot-Dry	Midland	TX	378	24%	0%	-2%
Hot-Dry	Phoenix	AZ	324	17%	-17%	-1%
Hot-Humid	Brownsville	TX	383	26%	8%	0%
Hot-Humid	Charleston	SC	373	30%	9%	-2%
Hot-Humid	Dallas	TX	380	22%	8%	0%
Hot-Humid	Houston	TX	381	26%	5%	0%
Hot-Humid	Jackson	MS	364	28%	9%	-2%
Hot-Humid	Jacksonville	FL	367	31%	-1%	-1%
Hot-Humid	Miami	FL	364	24%	57%	1%
Hot-Humid	Mobile	AL	367	29%	6%	-2%
Hot-Humid	New Orleans	LA	372	28%	1%	-1%
Hot-Humid	Orlando	FL	365	29%	3%	0%
Marine	Portland	OR	188	31%	22%	0%
Marine	San Francisco	CA	210	49%	-6%	-34%
Marine	Seattle	WA	186	38%	31%	-4%
Mixed-Dry	Albuquerque	NM	291	28%	16%	3%
Mixed-Dry	Amarillo	TX	377	27%	19%	2%
Mixed-Humid	Atlanta	GA	372	24%	5%	-1%
Mixed-Humid	Baltimore	MD	368	23%	10%	2%
Mixed-Humid	Charlotte	NC	373	28%	14%	0%
Mixed-Humid	Kansas City	MO	357	25%	18%	1%
Mixed-Humid	Memphis	TN	377	26%	13%	-1%
Mixed-Humid	Nashville	TN	378	29%	19%	1%
Mixed-Humid	New York City	NY	325	21%	10%	0%
Mixed-Humid	Norfolk	VA	356	30%	15%	0%
Mixed-Humid	Oklahoma	OK	371	24%	14%	0%
Mixed-Humid	Philadelphia	PA	319	23%	12%	1%
Mixed-Humid	St. Louis	MO	357	19%	11%	2%
Mixed-Humid	Tulsa	OK	372	24%	15%	1%
Mixed-Humid	Wichita Falls	TX	379	24%	11%	-2%
Very Cold	Caribou	ME	234	21%	16%	-7%
Very Cold	Duluth	MN	335	17%	10%	17%

Table A.4: Residential electricity rates and thermal discomfort slopes.

Climate	City	State	n	Electricity Rate [$/kWh]	Heating Slope [$/°C-hr]	Cooling Slope [$/°C-hr]
Cold	Boise	ID	254	0.117	0.011	0.006
Cold	Boston	MA	264	0.287	0.027	0.019
Cold	Buffalo	NY	326	0.230	0.030	0.021
Cold	Chicago	IL	350	0.149	0.014	0.011
Cold	Colorado Springs	CO	244	0.153	0.010	0.007
Cold	Columbus	OH	349	0.156	0.012	0.012
Cold	Dayton	OH	345	0.156	0.016	0.013
Cold	Detroit	MI	336	0.183	0.020	0.015
Cold	Eagle	CO	239	0.147	0.013	0.006
Cold	Goodland	KS	365	0.132	0.012	0.009
Cold	Madison	WI	328	0.167	0.018	0.011
Cold	Minneapolis	MN	342	0.172	0.019	0.012
Cold	Omaha	NE	373	0.118	0.012	0.010
Cold	Peoria	IL	346	0.151	0.016	0.012
Cold	Pittsburgh	PA	317	0.180	0.019	0.014
Cold	Salt Lake City	UT	250	0.111	0.011	0.008
Cold	Scranton	PA	317	0.180	0.018	0.013
Cold	Spokane	WA	186	0.110	0.011	0.005
Hot-Dry	El Paso	TX	380	0.148	0.008	0.011
Hot-Dry	Las Vegas	NV	312	0.149	0.010	0.014
Hot-Dry	Los Angeles	CA	204	0.252	0.007	0.014
Hot-Dry	Lubbock	TX	379	0.148	0.012	0.015
Hot-Dry	Midland	TX	378	0.148	0.008	0.012
Hot-Dry	Phoenix	AZ	324	0.148	0.005	0.013
Hot-Humid	Brownsville	TX	383	0.148	0.006	0.017
Hot-Humid	Charleston	SC	373	0.143	0.008	0.016
Hot-Humid	Dallas	TX	380	0.178	0.011	0.018
Hot-Humid	Houston	TX	381	0.195	0.009	0.020
Hot-Humid	Jackson	MS	364	0.137	0.009	0.014
Hot-Humid	Jacksonville	FL	367	0.148	0.006	0.013
Hot-Humid	Miami	FL	364	0.141	0.003	0.017
Hot-Humid	Mobile	AL	367	0.150	0.007	0.016
Hot-Humid	New Orleans	LA	372	0.131	0.005	0.013
Hot-Humid	Orlando	FL	365	0.148	0.003	0.014
Marine	Portland	OR	188	0.126	0.013	0.005
Marine	San Francisco	CA	210	0.303	0.017	0.005
Marine	Seattle	WA	186	0.118	0.012	0.004
Mixed-Dry	Albuquerque	NM	291	0.144	0.014	0.013
Mixed-Dry	Amarillo	TX	377	0.148	0.015	0.015
Mixed-Humid	Atlanta	GA	372	0.150	0.008	0.012
Mixed-Humid	Baltimore	MD	368	0.151	0.012	0.012
Mixed-Humid	Charlotte	NC	373	0.139	0.011	0.014
Mixed-Humid	Kansas City	MO	357	0.132	0.012	0.012
Mixed-Humid	Memphis	TN	377	0.128	0.009	0.014
Mixed-Humid	Nashville	TN	378	0.128	0.012	0.015
Mixed-Humid	New York City	NY	325	0.235	0.027	0.023
Mixed-Humid	Norfolk	VA	356	0.143	0.012	0.014
Mixed-Humid	Oklahoma	OK	371	0.138	0.011	0.015
Mixed-Humid	Philadelphia	PA	319	0.180	0.017	0.016
Mixed-Humid	St. Louis	MO	357	0.134	0.011	0.012
Mixed-Humid	Tulsa	OK	372	0.138	0.012	0.016
Mixed-Humid	Wichita Falls	TX	379	0.148	0.011	0.016
Very Cold	Caribou	ME	234	0.259	0.046	0.016
Very Cold	Duluth	MN	335	0.152	0.018	0.007

Table A.5: T0 optimization results for 54 U.S. cities.

City	Energy $	Externalities $	PeakDemand $	HeatDisc $	CoolDisc $
Albuquerque	1228 (48%)	1165 (46%)	149 (6%)	0 (0%)	0 (0%)
Amarillo	1447 (49%)	1305 (44%)	209 (7%)	0 (0%)	0 (0%)
Atlanta	1034 (47%)	1021 (46%)	165 (7%)	0 (0%)	0 (0%)
Baltimore	1599 (41%)	1985 (51%)	275 (7%)	0 (0%)	0 (0%)
Boise	978 (51%)	732 (38%)	201 (11%)	0 (0%)	0 (0%)
Boston	3668 (69%)	1216 (23%)	420 (8%)	0 (0%)	0 (0%)
Brownsville	825 (50%)	739 (45%)	75 (5%)	0 (0%)	0 (0%)
Buffalo	3897 (64%)	1839 (30%)	363 (6%)	0 (0%)	0 (0%)
Caribou	6448 (68%)	2320 (25%)	679 (7%)	0 (0%)	0 (0%)
Charleston	918 (46%)	911 (46%)	161 (8%)	0 (0%)	0 (0%)
Charlotte	1133 (46%)	1148 (47%)	183 (7%)	0 (0%)	0 (0%)
Chicago	1840 (42%)	2073 (48%)	425 (10%)	0 (0%)	0 (0%)
Colorado Springs	1006 (51%)	847 (43%)	107 (5%)	0 (0%)	0 (0%)
Columbus	1600 (43%)	1748 (47%)	340 (9%)	0 (0%)	0 (0%)
Dallas	1652 (54%)	1230 (40%)	165 (5%)	0 (0%)	0 (0%)
Dayton	1855 (43%)	2030 (47%)	455 (10%)	0 (0%)	0 (0%)
Detroit	2800 (49%)	2490 (43%)	451 (8%)	0 (0%)	0 (0%)
Duluth	3196 (43%)	3775 (51%)	484 (7%)	0 (0%)	0 (0%)
Eagle	1002 (49%)	873 (43%)	154 (8%)	0 (0%)	0 (0%)
El Paso	835 (50%)	748 (45%)	77 (5%)	0 (0%)	0 (0%)
Goodland	1502 (39%)	2065 (54%)	260 (7%)	0 (0%)	0 (0%)
Houston	1268 (57%)	856 (38%)	102 (5%)	0 (0%)	0 (0%)
Jackson	1080 (54%)	775 (39%)	158 (8%)	0 (0%)	0 (0%)
Jacksonville	830 (54%)	597 (39%)	109 (7%)	0 (0%)	0 (0%)
Kansas City	1939 (37%)	2905 (55%)	421 (8%)	0 (0%)	0 (0%)
Las Vegas	1064 (60%)	587 (33%)	130 (7%)	0 (0%)	0 (0%)
Los Angeles	500 (73%)	170 (25%)	20 (3%)	0 (0%)	0 (0%)
Lubbock	1297 (50%)	1166 (45%)	147 (6%)	0 (0%)	0 (0%)
Madison	2725 (48%)	2459 (44%)	467 (8%)	0 (0%)	0 (0%)
Memphis	1450 (45%)	1602 (49%)	202 (6%)	0 (0%)	0 (0%)
Miami	714 (54%)	545 (41%)	66 (5%)	0 (0%)	0 (0%)
Midland	1022 (50%)	916 (45%)	103 (5%)	0 (0%)	0 (0%)
Minneapolis	3423 (46%)	3564 (48%)	511 (7%)	0 (0%)	0 (0%)
Mobile	895 (52%)	719 (42%)	92 (5%)	0 (0%)	0 (0%)
Nashville	1533 (42%)	1703 (46%)	448 (12%)	0 (0%)	0 (0%)
New Orleans	839 (50%)	763 (45%)	88 (5%)	0 (0%)	0 (0%)
New York City	3312 (63%)	1542 (29%)	425 (8%)	0 (0%)	0 (0%)
Norfolk	1199 (51%)	976 (41%)	198 (8%)	0 (0%)	0 (0%)
Oklahoma	1675 (49%)	1506 (44%)	232 (7%)	0 (0%)	0 (0%)
Omaha	1851 (32%)	3503 (60%)	478 (8%)	0 (0%)	0 (0%)
Orlando	780 (54%)	563 (39%)	103 (7%)	0 (0%)	0 (0%)
Peoria	2383 (43%)	2635 (48%)	495 (9%)	0 (0%)	0 (0%)
Philadelphia	2278 (50%)	1864 (41%)	424 (9%)	0 (0%)	0 (0%)
Phoenix	894 (52%)	707 (41%)	108 (6%)	0 (0%)	0 (0%)
Pittsburgh	2301 (51%)	1875 (42%)	312 (7%)	0 (0%)	0 (0%)
Portland	994 (57%)	621 (35%)	139 (8%)	0 (0%)	0 (0%)
Salt Lake City	846 (39%)	1178 (55%)	132 (6%)	0 (0%)	0 (0%)
San Francisco	1005 (75%)	279 (21%)	49 (4%)	0 (0%)	0 (0%)
Scranton	2222 (51%)	1792 (41%)	323 (7%)	0 (0%)	0 (0%)
Seattle	1211 (43%)	1237 (44%)	338 (12%)	0 (0%)	0 (0%)
Spokane	1047 (44%)	1154 (49%)	169 (7%)	0 (0%)	0 (0%)
St. Louis	1629 (37%)	2405 (55%)	331 (8%)	0 (0%)	0 (0%)
Tulsa	1705 (48%)	1530 (43%)	353 (10%)	0 (0%)	0 (0%)
Wichita Falls	1517 (50%)	1360 (44%)	184 (6%)	0 (0%)	0 (0%)

Table A.6: T3.5 optimization results for 54 U.S. cities.

City	Energy $	Externalities $	PeakDemand $	HeatDisc $	CoolDisc $
Albuquerque	758 (40%)	717 (38%)	118 (6%)	199 (11%)	89 (5%)
Amarillo	894 (41%)	799 (37%)	171 (8%)	142 (7%)	176 (8%)
Atlanta	640 (40%)	630 (40%)	103 (6%)	77 (5%)	141 (9%)
Baltimore	1110 (37%)	1385 (46%)	223 (7%)	182 (6%)	86 (3%)
Boise	625 (44%)	465 (33%)	164 (11%)	133 (9%)	42 (3%)
Boston	2739 (61%)	907 (20%)	360 (8%)	407 (9%)	115 (3%)
Brownsville	512 (41%)	450 (36%)	43 (3%)	19 (2%)	236 (19%)
Buffalo	2720 (56%)	1286 (26%)	303 (6%)	476 (10%)	101 (2%)
Caribou	5190 (62%)	1880 (22%)	600 (7%)	673 (8%)	55 (1%)
Charleston	488 (37%)	482 (37%)	85 (6%)	64 (5%)	189 (14%)
Charlotte	649 (38%)	659 (38%)	151 (9%)	109 (6%)	160 (9%)
Chicago	1427 (37%)	1619 (42%)	512 (13%)	224 (6%)	74 (2%)
Colorado Springs	649 (45%)	544 (38%)	63 (4%)	144 (10%)	44 (3%)
Columbus	1161 (37%)	1269 (41%)	426 (14%)	181 (6%)	86 (3%)
Dallas	1104 (47%)	813 (35%)	89 (4%)	101 (4%)	226 (10%)
Dayton	1328 (37%)	1456 (40%)	505 (14%)	258 (7%)	81 (2%)
Detroit	2064 (44%)	1838 (39%)	379 (8%)	326 (7%)	90 (2%)
Duluth	2572 (40%)	3035 (48%)	424 (7%)	289 (5%)	43 (1%)
Eagle	621 (41%)	537 (36%)	128 (8%)	192 (13%)	32 (2%)
El Paso	506 (42%)	446 (37%)	51 (4%)	66 (5%)	136 (11%)
Goodland	1070 (35%)	1475 (49%)	215 (7%)	186 (6%)	75 (2%)
Houston	790 (47%)	525 (31%)	56 (3%)	63 (4%)	242 (14%)
Jackson	660 (44%)	476 (32%)	116 (8%)	85 (6%)	156 (10%)
Jacksonville	491 (44%)	352 (31%)	79 (7%)	44 (4%)	154 (14%)
Kansas City	1357 (34%)	2041 (51%)	343 (9%)	175 (4%)	105 (3%)
Las Vegas	665 (49%)	370 (27%)	80 (6%)	73 (5%)	172 (13%)
Los Angeles	168 (41%)	57 (14%)	13 (3%)	24 (6%)	151 (37%)
Lubbock	787 (42%)	700 (37%)	117 (6%)	110 (6%)	181 (10%)
Madison	2110 (44%)	1894 (40%)	420 (9%)	275 (6%)	74 (2%)
Memphis	955 (39%)	1051 (43%)	169 (7%)	97 (4%)	156 (6%)
Miami	488 (45%)	367 (34%)	34 (3%)	9 (1%)	182 (17%)
Midland	641 (43%)	567 (38%)	61 (4%)	71 (5%)	153 (10%)
Minneapolis	2772 (43%)	2879 (44%)	460 (7%)	285 (4%)	89 (1%)
Mobile	496 (41%)	397 (33%)	65 (5%)	47 (4%)	207 (17%)
Nashville	1008 (36%)	1120 (40%)	369 (13%)	135 (5%)	135 (5%)
New Orleans	521 (42%)	471 (38%)	51 (4%)	35 (3%)	175 (14%)
New York City	2370 (54%)	1104 (25%)	359 (8%)	409 (9%)	152 (3%)
Norfolk	685 (42%)	555 (34%)	103 (6%)	160 (10%)	114 (7%)
Oklahoma	1117 (43%)	1004 (39%)	181 (7%)	110 (4%)	185 (7%)
Omaha	1419 (30%)	2691 (56%)	422 (9%)	183 (4%)	81 (2%)
Orlando	496 (46%)	356 (33%)	52 (5%)	18 (2%)	159 (15%)
Peoria	1767 (39%)	1963 (44%)	441 (10%)	247 (5%)	87 (2%)
Philadelphia	1577 (44%)	1278 (36%)	355 (10%)	261 (7%)	105 (3%)
Phoenix	632 (46%)	500 (36%)	69 (5%)	28 (2%)	152 (11%)
Pittsburgh	1607 (45%)	1295 (36%)	273 (8%)	283 (8%)	96 (3%)
Portland	592 (47%)	368 (29%)	110 (9%)	169 (13%)	24 (2%)
Salt Lake City	505 (34%)	703 (47%)	100 (7%)	129 (9%)	68 (4%)
San Francisco	458 (55%)	127 (15%)	26 (3%)	206 (25%)	14 (2%)
Scranton	1571 (46%)	1251 (36%)	267 (8%)	276 (8%)	79 (2%)
Seattle	786 (38%)	799 (39%)	284 (14%)	188 (9%)	18 (1%)
Spokane	724 (39%)	784 (43%)	137 (7%)	160 (9%)	29 (2%)
St. Louis	1175 (34%)	1739 (50%)	269 (8%)	164 (5%)	101 (3%)
Tulsa	1148 (41%)	1030 (37%)	292 (11%)	128 (5%)	183 (7%)
Wichita Falls	985 (44%)	874 (39%)	94 (4%)	103 (5%)	205 (9%)

Table A.7: 1x optimization results for 54 U.S. cities.

City	Energy $	Externalities $	PeakDemand $	HeatDisc $	CoolDisc $
Albuquerque	1 (0%)	1 (0%)	0 (0%)	496 (69%)	220 (31%)
Amarillo	2 (0%)	2 (0%)	0 (0%)	364 (46%)	417 (53%)
Atlanta	8 (1%)	8 (1%)	0 (0%)	204 (36%)	342 (61%)
Baltimore	9 (1%)	10 (1%)	1 (0%)	604 (72%)	221 (26%)
Boise	23 (5%)	17 (3%)	1 (0%)	357 (70%)	109 (21%)
Boston	121 (6%)	40 (2%)	2 (0%)	1569 (78%)	282 (14%)
Brownsville	31 (4%)	28 (4%)	2 (0%)	34 (5%)	632 (87%)
Buffalo	54 (3%)	24 (1%)	1 (0%)	1587 (86%)	179 (10%)
Caribou	249 (7%)	82 (2%)	6 (0%)	2993 (88%)	82 (2%)
Charleston	6 (1%)	6 (1%)	0 (0%)	136 (26%)	378 (72%)
Charlotte	3 (0%)	3 (0%)	0 (0%)	267 (45%)	327 (54%)
Chicago	10 (1%)	11 (1%)	0 (0%)	817 (80%)	179 (18%)
Colorado Springs	18 (3%)	15 (3%)	1 (0%)	419 (75%)	105 (19%)
Columbus	4 (1%)	4 (1%)	0 (0%)	573 (73%)	199 (26%)
Dallas	15 (2%)	11 (1%)	1 (0%)	260 (26%)	695 (71%)
Dayton	12 (1%)	12 (1%)	1 (0%)	809 (80%)	174 (17%)
Detroit	21 (1%)	17 (1%)	1 (0%)	1216 (82%)	222 (15%)
Duluth	20 (1%)	23 (2%)	1 (0%)	1417 (91%)	96 (6%)
Eagle	30 (5%)	27 (4%)	1 (0%)	518 (82%)	57 (9%)
El Paso	11 (2%)	10 (2%)	1 (0%)	129 (24%)	382 (72%)
Goodland	2 (0%)	2 (0%)	0 (0%)	664 (77%)	194 (23%)
Houston	38 (4%)	26 (3%)	2 (0%)	141 (16%)	650 (76%)
Jackson	11 (2%)	7 (1%)	1 (0%)	224 (38%)	346 (59%)
Jacksonville	14 (3%)	10 (2%)	1 (0%)	101 (21%)	366 (75%)
Kansas City	2 (0%)	3 (0%)	0 (0%)	576 (67%)	278 (32%)
Las Vegas	25 (4%)	14 (2%)	1 (0%)	122 (18%)	515 (76%)
Los Angeles	9 (3%)	3 (1%)	0 (0%)	30 (11%)	233 (85%)
Lubbock	3 (0%)	3 (0%)	0 (0%)	272 (39%)	422 (60%)
Madison	28 (2%)	24 (2%)	1 (0%)	1162 (83%)	190 (14%)
Memphis	7 (1%)	8 (1%)	1 (0%)	290 (42%)	391 (56%)
Miami	117 (15%)	87 (11%)	6 (1%)	16 (2%)	539 (70%)
Midland	4 (1%)	4 (1%)	0 (0%)	178 (30%)	403 (68%)
Minneapolis	34 (2%)	35 (2%)	1 (0%)	1404 (81%)	258 (15%)
Mobile	22 (4%)	17 (3%)	1 (0%)	94 (16%)	461 (77%)
Nashville	8 (1%)	9 (1%)	1 (0%)	430 (60%)	272 (38%)
New Orleans	16 (3%)	14 (2%)	1 (0%)	73 (12%)	493 (83%)
New York City	77 (4%)	35 (2%)	2 (0%)	1472 (78%)	312 (16%)
Norfolk	10 (2%)	8 (1%)	1 (0%)	375 (59%)	243 (38%)
Oklahoma	2 (0%)	2 (0%)	0 (0%)	313 (38%)	504 (61%)
Omaha	4 (0%)	6 (1%)	0 (0%)	748 (74%)	250 (25%)
Orlando	38 (7%)	27 (5%)	2 (0%)	42 (8%)	441 (80%)
Peoria	7 (1%)	7 (1%)	0 (0%)	912 (79%)	231 (20%)
Philadelphia	14 (1%)	11 (1%)	1 (0%)	847 (76%)	242 (22%)
Phoenix	47 (6%)	35 (5%)	3 (0%)	48 (7%)	596 (82%)
Pittsburgh	21 (2%)	17 (1%)	1 (0%)	959 (79%)	217 (18%)
Portland	152 (22%)	94 (13%)	65 (9%)	347 (49%)	45 (6%)
Salt Lake City	6 (1%)	8 (2%)	0 (0%)	304 (62%)	169 (35%)
San Francisco	21 (5%)	6 (1%)	1 (0%)	376 (89%)	20 (5%)
Scranton	32 (3%)	25 (2%)	1 (0%)	969 (81%)	161 (14%)
Seattle	5 (1%)	5 (1%)	0 (0%)	515 (92%)	35 (6%)
Spokane	18 (3%)	17 (3%)	1 (0%)	531 (83%)	69 (11%)
St. Louis	7 (1%)	10 (1%)	1 (0%)	585 (65%)	295 (33%)
Tulsa	3 (0%)	3 (0%)	0 (0%)	390 (44%)	483 (55%)
Wichita Falls	5 (1%)	5 (1%)	0 (0%)	275 (33%)	555 (66%)

Table A.8: 3x optimization results for 54 U.S. cities

City	Energy $	Externalities $	PeakDemand $	HeatDisc $	CoolDisc $
Albuquerque	404 (22%)	372 (20%)	17 (1%)	779 (43%)	256 (14%)
Amarillo	419 (21%)	377 (18%)	17 (1%)	667 (33%)	564 (28%)
Atlanta	255 (31%)	258 (31%)	13 (2%)	163 (20%)	131 (16%)
Baltimore	300 (14%)	360 (16%)	11 (0%)	1223 (55%)	311 (14%)
Boise	270 (37%)	196 (27%)	16 (2%)	178 (24%)	70 (10%)
Boston	1901 (60%)	628 (20%)	46 (1%)	491 (16%)	82 (3%)
Brownsville	531 (37%)	473 (33%)	28 (2%)	97 (7%)	293 (21%)
Buffalo	1331 (30%)	611 (14%)	36 (1%)	2235 (50%)	251 (6%)
Caribou	3040 (41%)	1050 (14%)	81 (1%)	3104 (42%)	119 (2%)
Charleston	270 (21%)	266 (21%)	17 (1%)	377 (29%)	353 (28%)
Charlotte	261 (17%)	263 (17%)	12 (1%)	607 (39%)	419 (27%)
Chicago	401 (28%)	437 (30%)	14 (1%)	509 (35%)	79 (5%)
Colorado Springs	300 (37%)	252 (31%)	12 (1%)	208 (25%)	46 (6%)
Columbus	260 (25%)	273 (26%)	10 (1%)	415 (39%)	95 (9%)
Dallas	648 (28%)	480 (21%)	30 (1%)	552 (24%)	595 (26%)
Dayton	407 (16%)	432 (17%)	16 (1%)	1509 (58%)	233 (9%)
Detroit	691 (19%)	598 (16%)	22 (1%)	2074 (56%)	334 (9%)
Duluth	540 (13%)	627 (15%)	25 (1%)	2658 (66%)	207 (5%)
Eagle	343 (24%)	299 (21%)	16 (1%)	703 (49%)	89 (6%)
El Paso	309 (25%)	276 (22%)	17 (1%)	259 (21%)	399 (32%)
Goodland	302 (13%)	411 (18%)	12 (1%)	1247 (55%)	307 (13%)
Houston	644 (36%)	429 (24%)	31 (2%)	356 (20%)	323 (18%)
Jackson	361 (25%)	253 (18%)	19 (1%)	503 (35%)	285 (20%)
Jacksonville	320 (29%)	231 (21%)	19 (2%)	273 (25%)	251 (23%)
Kansas City	187 (17%)	267 (24%)	9 (1%)	467 (42%)	175 (16%)
Las Vegas	559 (38%)	308 (21%)	27 (2%)	157 (11%)	425 (29%)
Los Angeles	293 (49%)	99 (17%)	9 (2%)	57 (9%)	141 (24%)
Lubbock	355 (20%)	316 (17%)	18 (1%)	602 (33%)	516 (29%)
Madison	682 (19%)	605 (17%)	27 (1%)	1902 (54%)	305 (9%)
Memphis	257 (14%)	277 (15%)	16 (1%)	748 (41%)	521 (29%)
Miami	557 (48%)	425 (36%)	32 (3%)	48 (4%)	106 (9%)
Midland	322 (22%)	285 (19%)	19 (1%)	431 (29%)	417 (28%)
Minneapolis	722 (17%)	737 (17%)	28 (1%)	2475 (57%)	371 (9%)
Mobile	388 (31%)	308 (24%)	21 (2%)	256 (20%)	298 (23%)
Nashville	248 (13%)	265 (14%)	13 (1%)	1020 (54%)	360 (19%)
New Orleans	387 (30%)	350 (27%)	24 (2%)	209 (16%)	311 (24%)
New York City	1576 (53%)	723 (24%)	41 (1%)	545 (18%)	83 (3%)
Norfolk	331 (35%)	266 (28%)	13 (1%)	234 (25%)	91 (10%)
Oklahoma	368 (17%)	329 (15%)	18 (1%)	742 (34%)	742 (34%)
Omaha	222 (8%)	410 (15%)	10 (0%)	1660 (60%)	454 (16%)
Orlando	402 (39%)	292 (29%)	25 (2%)	126 (12%)	180 (18%)
Peoria	433 (14%)	465 (15%)	16 (1%)	1769 (58%)	356 (12%)
Philadelphia	522 (33%)	426 (27%)	17 (1%)	514 (32%)	115 (7%)
Phoenix	520 (37%)	407 (29%)	31 (2%)	121 (9%)	335 (24%)
Pittsburgh	631 (21%)	504 (17%)	23 (1%)	1532 (50%)	348 (11%)
Portland	455 (34%)	283 (21%)	195 (15%)	347 (26%)	45 (3%)
Salt Lake City	147 (12%)	204 (16%)	7 (1%)	609 (48%)	299 (24%)
San Francisco	62 (13%)	17 (4%)	2 (0%)	376 (79%)	20 (4%)
Scranton	615 (21%)	489 (17%)	22 (1%)	1569 (53%)	243 (8%)
Seattle	16 (3%)	14 (2%)	1 (0%)	515 (89%)	35 (6%)
Spokane	310 (20%)	312 (20%)	20 (1%)	743 (49%)	142 (9%)
St. Louis	264 (22%)	370 (30%)	13 (1%)	433 (35%)	146 (12%)
Tulsa	426 (19%)	381 (17%)	20 (1%)	849 (37%)	621 (27%)
Wichita Falls	452 (21%)	402 (19%)	25 (1%)	639 (30%)	628 (29%)

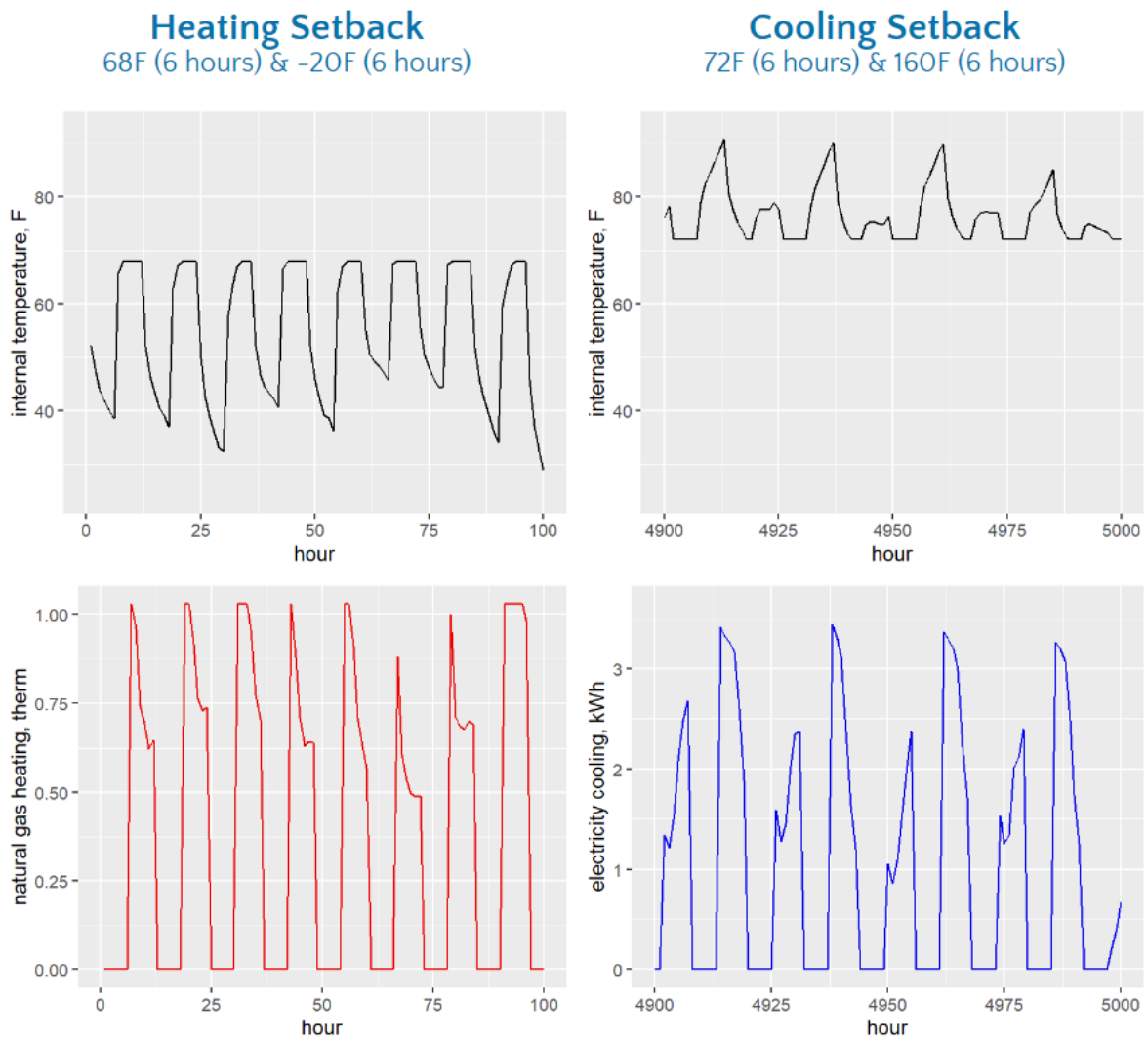


Figure A.1: Customized thermostat setback on EnergyPlus.

By default, EnergyPlus maintains a user-defined setpoint internal temperature, which results in minimal internal temperature variation. This poses a challenge for fitting a surrogate model that explains hourly energy flows as a function of indoor temperature and various weather variables. To introduce variations in indoor temperatures, we modified the setpoint temperature in our customized run, causing the HVAC systems to cycle on and off every six hours. The rate at which the temperature decays, and the energy input needed for the internal temperature to recover to the setpoint, given ambient weather conditions, characterize the building's thermal properties. These characteristics are embedded in our regression model's coefficients.

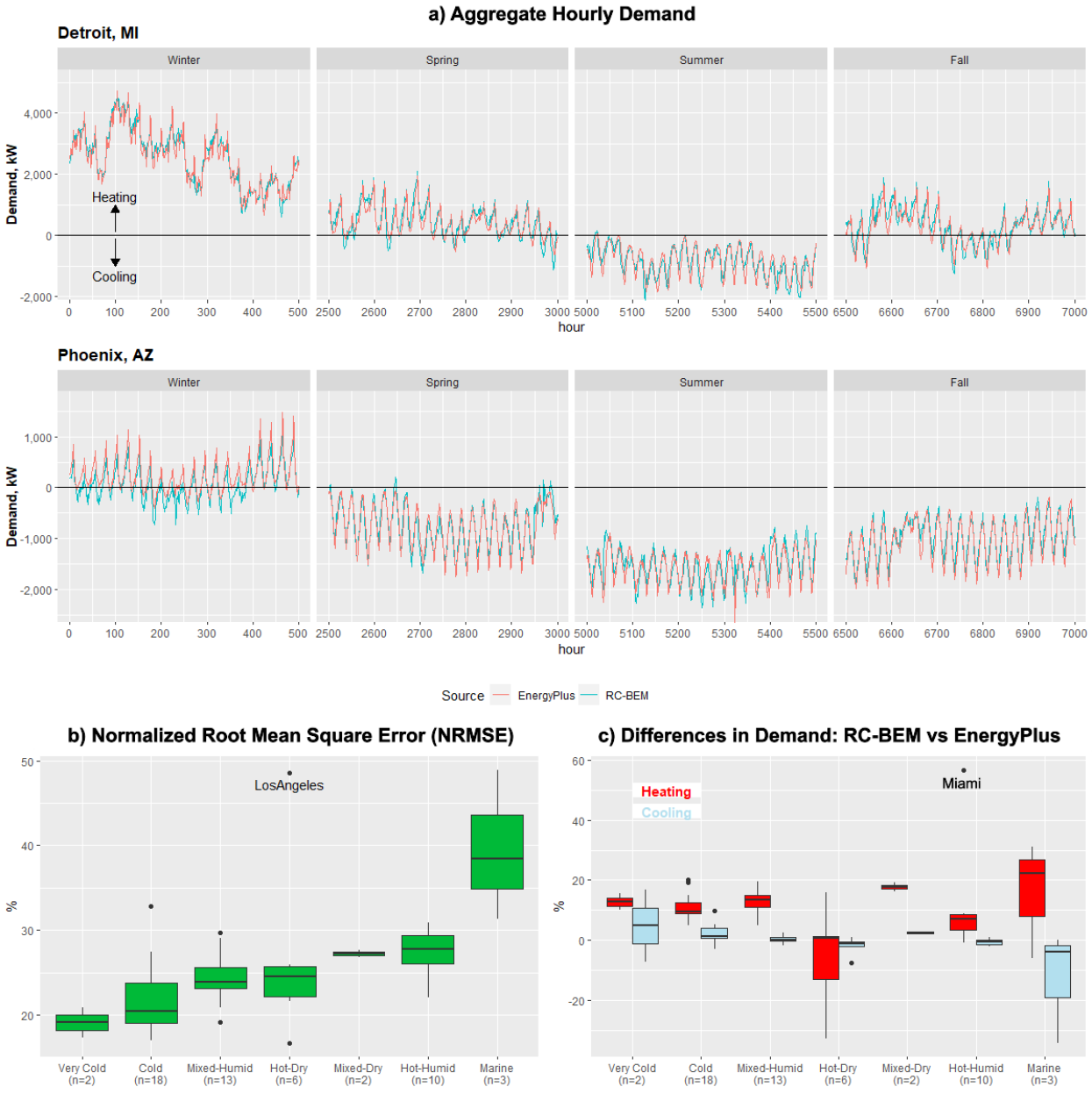


Figure A.2: RC-BEM validation against EnergyPlus Simulations.

a) Comparison of hourly demand predictions by the RC-BEM (blue) and EnergyPlus (red) simulations for Detroit, MI (n = 336 modeled homes) and Phoenix AZ (n = 324) across four seasons. Positive demand values indicate heating requirements (adding heat to the home), while negative values indicate cooling requirements (removing heat from the home) to maintain the setpoint temperature. b) Normalized Root Mean Square Error (NRMSE) analysis quantifies the accuracy of RC-BEM's hourly demand predictions relative to EnergyPlus simulations (validation dataset) across 54 cities within seven climate zones. The number of cities (n) is indicated for each climate zone. c) Boxplots show the percentage differences in aggregate annual heating (red) and cooling (blue) demand between RC-BEM predictions and EnergyPlus simulations for each city.

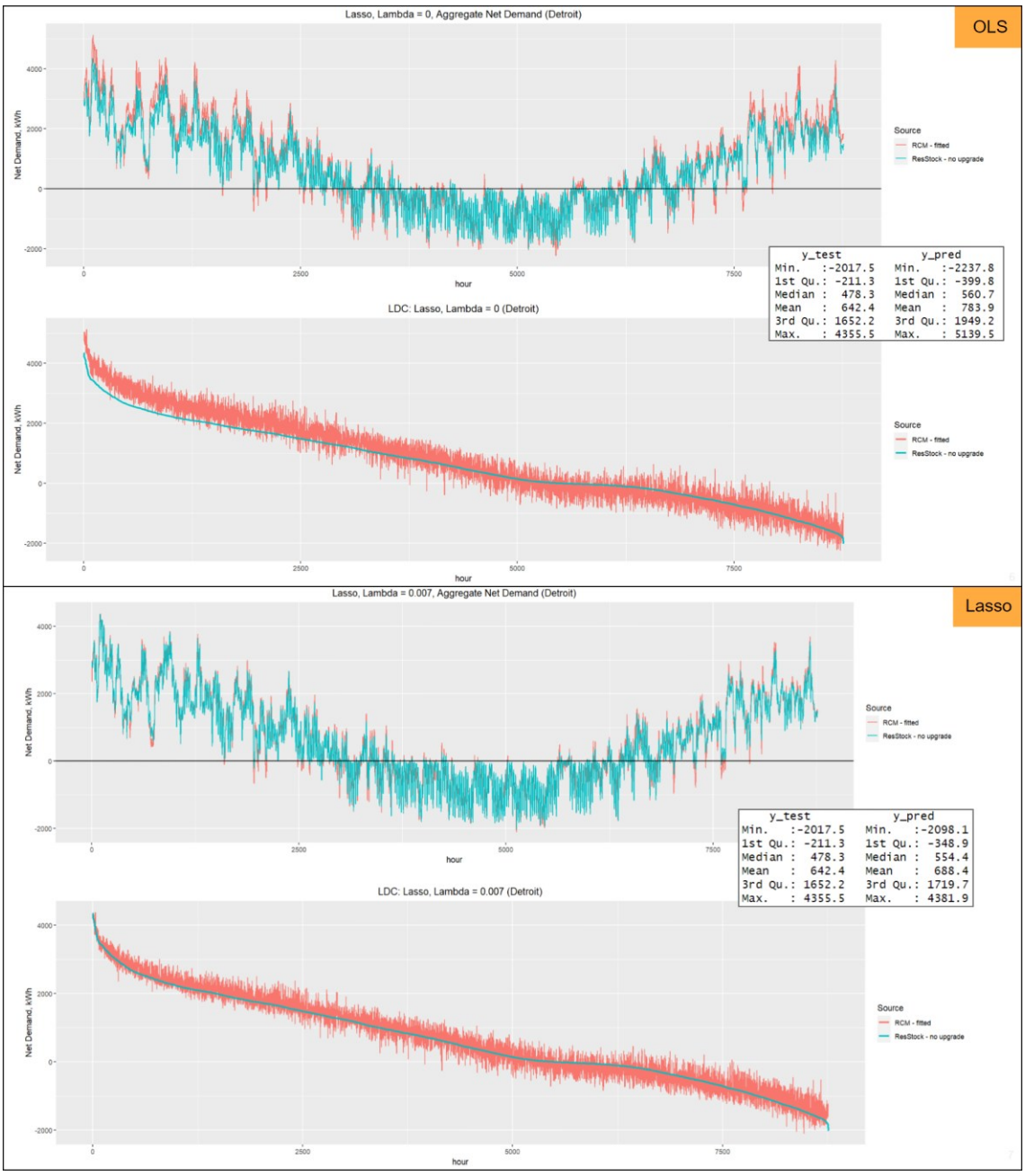


Figure A.3: Comparison of ordinary least squares (OLS) and penalized regressions.

Example of how Lasso regression improves prediction for Detroit, MI.
Panel a: Hourly RC-BEM heat flow prediction and the load duration curve via ordinary least square regression (OLS).
Panel b: Hourly RC-BEM heat flow prediction and the load duration curve via a penalized linear regression (Lasso). The shrinkage penalty term, lambda, was tuned for each city to reduce such overprediction of hourly peak demand.

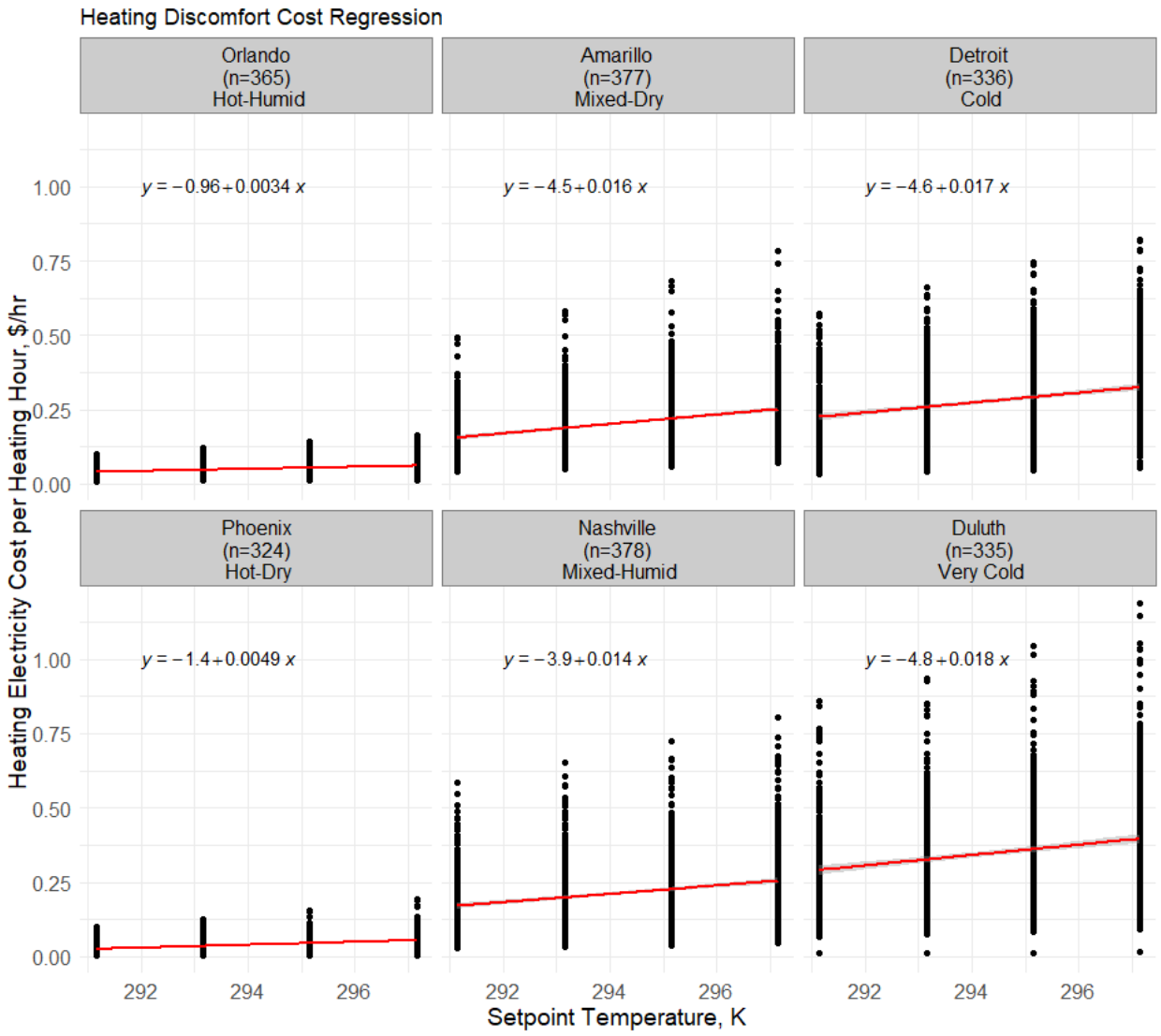


Figure A.4: Heating discomfort costs across six representative cities.

Regression analysis of heating electricity costs per heating hour ($/hr) across a range of internal setpoint temperatures (K) for six representative cities. The scatterplots display the distribution of heating costs (y-axis) relative to setpoint temperatures (x-axis) for individual homes in each city, represented by black dots. The red lines indicate the best-fit linear regression for each city, capturing the relationship between setpoint temperature and heating costs. The slopes of these lines, shown in the equation on each panel, represent the incremental change in heating discomfort costs with increasing setpoint temperature, expressed in $/K-hr. The analysis includes cities from diverse climate regions, highlighting variability in heating discomfort sensitivity across hot-humid (Orlando), hot-dry (Phoenix), mixed-dry (Amarillo), mixed-humid (Nashville), cold (Detroit), and very cold (Duluth) climates.

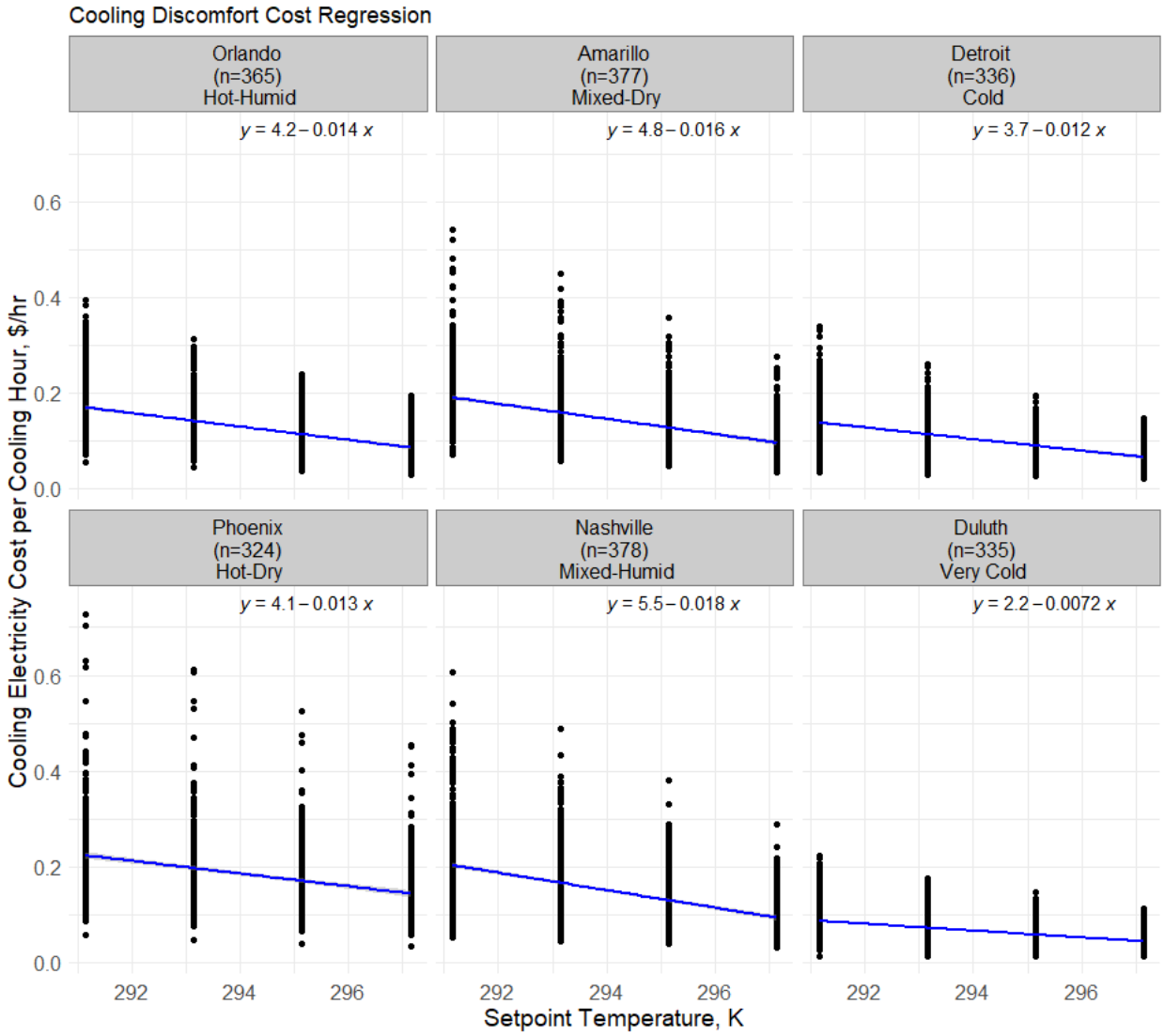


Figure A.5: Cooling discomfort cost across six representative cities.

Regression analysis of heating electricity costs per heating hour ($/hr) across a range of internal setpoint temperatures (K) for six representative cities. The scatterplots display the distribution of heating costs (y-axis) relative to setpoint temperatures (x-axis) for individual homes in each city, represented by black dots. The red lines indicate the best-fit linear regression for each city, capturing the relationship between setpoint temperature and heating costs. The slopes of these lines, shown in the equation on each panel, represent the incremental change in heating discomfort costs with increasing setpoint temperature, expressed in $/K-hr. The analysis includes cities from diverse climate regions, highlighting variability in heating discomfort sensitivity across hot-humid (Orlando), hot-dry (Phoenix), mixed-dry (Amarillo), mixed-humid (Nashville), cold (Detroit), and very cold (Duluth) climates.

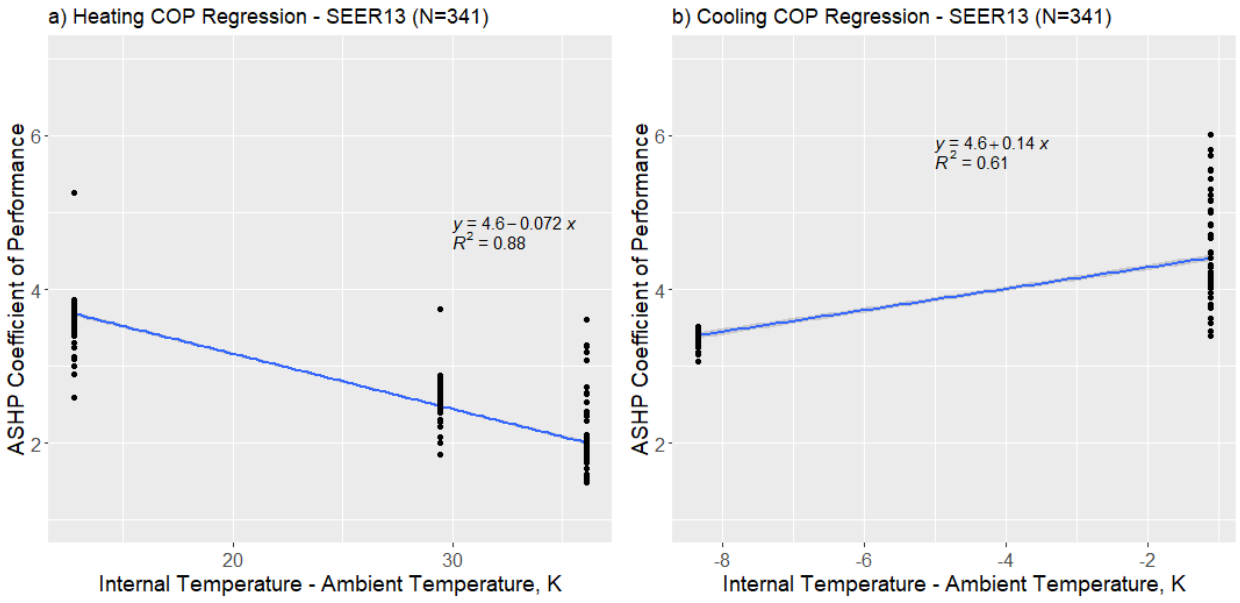


Figure A.6: Temperature-dependent ASHP coefficient of performance (COP).

Example of temperature-dependent regression of ASHP Coefficient of Performance (COP) as a function of the temperature difference between indoor and ambient environments. The COP is calculated from performance data of commercially available heat pumps and correlates with the SEER rating provided in the building metadata. This regression model is trained using data from the Cold Climate Air Source Heat Pump (ccASHP) Product List and Specifications, compiled by the Northeast Energy Efficiency Partnerships. Panel a shows the COP of ASHP under heating mode, while panel b shows the COP of ASHP under cooling mode.

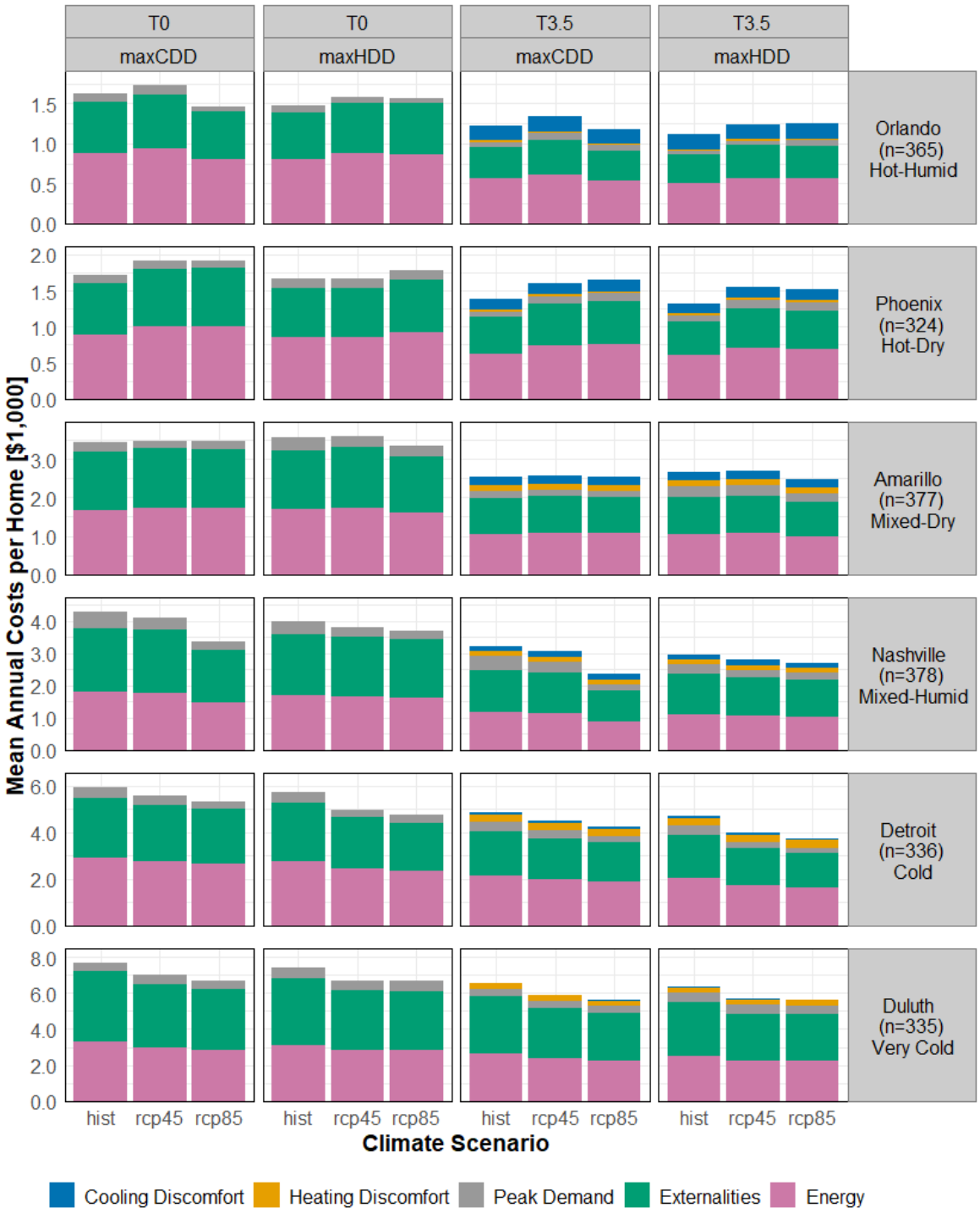


Figure A.7: Annual cost trade-offs under historical, RCP4.5, and RCP8.5.

Annual cost trade-offs across six representative cities from diverse climate regions for different climate scenarios: maxCDD and maxHDD under historical, RCP4.5, and RCP8.5. The bars illustrate the mean annual costs per home (in $1,000) for different cost components—energy, externalities, peak demand, heating discomfort, and cooling discomfort—across four optimization scenarios: T0 (no deviation from setpoint), T3.5 (3.5°C deviation allowed).

Appendix B: Supplementary Information for Chapter 3

Table B.1: Distribution of baseline heating setpoint temperatures (°F).

City	*P25*	*P50*	*P75*
Caribou	67	68	70
Spokane	67	68	70
Madison	67	68	70
Buffalo	68	70	70
Detroit	68	70	70
Scranton	67	68	70
Chicago	68	70	70
Dayton	68	70	70
Duluth	67	68	70
Goodland	68	70	70
Minneapolis	67	68	70
Pittsburgh	68	70	70
Seattle	68	70	72
Columbus	68	70	70
Kansas City	68	70	72
Peoria	68	70	70
Boise	68	70	70
Omaha	67	68	70
Eagle	67	68	70
Philadelphia	68	70	72
Boston	68	70	70
StLouis	68	70	72
Baltimore	68	70	72
Nashville	68	70	72
New York City	68	70	72

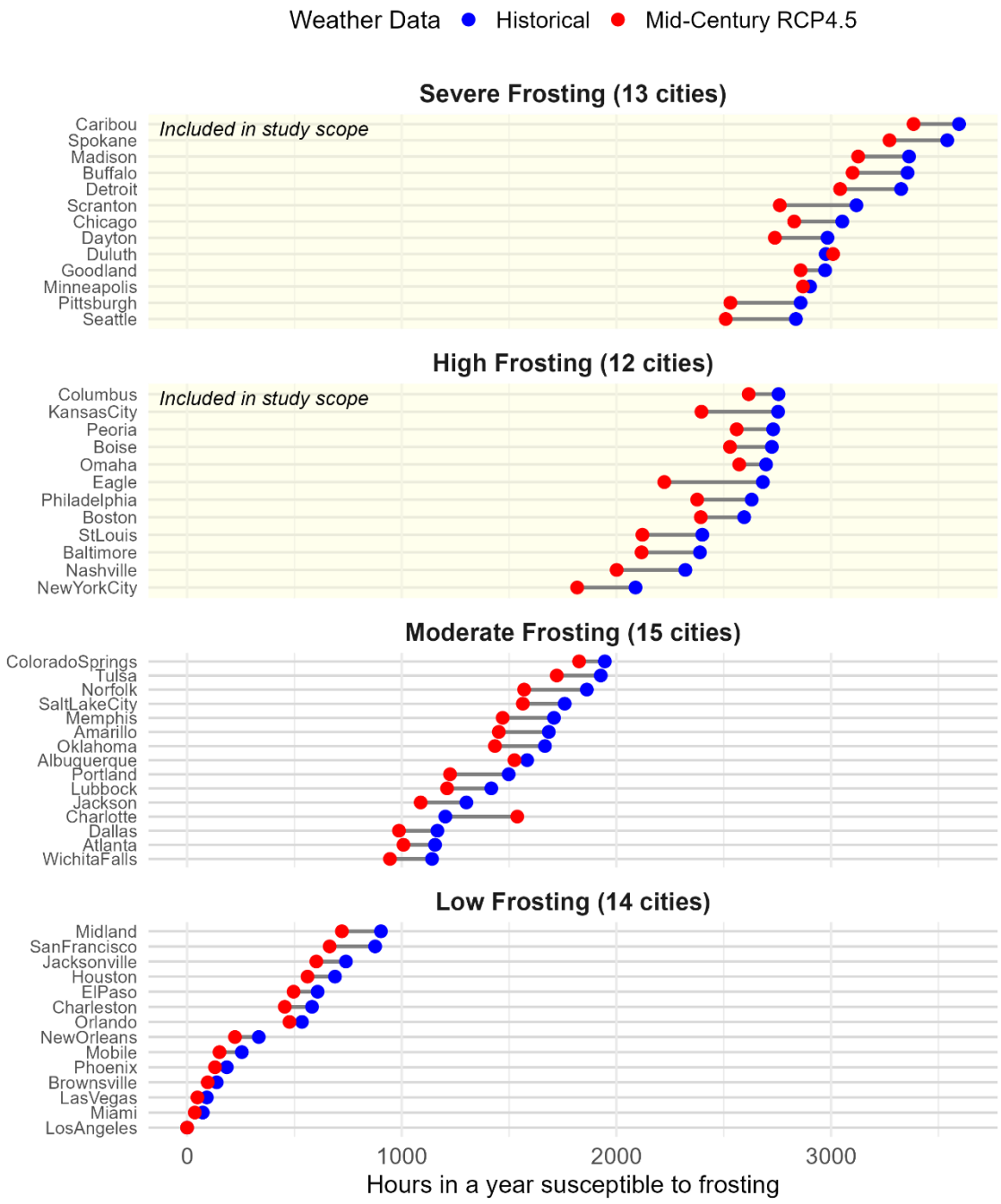


Figure B.1: City selection based on frosting severity.

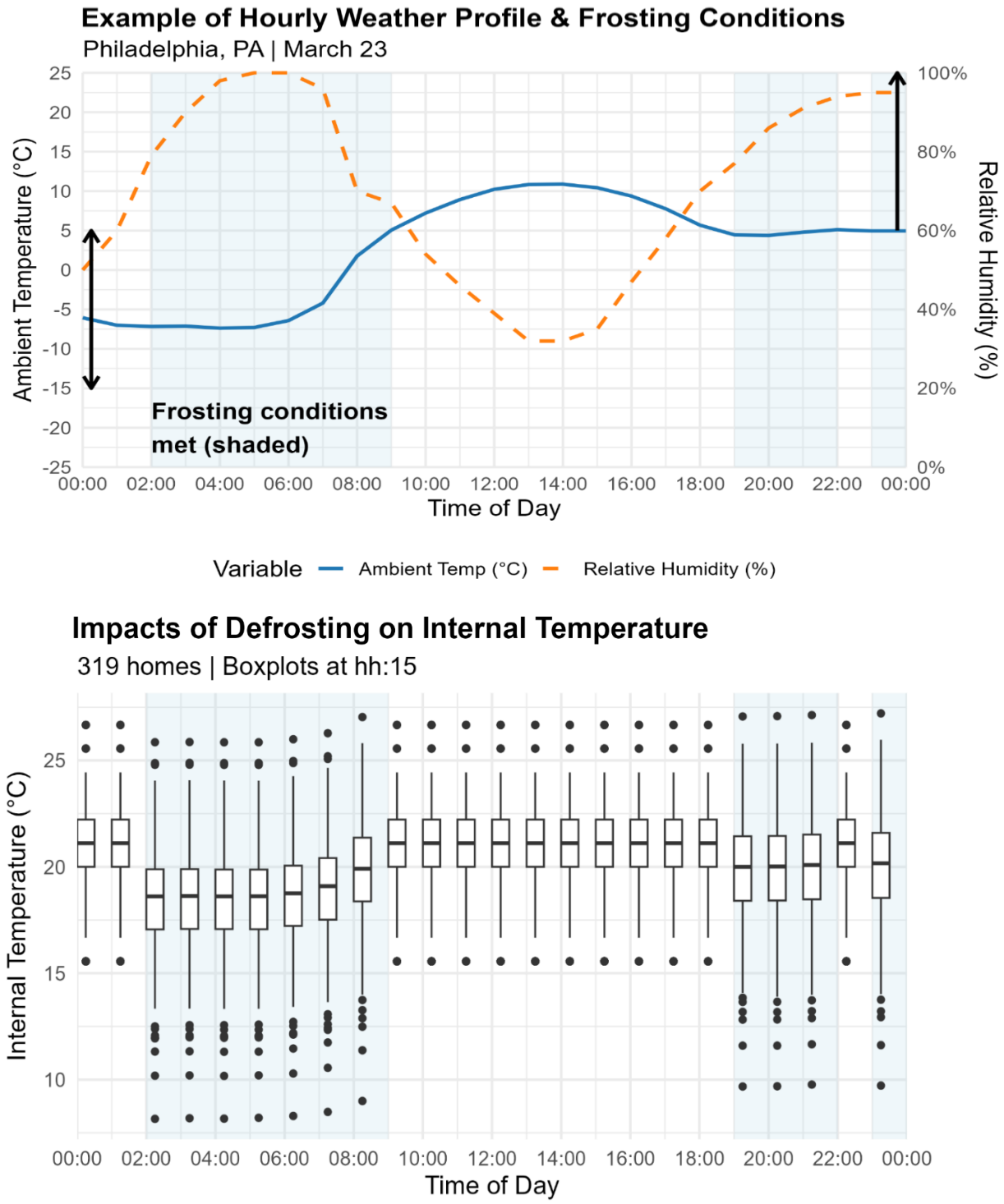


Figure B.2: Example of internal temperature drop after 15 minutes of defrosting.

Appendix C: Supplementary Information for Chapter 4

Table C.1: Comparison of key literatures focusing on U.S. residential decarbonization.

	Energy Efficiency	*Structural Sufficiency*	*Behavioral Sufficiency*	*Stock Turnover*	*Climate Change*	*Grid Decarbonization*
van Heerden et al (2025) [122]	Yes	Yes	Yes Note: Thermostat adjustments are classified as efficiency improvements	Yes	No	Yes
Zhang et al (2025) [125]	Yes	No	No	No	Yes Note: Via Cooling/Heating Degree Days approach	Yes
Wilson et al (2024) [138]	Yes	No	No	No	No Note: All simulations use TMY3 data	Yes
Berrill et al. (2022) [121]	Yes	Yes	No	Yes	No Note: All simulations use TMY3 data	Yes
This paper	Yes	Yes	Yes	Yes	Yes Note: Consider hourly future weather conditions	Yes

Table C.2: Shares of rural residential building archetypes in 2020 by state.

STATE	MFH_LARGE	MFH_SMALL	SFH_ATTACHED	SFH_DETACHED
AL	5.2%	5.6%	1.2%	88%
AR	5.8%	6.1%	1.2%	87%
AZ	5.0%	4.2%	2.6%	88%
CA	5.1%	4.2%	2.9%	88%
CO	6.8%	3.9%	5.3%	84%
CT	5.4%	8.1%	4.2%	82%
DC	0.0%	0.0%	0.0%	0.0%
DE	0.0%	0.0%	0.0%	0.0%
FL	7.4%	5.6%	3.9%	83%
GA	5.0%	5.4%	1.8%	88%
IA	6.0%	3.6%	2.4%	88%
ID	4.7%	4.3%	3.1%	88%
IL	4.0%	4.1%	1.7%	90%
IN	4.5%	3.3%	1.8%	90%
KS	4.8%	4.0%	3.0%	88%
KY	6.2%	6.2%	2.1%	86%
LA	4.7%	6.0%	1.6%	88%
MA	6.7%	7.3%	4.3%	82%
MD	6.9%	3.7%	5.7%	84%
ME	4.7%	5.6%	1.6%	88%
MI	4.9%	2.8%	2.2%	90%
MN	7.7%	2.6%	3.4%	86%
MO	3.6%	5.3%	2.1%	89%
MS	6.6%	5.4%	1.2%	87%
MT	5.5%	4.9%	4.6%	85%
NC	4.5%	4.8%	1.9%	89%
ND	14%	4.2%	6.3%	75%
NE	5.4%	3.9%	2.8%	88%
NH	8.6%	6.8%	5.1%	79%

NJ	0.0%	0.0%	0.0%	0.0%
NM	4.5%	4.3%	2.8%	88%
NV	5.9%	5.3%	3.7%	85%
NY	5.1%	6.9%	2.2%	86%
OH	4.4%	4.4%	2.4%	89%
OK	4.3%	3.6%	1.5%	91%
OR	5.6%	5.1%	3.2%	86%
PA	3.7%	3.9%	6.5%	86%
RI	0.0%	0.0%	0.0%	0.0%
SC	5.9%	5.1%	2.1%	87%
SD	9.2%	3.4%	3.7%	84%
TN	5.0%	5.5%	1.5%	88%
TX	4.9%	4.9%	1.6%	89%
UT	5.8%	4.6%	5.2%	84%
VA	5.7%	3.0%	3.6%	88%
VT	5.1%	7.3%	1.9%	86%
WA	6.3%	3.9%	2.6%	87%
WI	6.0%	4.0%	3.3%	87%
WV	5.1%	3.2%	2.8%	89%
WY	6.0%	4.3%	6.2%	83%

Table C.3: Shares of suburban residential building archetypes in 2020 by state.

STATE	MFH_LARGE	MFH_SMALL	SFH_ATTACHED	SFH_DETACHED
AL	12%	3.8%	2.3%	82%
AR	12%	5.8%	2.9%	79%
AZ	11%	3.5%	5.9%	79%
CA	14%	5.3%	8.2%	73%
CO	13%	3.1%	8.3%	76%
CT	10%	7.6%	6.7%	76%
DC	0.0%	0.0%	0.0%	0.0%
DE	11%	2.90%	17%	69%
FL	20%	5.5%	7.8%	67%
GA	14%	4.2%	5.6%	77%
IA	13%	3.3%	8.3%	76%
ID	6.9%	4.9%	4.4%	84%
IL	11%	4.7%	9.0%	75%
IN	9.6%	3.9%	5.0%	82%
KS	12%	3.70%	7.50%	77%
KY	12%	6.90%	4.10%	77%
LA	9.7%	5.7%	2.6%	82%
MA	12%	11%	6.80%	71%
MD	17%	1.9%	20%	61%
ME	7.7%	7.7%	4.7%	80%
MI	9.7%	3.1%	6.3%	81%
MN	14%	2.0%	12%	72%
MO	8.8%	4.3%	5.0%	82%
MS	11%	4.5%	1.9%	83%
MT	9.3%	7.3%	8.1%	75%
NC	13%	4.0%	6.3%	76%
ND	32%	4.0%	11%	53%
NE	15%	2.8%	6.1%	76%

NH	10%	5%	8.40%	76%
NJ	12%	8.3%	11%	68%
NM	9.3%	5.0%	5.2%	80%
NV	18%	6.5%	5.5%	70%
NY	8.8%	7.0%	5.1%	79%
OH	10%	4.7%	6.0%	79%
OK	12%	3.8%	2.8%	82%
OR	15%	5.0%	6.2%	74%
PA	7.3%	4.1%	16%	72%
RI	10%	10%	4.4%	75%
SC	11%	4.4%	4.2%	80%
SD	21%	3.1%	8.8%	67%
TN	13%	4.9%	4.7%	77%
TX	18%	4.1%	3.1%	75%
UT	10%	4.2%	7.6%	78%
VA	14%	2.8%	17%	67%
VT	12%	8.2%	9.8%	70%
WA	14%	4.0%	4.9%	77%
WI	14%	5.9%	6.1%	74%
WV	8.70%	4.9%	3.1%	83%
WY	0.0%	0.0%	0.0%	0.0%

Table C.4: Shares of urban residential building archetypes in 2020 by state.

STATE	MFH_LARGE	MFH_SMALL	SFH_ATTACHED	SFH_DETACHED
AL	18%	8.1%	2.5%	72%
AR	0.0%	0.0%	0.0%	0.0%
AZ	23%	5.8%	5.9%	65%
CA	33%	8.1%	9.9%	49%
CO	23%	4.0%	12%	61%
CT	28%	30%	7.6%	34%
DC	43%	7.8%	33%	16%
DE	0.0%	0.0%	0.0%	0.0%
FL	30%	7.0%	6.9%	56%
GA	44%	5.3%	6.9%	44%
IA	17%	2.6%	4.4%	75%
ID	0.0%	0.0%	0.0%	0.0%
IL	33%	23%	5.4%	39%
IN	22%	7.0%	11%	60%
KS	11%	5.9%	4.1%	79%
KY	19%	7.0%	6.6%	67%
LA	16%	15%	8.9%	60%
MA	34%	27%	9.3%	30%
MD	18%	7.0%	57%	17%
ME	0.0%	0.0%	0.0%	0.0%
MI	12%	4.2%	6.7%	77%
MN	31%	7.6%	4.4%	57%
MO	21%	14%	4.0%	61%
MS	17%	7.3%	2.9%	73%
MT	0.0%	0.0%	0.0%	0.0%
NC	34%	7.0%	7.1%	52%
ND	0.0%	0.0%	0.0%	0.0%
NE	17%	3.9%	5.6%	74%
NH	25%	16%	7.6%	51%

NJ	37%	35%	13%	15%
NM	13%	6.4%	4.8%	76%
NV	32%	12%	5.4%	50%
NY	45%	21%	13%	22%
OH	15%	12%	7.8%	65%
OK	25%	6.1%	4.8%	64%
OR	15%	6.5%	4.4%	74%
PA	14%	8.7%	63%	15%
RI	20%	34%	5.2%	41%
SC	0.0%	0.0%	0.0%	0.0%
SD	0.0%	0.0%	0.0%	0.0%
TN	21%	6.9%	6.0%	67%
TX	27%	6.0%	4.2%	63%
UT	26%	11%	11%	52%
VA	27%	6.3%	14%	52%
VT	0.0%	0.0%	0.0%	0.0%
WA	32%	5.0%	6.4%	57%
WI	13%	21%	7.1%	59%
WV	0.0%	0.0%	0.0%	0.0%
WY	0.0%	0.0%	0.0%	0.0%

Table C.5: 2020 site end-use consumption [trillion BTU] in the U.S.

	SPACE HEATING	AIR CONDITIONING
ALL HOMES	**4,026**	**866**
CENSUS REGION AND DIVISION		
NORTHEAST	1,030	93
NEW ENGLAND	293	19
MIDDLE ATLANTIC	737	74
MIDWEST	1,484	131
EAST NORTH CENTRAL	1,054	84
WEST NORTH CENTRAL	430	47
SOUTH	906	497
SOUTH ATLANTIC	459	248
EAST SOUTH CENTRAL	184	66
WEST SOUTH CENTRAL	263	183
WEST	605	145
MOUNTAIN	284	80
MOUNTAIN NORTH	208	18
MOUNTAIN SOUTH	75	62
PACIFIC	322	65

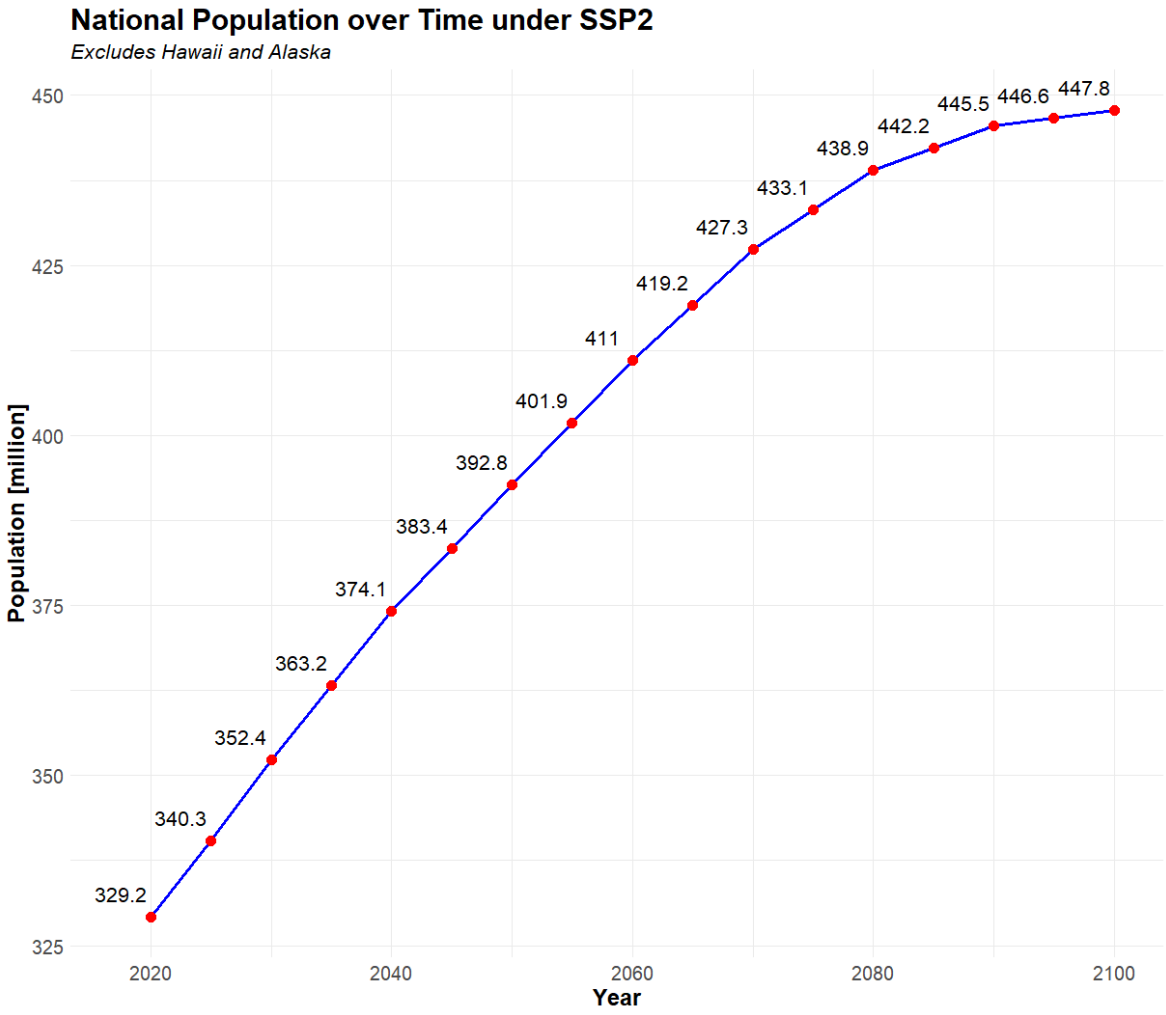


Figure C.1: National population trajectory under SSP2.

U.S. population projections from 2020 to 2100 under Shared Socioeconomic Pathway 2 ("Middle of the Road"), excluding Hawaii and Alaska. This population trajectory is applied uniformly across all policy scenarios. Source: GCAM-USA [139,140]

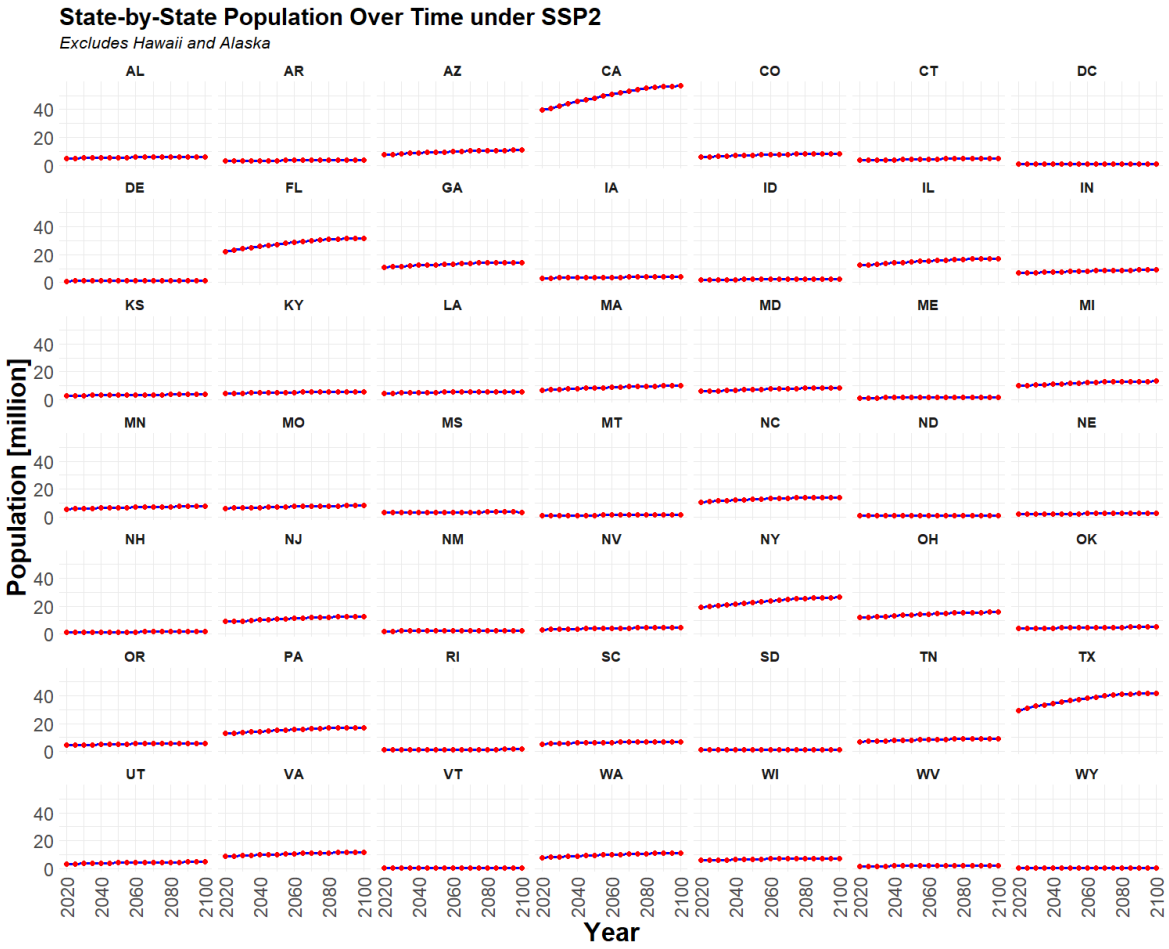


Figure C.2: State-level population trajectories under SSP2.

State-by-state population projections from 2020 to 2100 under Shared Socioeconomic Pathway 2, excluding Hawaii and Alaska. State-level population trajectories are held constant across all policy scenarios to isolate the effects of housing structure, energy efficiency, and comfort assumptions on residential energy demand and emissions. Source: GCAM-USA [139,140]

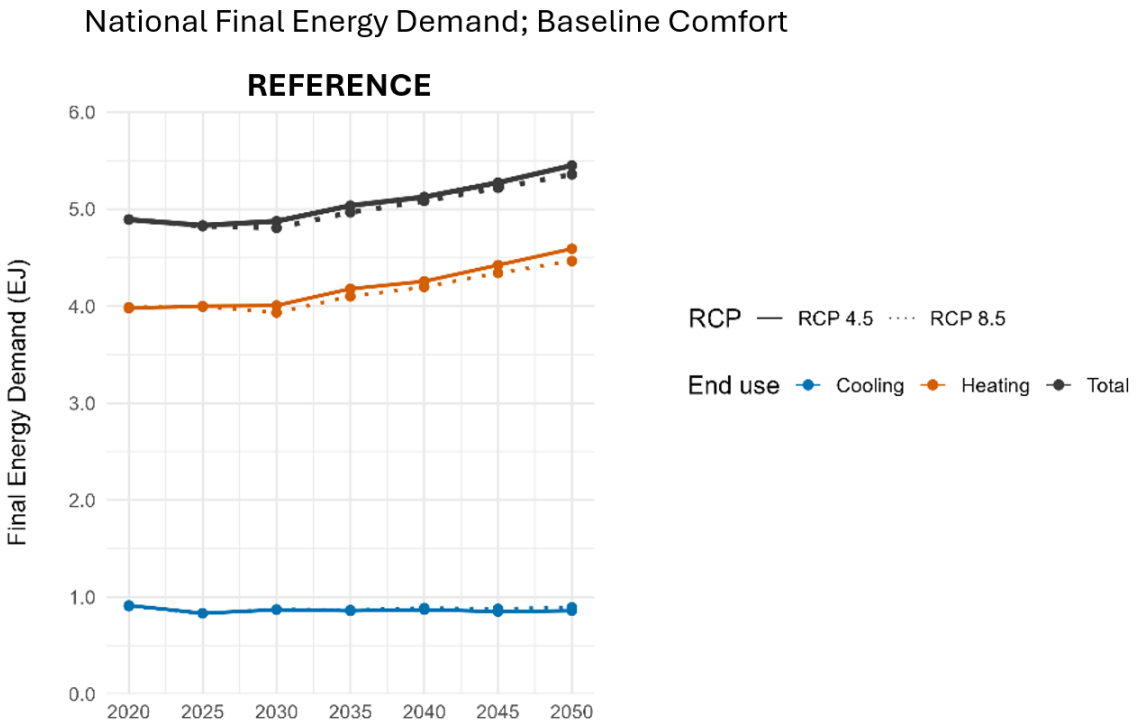


Figure C.3: Sensitivity of national final residential energy demand to climate pathways.

Final residential energy demand for heating, cooling, and total use under RCP4.5 and RCP8.5 using Baseline Comfort assumptions. The Reference scenario is shown as a representative case to illustrate that differences in climate pathways produce relatively small changes in mid-century energy demand compared with differences across policy scenarios.

Bibliography

(1) US EPA, O. *Commercial and Residential Sector Emissions*. https://www.epa.gov/ghgemissions/commercial-and-residential-sector-emissions (accessed 2026-02-10).

(2) US EPA, O. *Inventory of U.S. Greenhouse Gas Emissions and Sinks: 1990-2022*. https://www.epa.gov/ghgemissions/inventory-us-greenhouse-gas-emissions-and-sinks-1990-2022 (accessed 2025-01-11).

(3) *U.S. Energy Information Administration - EIA - Independent Statistics and Analysis*. https://www.eia.gov/environment/emissions/carbon/ (accessed 2026-02-10).

(4) *Annual Energy Outlook 2025 - U.S. Energy Information Administration (EIA)*. https://www.eia.gov/outlooks/aeo/ (accessed 2026-02-10).

(5) *Residential Buildings Factsheet | Center for Sustainable Systems*. https://css.umich.edu/publications/factsheets/built-environment/residential-buildings-factsheet (accessed 2026-02-10).

(6) van Ruijven, B. J.; De Cian, E.; Sue Wing, I. Amplification of Future Energy Demand Growth Due to Climate Change. *Nat. Commun.* **2019**, *10* (1), 2762. https://doi.org/10.1038/s41467-019-10399-3.

(7) *The Paris Agreement - Publication | UNFCCC*. https://unfccc.int/documents/184656 (accessed 2026-01-31).

(8) Camarasa, C.; Mata, É.; Navarro, J. P. J.; Reyna, J.; Bezerra, P.; Angelkorte, G. B.; Feng, W.; Filippidou, F.; Forthuber, S.; Harris, C.; Sandberg, N. H.; Ignatiadou, S.; Kranzl, L.; Langevin, J.; Liu, X.; Müller, A.; Soria, R.; Villamar, D.; Dias, G. P.; Wanemark, J.; Yaramenka, K. A Global Comparison of Building Decarbonization Scenarios by 2050 towards 1.5–2 °C Targets. *Nat. Commun.* **2022**, *13* (1), 3077. https://doi.org/10.1038/s41467-022-29890-5.

(9) Cannon, A. J. Twelve Months at 1.5 °C Signals Earlier than Expected Breach of Paris Agreement Threshold. *Nat. Clim. Change* **2025**, *15* (3), 266–269. https://doi.org/10.1038/s41558-025-02247-8.

(10) *World on track to breach 1.5C target by 2030*. SciDev.Net. https://www.scidev.net/global/news/world-on-track-to-breach-1-5c-target-by-2030/ (accessed 2026-02-10).

(11) *Chapter 9: Buildings*. https://www.ipcc.ch/report/ar6/wg3/chapter/chapter-9/ (accessed 2026-01-12).

(12) Wright, D.; Meadows, D. H. *Thinking in Systems*, 0 ed.; Routledge, 2012. https://doi.org/10.4324/9781849773386.

(13) Casquero-Modrego, N.; Antonopoulos, C.; Fuentes, T. L.; McCord, K. H.; Walker, I. S. Decarbonizing Residential Buildings in the United States: A Comparative Analysis of Households and Construction Professionals. *Energy Res. Soc. Sci.* **2025**, *120*, 103908. https://doi.org/10.1016/j.erss.2024.103908.

(14) Misconel, S.; Zimmermann, F.; Mikurda, J.; Möst, D.; Kunze, R.; Gnann, T.; Kühnbach, M.; Speth, D.; Pelka, S.; Yu, S. Model Coupling and Comparison on Optimal Load Shifting of Battery Electric Vehicles and Heat Pumps Focusing on Generation Adequacy. *Energy* **2024**, *305*, 132266. https://doi.org/10.1016/j.energy.2024.132266.
(15) White, P. R.; Rhodes, J. D.; Wilson, E. J. H.; Webber, M. E. Quantifying the Impact of Residential Space Heating Electrification on the Texas Electric Grid. *Appl. Energy* **2021**, *298*, 117113. https://doi.org/10.1016/j.apenergy.2021.117113.
(16) Wildstein, P. J.; Craig, M. T.; Vaishnav, P. Participant Overrides Can Halve the Reliability Value of Direct Load Control Programs. *Energy Build.* **2023**, *299*, 113606. https://doi.org/10.1016/j.enbuild.2023.113606.
(17) Waite, M.; Modi, V. Electricity Load Implications of Space Heating Decarbonization Pathways. *Joule* **2020**, *4* (2), 376–394. https://doi.org/10.1016/j.joule.2019.11.011.
(18) Rep. Yarmuth, J. A. [D-K.-3. *Text - H.R.5376 - 117th Congress (2021-2022): Inflation Reduction Act of 2022*. https://www.congress.gov/bill/117th-congress/house-bill/5376/text (accessed 2025-09-30).
(19) Heinz, E.; Sovacool, B. K.; Kwan, T.; Petit, V. Reviewing the 95 Sociotechnical Barriers to the Decarbonization of Buildings. *Nat. Commun.* **2025**, *16* (1), 9983. https://doi.org/10.1038/s41467-025-64923-9.
(20) Singhal, P.; Sommer, S.; Kaestner, K.; Pahle, M. Split-Incentives in Energy Efficiency Investments? Evidence from Rental Housing. *Resour. Energy Econ.* **2025**, *82*, 101488. https://doi.org/10.1016/j.reseneeco.2025.101488.
(21) Huang, L.; Nock, D.; Cong, S.; Qiu, Y. (Lucy). Inequalities across Cooling and Heating in Households: Energy Equity Gaps. *Energy Policy* **2023**, *182*, 113748. https://doi.org/10.1016/j.enpol.2023.113748.
(22) Sovacool, B. K.; Dworkin, M. H. Energy Justice: Conceptual Insights and Practical Applications. *Appl. Energy* **2015**, *142*, 435–444. https://doi.org/10.1016/j.apenergy.2015.01.002.
(23) Bednar, D. J.; Reames, T. G.; Keoleian, G. A. The Intersection of Energy and Justice: Modeling the Spatial, Racial/Ethnic and Socioeconomic Patterns of Urban Residential Heating Consumption and Efficiency in Detroit, Michigan. *Energy Build.* **2017**, *143*, 25–34. https://doi.org/10.1016/j.enbuild.2017.03.028.
(24) McKenna, C.; Gronlund, C.; Vaishnav, P. Heating with Justice: Barriers and Solutions to a Just Energy Transition in Cold Climates. *Resour. Conserv. Recycl.* **2024**, *208*, 107699. https://doi.org/10.1016/j.resconrec.2024.107699.
(25) Mastrucci, A.; van Ruijven, B.; Byers, E.; Poblete-Cazenave, M.; Pachauri, S. Global Scenarios of Residential Heating and Cooling Energy Demand and CO2 Emissions. *Clim. Change* **2021**, *168* (3), 14. https://doi.org/10.1007/s10584-021-03229-3.
(26) Ürge-Vorsatz, D.; Rosenzweig, C.; Dawson, R. J.; Sanchez Rodriguez, R.; Bai, X.; Barau, A. S.; Seto, K. C.; Dhakal, S. Locking in Positive Climate Responses in Cities. *Nat. Clim. Change* **2018**, *8* (3), 174–177. https://doi.org/10.1038/s41558-018-0100-6.
(27) Li, X. 'Cathy'; Zhao, L.; Qin, Y.; Oleson, K.; Zhang, Y. Elevated Urban Energy Risks Due to Climate-Driven Biophysical Feedbacks. *Nat. Clim. Change* **2024**, *14* (10), 1056–1063. https://doi.org/10.1038/s41558-024-02108-w.
(28) Friedlingstein, P.; O'Sullivan, M.; Jones, M. W.; Andrew, R. M.; Bakker, D. C. E.; Hauck, J.; Landschützer, P.; Le Quéré, C.; Li, H.; Luijkx, I. T.; Peters, G. P.; Peters, W.; Pongratz, J.; Schwingshackl, C.; Sitch, S.; Canadell, J. G.; Ciais, P.; Aas, K.; Alin, S. R.; Anthoni,

P.; Barbero, L.; Bates, N. R.; Bellouin, N.; Benoit-Cattin, A.; Berghoff, C. F.; Bernardello, R.; Bopp, L.; Brasika, I. B. M.; Chamberlain, M. A.; Chandra, N.; Chevallier, F.; Chini, L. P.; Collier, N. O.; Colligan, T. H.; Cronin, M.; Djeutchouang, L.; Dou, X.; Enright, M. P.; Enyo, K.; Erb, M.; Evans, W.; Feely, R. A.; Feng, L.; Ford, D. J.; Foster, A.; Fransner, F.; Gasser, T.; Gehlen, M.; Gkritzalis, T.; Goncalves De Souza, J.; Grassi, G.; Gregor, L.; Gruber, N.; Guenet, B.; Gürses, Ö.; Harrington, K.; Harris, I.; Heinke, J.; Hurtt, G. C.; Iida, Y.; Ilyina, T.; Ito, A.; Jacobson, A. R.; Jain, A. K.; Jarníková, T.; Jersild, A.; Jiang, F.; Jones, S. D.; Kato, E.; Keeling, R. F.; Klein Goldewijk, K.; Knauer, J.; Kong, Y.; Korsbakken, J. I.; Koven, C.; Kunimitsu, T.; Lan, X.; Liu, J.; Liu, Z.; Liu, Z.; Lo Monaco, C.; Ma, L.; Marland, G.; McGuire, P. C.; McKinley, G. A.; Melton, J.; Monacci, N.; Monier, E.; Morgan, E. J.; Munro, D. R.; Müller, J. D.; Nakaoka, S.-I.; Nayagam, L. R.; Niwa, Y.; Nutzel, T.; Olsen, A.; Omar, A. M.; Pan, N.; Pandey, S.; Pierrot, D.; Qin, Z.; Regnier, P. A. G.; Rehder, G.; Resplandy, L.; Roobaert, A.; Rosan, T. M.; Rödenbeck, C.; Schwinger, J.; Skjelvan, I.; Smallman, T. L.; Spada, V.; Sreeush, M. G.; Sun, Q.; Sutton, A. J.; Sweeney, C.; Swingedouw, D.; Séférian, R.; Takao, S.; Tatebe, H.; Tian, H.; Tian, X.; Tilbrook, B.; Tsujino, H.; Tubiello, F.; van Ooijen, E.; van der Werf, G.; van de Velde, S. J.; Walker, A.; Wanninkhof, R.; Yang, X.; Yuan, W.; Yue, X.; Zeng, J. Global Carbon Budget 2025. *Earth Syst. Sci. Data Discuss.* **2025**, 1–139. https://doi.org/10.5194/essd-2025-659.

(29) *Building America Climate-Specific Guidance*. Energy.gov. https://www.energy.gov/eere/buildings/building-america-climate-specific-guidance (accessed 2026-02-01).

(30) Reyna, J.; Wilson, E.; Parker, A.; Satre-Meloy, A.; Egerter, A.; Bianchi, C.; Praprost, M.; Speake, A.; Liu, L.; Horsey, R.; Dahlhausen, M.; Caradonna, C.; Rothgeb, S. U.S. Building Stock Characterization Study: A National Typology for Decarbonizing U.S. Buildings. *Renew. Energy* **2022**.

(31) Gagnon, P.; Sanchez Perez, P. A.; Florez, J.; Morris, J.; Llerena Velasquez, M.; Eisenman, J. *Cambium 2024 Scenario Descriptions and Documentation*; NREL/TP-6A40-93005; National Renewable Energy Laboratory (NREL), Golden, CO (United States), 2025. https://doi.org/10.2172/2558937.

(32) Habeeb, D.; Vargo, J.; Stone, B. Rising Heat Wave Trends in Large US Cities. *Nat. Hazards* **2015**, *76* (3), 1651–1665. https://doi.org/10.1007/s11069-014-1563-z.

(33) Jones, A.; Nock, D.; Samaras, C.; Qiu, Y. (Lucy); Xing, B. Climate Change Impacts on Future Residential Electricity Consumption and Energy Burden: A Case Study in Phoenix, Arizona. *Energy Policy* **2023**, *183*, 113811. https://doi.org/10.1016/j.enpol.2023.113811.

(34) Cong, S.; Nock, D.; Qiu, Y. L.; Xing, B. Unveiling Hidden Energy Poverty Using the Energy Equity Gap. *Nat. Commun.* **2022**, *13* (1), 2456. https://doi.org/10.1038/s41467-022-30146-5.

(35) *Lifting the High Energy Burden in America's Largest Cities: How Energy Efficiency Can Improve Low Income and Underserved Communities*. Energy Efficiency for All. https://energyefficiencyforall.org/resources/lifting-the-high-energy-burden-in-americas-largest-cities-how-energy/ (accessed 2026-02-01).

(36) DeCarolis, J.; Hunter, K.; Sreepathi, S. The TEMOA Project: Tools for Energy Model Optimization and Analysis.

(37) Craig, M. T.; Jaramillo, P.; Hodge, B.-M.; Nijssen, B.; Brancucci, C. Compounding Climate Change Impacts during High Stress Periods for a High Wind and Solar Power

System in Texas. *Environ. Res. Lett.* **2020**, *15* (2), 024002. https://doi.org/10.1088/1748-9326/ab6615.
(38) *Buildings – Analysis*. IEA. https://www.iea.org/reports/buildings (accessed 2023-06-26).
(39) Davis, S. J.; Lewis, N. S.; Shaner, M.; Aggarwal, S.; Arent, D.; Azevedo, I. L.; Benson, S. M.; Bradley, T.; Brouwer, J.; Chiang, Y.-M.; Clack, C. T. M.; Cohen, A.; Doig, S.; Edmonds, J.; Fennell, P.; Field, C. B.; Hannegan, B.; Hodge, B.-M.; Hoffert, M. I.; Ingersoll, E.; Jaramillo, P.; Lackner, K. S.; Mach, K. J.; Mastrandrea, M.; Ogden, J.; Peterson, P. F.; Sanchez, D. L.; Sperling, D.; Stagner, J.; Trancik, J. E.; Yang, C.-J.; Caldeira, K. Net-Zero Emissions Energy Systems. *Science* **2018**, *360* (6396), eaas9793. https://doi.org/10.1126/science.aas9793.
(40) The Heat Is On. *Nat. Energy* **2016**, *1* (12), 1–1. https://doi.org/10.1038/nenergy.2016.193.
(41) Rosenow, J.; Gibb, D.; Nowak, T.; Lowes, R. Heating up the Global Heat Pump Market. *Nat. Energy* **2022**, *7* (10), 901–904. https://doi.org/10.1038/s41560-022-01104-8.
(42) Berrill, P.; Wilson, E. J. H.; Reyna, J. L.; Fontanini, A. D.; Hertwich, E. G. Decarbonization Pathways for the Residential Sector in the United States. *Nat. Clim. Change* **2022**, *12* (8), 712–718. https://doi.org/10.1038/s41558-022-01429-y.
(43) Heating – Analysis. *IEA*. https://www.iea.org/reports/heating (accessed 2023-05-11).
(44) Jenkins, J. D.; Mayfield, E. N.; Larson, E. D.; Pacala, S. W.; Greig, C. Mission Net-Zero America: The Nation-Building Path to a Prosperous, Net-Zero Emissions Economy. *Joule* **2021**, *5* (11), 2755–2761. https://doi.org/10.1016/j.joule.2021.10.016.
(45) Gibb, D.; Rosenow, J.; Lowes, R.; Hewitt, N. J. Coming in from the Cold: Heat Pump Efficiency at Low Temperatures. *Joule* **2023**, *7* (9), 1939–1942. https://doi.org/10.1016/j.joule.2023.08.005.
(46) Wu, C.; Liu, F.; Li, X.; Wang, Z.; Xu, Z.; Zhao, W.; Yang, Y.; Wu, P.; Xu, C.; Wang, Y. Low-Temperature Air Source Heat Pump System for Heating in Severely Cold Area: Long-Term Applicability Evaluation. *Build. Environ.* **2022**, *208*, 108594. https://doi.org/10.1016/j.buildenv.2021.108594.
(47) Schoenbauer, B.; Kessler, N.; Bohac, D.; Kushler, M. Field Assessment of Cold Climate Air Source Heat Pumps.
(48) Deetjen, T. A.; Walsh, L.; Vaishnav, P. US Residential Heat Pumps: The Private Economic Potential and Its Emissions, Health, and Grid Impacts. *Environ. Res. Lett.* **2021**, *16* (8), 084024. https://doi.org/10.1088/1748-9326/ac10dc.
(49) Vaishnav, P.; Fatimah, A. M. The Environmental Consequences of Electrifying Space Heating. *Environ. Sci. Technol.* **2020**, *54* (16), 9814–9823. https://doi.org/10.1021/acs.est.0c02705.
(50) White, L. V.; Sintov, N. D. Health and Financial Impacts of Demand-Side Response Measures Differ across Sociodemographic Groups. *Nat. Energy* **2020**, *5* (1), 50–60. https://doi.org/10.1038/s41560-019-0507-y.
(51) Pergantis, E. N.; Priyadarshan; Theeb, N. A.; Dhillon, P.; Ore, J. P.; Ziviani, D.; Groll, E. A.; Kircher, K. J. Field Demonstration of Predictive Heating Control for an All-Electric House in a Cold Climate. *Appl. Energy* **2024**, *360*, 122820. https://doi.org/10.1016/j.apenergy.2024.122820.
(52) Pelletier, F.; Faruqui, A. Does Dynamic Pricing Work in a Winter-Peaking Climate? A Case Study of Hydro Quebec. *Electr. J.* **2022**, *35* (2), 107080. https://doi.org/10.1016/j.tej.2022.107080.

(53) *EnergyPlus™*; EnergyPlus™ (e+); 005462MLTPL00; National Renewable Energy Laboratory (NREL), Golden, CO (United States); Lawrence Berkeley National Laboratory (LBNL), Berkeley, CA (United States), 2017. https://www.osti.gov/biblio/1395882 (accessed 2023-06-26).
(54) *Wilson: A high-granularity approach to modeling energy... - Google Scholar*. https://scholar.google.com/scholar_lookup?title=A%20High-Granularity%20Approach%20to%20Modeling%20Energy%20Consumption%20and%20Savings%20Potential%20in%20the%20u.S.%20Residential%20Building%20stock%3A%20Preprint&author=E.%20Wilson&publication_year=2022 (accessed 2026-02-12).
(55) *Average energy prices for the United States, regions, census divisions, and selected metropolitan areas : Midwest Information Office : U.S. Bureau of Labor Statistics*. https://www.bls.gov/regions/midwest/data/averageenergyprices_selectedareas_table.htm (accessed 2023-05-23).
(56) *Electricity Marginal Factors Estimates*. https://cedm.shinyapps.io/MarginalFactors/ (accessed 2023-05-23).
(57) *Avoided Cost Calculator for Distributed Energy Resources (DER)*. E3. https://www.ethree.com/public_proceedings/energy-efficiency-calculator/ (accessed 2026-02-15).
(58) Wilson, E. J.; Christensen, C. B.; Horowitz, S. G.; Robertson, J. J.; Maguire, J. B. *Energy Efficiency Potential in the U.S. Single-Family Housing Stock*; NREL/TP-5500-68670; National Renewable Energy Lab. (NREL), Golden, CO (United States), 2017. https://doi.org/10.2172/1414819.
(59) *TMY3 Weather Data for ComStock and ResStock | NLR Data Catalog*. https://data.nrel.gov/submissions/156 (accessed 2026-02-12).
(60) *ccASHP Specification & Product List | Northeast Energy Efficiency Partnerships*. https://neep.org/heating-electrification/ccashp-specification-product-list (accessed 2023-07-07).
(61) US EPA, O. *EPA Issues Supplemental Proposal to Reduce Methane and Other Harmful Pollution from Oil and Natural Gas Operations*. https://www.epa.gov/controlling-air-pollution-oil-and-natural-gas-operations/epa-issues-supplemental-proposal-reduce (accessed 2024-08-20).
(62) *Notice of Availability: Proposed Draft Guidance for Estimating Value per Statistical Life*. Federal Register. https://www.federalregister.gov/documents/2023/03/24/2023-06081/notice-of-availability-proposed-draft-guidance-for-estimating-value-per-statistical-life (accessed 2024-08-20).
(63) Carson, R. T.; Hanemann, W. M. Chapter 17 Contingent Valuation. In *Handbook of Environmental Economics*; Mler, K.-G., Vincent, J. R., Eds.; Valuing Environmental Changes; Elsevier, 2005; Vol. 2, pp 821–936. https://doi.org/10.1016/S1574-0099(05)02017-6.
(64) *Standard 90.1*. https://www.ashrae.org/technical-resources/bookstore/standard-90-1 (accessed 2024-09-06).
(65) Naderi, S.; Heslop, S.; Chen, D.; MacGill, I.; Pignatta, G. Consumer Cost Savings, Improved Thermal Comfort, and Reduced Peak Air Conditioning Demand through Pre-Cooling in Australian Housing. *Energy Build.* **2022**, *271*, 112172. https://doi.org/10.1016/j.enbuild.2022.112172.

(66) Nicol, F.; Humphreys, M. Derivation of the Adaptive Equations for Thermal Comfort in Free-Running Buildings in European Standard EN15251. *Build. Environ.* **2010**, *45* (1), 11–17. https://doi.org/10.1016/j.buildenv.2008.12.013.
(67) Kwon, M.; Cong, S.; Nock, D.; Huang, L.; Qiu, Y. (Lucy); Xing, B. Forgone Summertime Comfort as a Function of Avoided Electricity Use. *Energy Policy* **2023**, *183*, 113813. https://doi.org/10.1016/j.enpol.2023.113813.
(68) Acton, J. P.; Mitchell, B. M. *Welfare Analysis of Electricity Rate Changes*; 1983. https://www.rand.org/pubs/notes/N2010.html (accessed 2026-02-12).
(69) Jones, A. D.; Rastogi, D.; Vahmani, P.; Stansfield, A. M.; Reed, K. A.; Thurber, T.; Ullrich, P. A.; Rice, J. S. Continental United States Climate Projections Based on Thermodynamic Modification of Historical Weather. *Sci. Data* **2023**, *10*, 664. https://doi.org/10.1038/s41597-023-02485-5.
(70) Wilson, E. J. H.; Harris, C. B.; Robertson, J. J.; Agan, J. Evaluating Energy Efficiency Potential in Low-Income Households: A Flexible and Granular Approach. *Energy Policy* **2019**, *129*, 710–737. https://doi.org/10.1016/j.enpol.2019.01.054.
(71) Deming, W. E.; Stephan, F. F. On a Least Squares Adjustment of a Sampled Frequency Table When the Expected Marginal Totals Are Known. *Ann. Math. Stat.* **1940**, *11* (4), 427–444.
(72) *Standard 55 – Thermal Environmental Conditions for Human Occupancy*. https://www.ashrae.org/technical-resources/bookstore/standard-55-thermal-environmental-conditions-for-human-occupancy (accessed 2024-09-06).
(73) *Hours of Safety in Cold Weather*. RMI. https://rmi.org/insight/hours-of-safety-in-cold-weather/ (accessed 2024-09-16).
(74) High Indoor Temperatures. In *WHO Housing and Health Guidelines*; World Health Organization, 2018.
(75) Information (NCEI), N. C. for E. *U.S. Monthly Climate Normals (1981-2010)*. https://www.ncei.noaa.gov/access/metadata/landing-page/bin/iso?id=gov.noaa.ncdc:C00822 (accessed 2025-01-21).
(76) Cong, S.; Ku, A. L.; Nock, D.; Ng, C.; Qiu, Y. (Lucy). Comfort or Cash? Lessons from the COVID-19 Pandemic's Impact on Energy Insecurity and Energy Limiting Behavior in Households. *Energy Res. Soc. Sci.* **2024**, *113*, 103528. https://doi.org/10.1016/j.erss.2024.103528.
(77) Ballester, J.; Quijal-Zamorano, M.; Méndez Turrubiates, R. F.; Pegenaute, F.; Herrmann, F. R.; Robine, J. M.; Basagaña, X.; Tonne, C.; Antó, J. M.; Achebak, H. Heat-Related Mortality in Europe during the Summer of 2022. *Nat. Med.* **2023**, *29* (7), 1857–1866. https://doi.org/10.1038/s41591-023-02419-z.
(78) Martínez-Solanas, È.; Quijal-Zamorano, M.; Achebak, H.; Petrova, D.; Robine, J.-M.; Herrmann, F. R.; Rodó, X.; Ballester, J. Projections of Temperature-Attributable Mortality in Europe: A Time Series Analysis of 147 Contiguous Regions in 16 Countries. *Lancet Planet. Health* **2021**, *5* (7), e446–e454. https://doi.org/10.1016/S2542-5196(21)00150-9.
(79) Tessum, C. W.; Hill, J. D.; Marshall, J. D. InMAP: A Model for Air Pollution Interventions. *PLOS ONE* **2017**, *12* (4), e0176131. https://doi.org/10.1371/journal.pone.0176131.
(80) Heo, J.; Adams, P. J.; Gao, H. O. Reduced-Form Modeling of Public Health Impacts of Inorganic PM2.5 and Precursor Emissions. *Atmos. Environ.* **2016**, *137*, 80–89. https://doi.org/10.1016/j.atmosenv.2016.04.026.

(81) *APModel*. https://nickmuller.tepper.cmu.edu/APModel.aspx (accessed 2024-09-16).
(82) Mai, T. T.; Jadun, P.; Logan, J. S.; McMillan, C. A.; Muratori, M.; Steinberg, D. C.; Vimmerstedt, L. J.; Haley, B.; Jones, R.; Nelson, B. *Electrification Futures Study: Scenarios of Electric Technology Adoption and Power Consumption for the United States*; NREL/TP--6A20-71500; National Renewable Energy Laboratory (NREL), Golden, CO (United States), 2018. https://doi.org/10.2172/1459351.
(83) Garimella, S.; Lockyear, K.; Pharis, D.; Chawa, O. E.; Hughes, M. T.; Kini, G. Realistic Pathways to Decarbonization of Building Energy Systems. *Joule* **2022**, *6* (5), 956–971. https://doi.org/10.1016/j.joule.2022.04.003.
(84) Ma, L.; Sun, Y.; Wang, F.; Wang, M.; Zhang, S.; Wang, Z. Advancements in Anti-Frosting and Defrosting Techniques for Air Source Heat Pumps: A Comprehensive Review of Recent Progress. *Appl. Energy* **2025**, *377*, 124358. https://doi.org/10.1016/j.apenergy.2024.124358.
(85) Zhu, J. H.; Sun, Y. Y.; Wang, W.; Deng, S. M.; Ge, Y. J.; Li, L. T. Developing a New Frosting Map to Guide Defrosting Control for Air-Source Heat Pump Units. *Appl. Therm. Eng.* **2015**, *90*, 782–791. https://doi.org/10.1016/j.applthermaleng.2015.06.076.
(86) Song, M.; Deng, S.; Dang, C.; Mao, N.; Wang, Z. Review on Improvement for Air Source Heat Pump Units during Frosting and Defrosting. *Appl. Energy* **2018**, *211*, 1150–1170. https://doi.org/10.1016/j.apenergy.2017.12.022.
(87) Nawaz, K.; Elatar, A. F.; Fricke, B. A. *A Critical Literature Review of Defrost Technologies for Heat Pumps and Refrigeration Systems*; ORNL/SPR-2018/1007; Oak Ridge National Laboratory (ORNL), Oak Ridge, TN (United States), 2018. https://doi.org/10.2172/1474464.
(88) Dongellini, M.; Piazzi, A.; Biagi, F. D.; Morini, G. L. The Modelling of Reverse Defrosting Cycles of Air-to-Water Heat Pumps with TRNSYS. *E3S Web Conf.* **2019**, *111*, 01063. https://doi.org/10.1051/e3sconf/201911101063.
(89) Milev, G.; Al-Habaibeh, A.; Fanshawe, S.; Siena, F. L. Investigating the Effect of the Defrost Cycles of Air-Source Heat Pumps on Their Electricity Demand in Residential Buildings. *Energy Build.* **2023**, *300*, 113656. https://doi.org/10.1016/j.enbuild.2023.113656.
(90) Winkler, J.; Ramaraj, S. *Field Validation of Air-Source Heat Pumps for Cold Climates*; NREL/TP--5500-84745; National Renewable Energy Laboratory (NREL), Golden, CO (United States), 2023. https://doi.org/10.2172/1973090.
(91) *Cold Climate Air Source Heat Pump Final Report | Center for Energy and Environment*. https://www.mncee.org/cold-climate-air-source-heat-pump-final-report (accessed 2025-10-08).
(92) Wang, W.; Feng, Y. C.; Zhu, J. H.; Li, L. T.; Guo, Q. C.; Lu, W. P. Performances of Air Source Heat Pump System for a Kind of Mal-Defrost Phenomenon Appearing in Moderate Climate Conditions. *Appl. Energy* **2013**, *112*, 1138–1145. https://doi.org/10.1016/j.apenergy.2012.12.054.
(93) Guo, X.-M.; Chen, Y.-G.; Wang, W.-H.; Chen, C.-Z. Experimental Study on Frost Growth and Dynamic Performance of Air Source Heat Pump System. *Appl. Therm. Eng.* **2008**, *28* (17), 2267–2278. https://doi.org/10.1016/j.applthermaleng.2008.01.007.
(94) Wu, C.; Wang, Z.; Li, X.; Xu, Z.; Xu, C.; Yang, Y.; Zhao, W.; Wang, Y. Field Experimental Research on Retarding Frosting and Improving Defrosting Performance of

Air Source Heat Pumps through Variable Frequency Technology. *J. Build. Eng.* **2023**, *64*, 105628. https://doi.org/10.1016/j.jobe.2022.105628.
(95) Liang, S.; Wang, H.; Gao, X.; Tian, X.; Zhu, H.; Hu, S.; Lin, C. Experimental Study on the Operating Performance of the Air Source Heat Pump (ASHP) with Variable Outdoor Airflow Rate under the Standard Frosting Condition. *Energy Built Environ.* **2024**, *5* (5), 719–726. https://doi.org/10.1016/j.enbenv.2023.06.001.
(96) Kwak, K.; Bai, C. A Study on the Performance Enhancement of Heat Pump Using Electric Heater under the Frosting Condition: Heat Pump under Frosting Condition. *Appl. Therm. Eng.* **2010**, *30* (6), 539–543. https://doi.org/10.1016/j.applthermaleng.2009.10.016.
(97) Wei, W.; Jin, X.; Dong, Q.; Ni, L.; Zhao, S.; Wang, W.; Sun, Y. Frosting Performance Variations of Variable-Frequency Air Source Heat Pump in Different Climatic Regions. *Appl. Therm. Eng.* **2023**, *219*, 119356. https://doi.org/10.1016/j.applthermaleng.2022.119356.
(98) Li, Z.; Sun, Y.; Wang, W.; Wei, W. An Improved Equivalent Temperature Drop Method for Evaluating the Operating Performances of ASHP Units under Frosting Conditions Considering Their Configuration and Operation. *Energy Build.* **2025**, *331*, 115370. https://doi.org/10.1016/j.enbuild.2025.115370.
(99) Munk, J.; Shen, B.; Gehl, A. C. *Cost-Optimized Cold Climate Heat Pump Development and Field Test*; ORNL/TM-2021/2044; Oak Ridge National Laboratory (ORNL), Oak Ridge, TN (United States), 2021. https://doi.org/10.2172/1814297.
(100) Winkler, J.; Shoukas, G. *Cold Climate Air-Source Heat Pump Demonstration and Analysis: Experimental Study on Cold Temperature Performance*; NREL/TP--5500-89413; National Renewable Energy Laboratory (NREL), Golden, CO (United States); Xcel Energy, Minneapolis, MN (United States), 2024. https://doi.org/10.2172/2352707.
(101) Shoukas, G.; Bonnema, E.; Paranjothi, G.; Faramarzi, R.; Klun, L. *Performance Assessment of High Efficiency Variable Speed Air-Source Heat Pump in Cold Climate Applications*; NREL/TP-5500-80802; National Renewable Energy Laboratory (NREL), Golden, CO (United States), 2022. https://doi.org/10.2172/1847877.
(102) *Residential Cold Climate Heat Pump Challenge*. Energy.gov. https://www.energy.gov/eere/buildings/residential-cold-climate-heat-pump-challenge (accessed 2025-12-05).
(103) *Improving the Frost Resistance Performance of Hydrophilic Coatings by Modulating the Formation of Zwitterionic Polymers | ACS Applied Polymer Materials*. https://pubs.acs.org/doi/full/10.1021/acsapm.3c00687?casa_token=V1PH77UKBboAAAAA%3AhI6lCI8Mkuto2pHgsRl60AdB8OrGe6-6bff685UnRnqXRYoLaFYYlF0H3sOAbcVR_L1KVlzC6N52Nw (accessed 2025-12-05).
(104) *A multifunctional antifog, antifrost, and self-cleaning zwitterionic polymer coating based on poly(SBMA-co-AA) | Journal of Coatings Technology and Research*. https://link.springer.com/article/10.1007/s11998-020-00324-5 (accessed 2025-12-05).
(105) Lee, E.; Lee, J.; Kim, D.; Jeong, K.; Seo, J.-H. Investigation of Hydration State Effects on Ice and Frost Formation on Hydrogel-Coated Surfaces for Enhanced Anti-Icing/Frosting Properties. *Prog. Org. Coat.* **2024**, *197*, 108857. https://doi.org/10.1016/j.porgcoat.2024.108857.
(106) Zhang, S.; Gao, F.; Jiang, Z.; He, Q.; Lu, J.; Hou, Y.; Zhan, X.; Zhang, Q. Bioinspired Durable Interpenetrating Network Anti-Icing Coatings Enabled by Binders and

Hydrophobic-Ion Specific Synergies. *Chem. Eng. J.* **2024**, *479*, 147836. https://doi.org/10.1016/j.cej.2023.147836.
(107) Lee, E.; Seo, S.; Seo, J.-H. Effect of Hydration States on the Anti-Icing/Frosting Performance of Zwitterionic Hydrogel-Coated Surfaces. *Langmuir* **2025**, *41* (5), 3367–3376. https://doi.org/10.1021/acs.langmuir.4c04359.
(108) *Index of /Download/Weather/TMY3*. https://doe2.com/Download/Weather/TMY3/ (accessed 2026-01-10).
(109) Nawawi, S.; Yi, M.; Craig, M.; Deetjen, T.; Vaishnav, P. Cross-Sectoral Trade-Offs in a Changing Climate: Surrogate Models to Balance Home Energy Bills, Occupant Comfort, and Power System Externalities. *iScience* **2025**, *28* (6), 112728. https://doi.org/10.1016/j.isci.2025.112728.
(110) White_Rodgers_47D01U_843_Instruction_Installation_Manual.Pdf.
(111) National Academies of Sciences, Engineering; Medicine. *Current Methods for Life-Cycle Analyses of Low-Carbon Transportation Fuels in the United States*; The National Academies Press: Washington, DC, 2022. https://doi.org/10.17226/26402.
(112) *Residential Energy Consumption Survey (RECS) - Energy Information Administration*. https://www.eia.gov/consumption/residential/ (accessed 2024-08-20).
(113) Cheng, L.; Vaishnav, P. How Do Distributed Energy Resources Change the Economics of Decarbonization in Michigan. *Energy Build.* **2025**, *345*, 116051. https://doi.org/10.1016/j.enbuild.2025.116051.
(114) US EPA, O. *Fast Facts on Transportation Greenhouse Gas Emissions*. https://www.epa.gov/greenvehicles/fast-facts-transportation-greenhouse-gas-emissions (accessed 2024-04-14).
(115) White, L. A. Demand Defrost Control Method and Apparatus. US4882908A, November 28, 1989. https://patents.google.com/patent/US4882908A/en (accessed 2025-12-10).
(116) Kneifel, J.; O'Rear, E. An Assessment of Typical Weather Year Data Impacts vs. Multi-Year Weather Data on Net-Zero Energy Building Simulations. *NIST Spec. Publ.* **2016**, *1204*.
(117) of 3.5, T. E. claims its new heat pump system can achieve a seasonal coefficient performance; Bellini, deliver 30 C. of heat indoors at-50 C. C. L. R. told pv magazine that the system could be produced at a lower cost than conventional models E. *US startup developing defrost-free residential heat pump for cold climates*. pv magazine International. https://www.pv-magazine.com/2025/02/11/u-s-startup-developing-defrost-free-residential-heat-pump-for-cold-climates/ (accessed 2026-02-09).
(118) *Total Energy Monthly Data - U.S. Energy Information Administration (EIA)*. https://www.eia.gov/totalenergy/data/monthly/ (accessed 2025-09-22).
(119) *COP26: Sufficiency Should be First*. Buildings and Cities. https://www.buildingsandcities.org/insights/commentaries/cop26-sufficiency.html (accessed 2025-11-24).
(120) Hu, S.; Zhou, X.; Yan, D.; Guo, F.; Hong, T.; Jiang, Y. A Systematic Review of Building Energy Sufficiency towards Energy and Climate Targets. *Renew. Sustain. Energy Rev.* **2023**, *181*, 113316. https://doi.org/10.1016/j.rser.2023.113316.
(121) Berrill, P.; Wilson, E. J. H.; Reyna, J. L.; Fontanini, A. D.; Hertwich, E. G. Decarbonization Pathways for the Residential Sector in the United States. *Nat. Clim. Change* **2022**, *12* (8), 712–718. https://doi.org/10.1038/s41558-022-01429-y.

(122) van Heerden, R.; Edelenbosch, O. Y.; Daioglou, V.; Le Gallic, T.; Baptista, L. B.; Di Bella, A.; Colelli, F. P.; Emmerling, J.; Fragkos, P.; Hasse, R.; Hoppe, J.; Kishimoto, P.; Leblanc, F.; Lefèvre, J.; Luderer, G.; Marangoni, G.; Mastrucci, A.; Pettifor, H.; Pietzcker, R.; Rochedo, P.; van Ruijven, B.; Schaeffer, R.; Wilson, C.; Yeh, S.; Zisarou, E.; van Vuuren, D. Demand-Side Policies Can Significantly Reduce Emissions from Energy Use in Buildings and Transport. *Nat. Energy* **2025**, *10* (3), 293–294. https://doi.org/10.1038/s41560-025-01721-z.
(123) Levesque, A.; Pietzcker, R. C.; Luderer, G. Halving Energy Demand from Buildings: The Impact of Low Consumption Practices. *Technol. Forecast. Soc. Change* **2019**, *146*, 253–266. https://doi.org/10.1016/j.techfore.2019.04.025.
(124) Mastrucci, A.; Niamir, L.; Boza-Kiss, B.; Bento, N.; Wiedenhofer, D.; Streeck, J.; Pachauri, S.; Wilson, C.; Chatterjee, S.; Creutzig, F.; Dukkipati, S.; Feng, W.; Grubler, A.; Jupesta, J.; Kumar, P.; Marangoni, G.; Saheb, Y.; Shimoda, Y.; Shoai-Tehrani, B.; Yamaguchi, Y.; Ruijven, B. van. Modeling Low Energy Demand Futures for Buildings: Current State and Research Needs. *Annu. Rev. Environ. Resour.* **2023**, *48* (Volume 48, 2023), 761–792. https://doi.org/10.1146/annurev-environ-112321-102921.
(125) Zhang, Y.; Ou, Y.; Waldhoff, S.; O'Neill, B.; Iyer, G.; Sampedro, J.; Casper, K. Long-Term Decarbonization Impacts on Residential Energy Security across Income Groups and US States. *Environ. Res. Lett.* **2025**, *20* (5), 054040. https://doi.org/10.1088/1748-9326/adca4c.
(126) *Chapter 5: Demand, services and social aspects of mitigation*. https://www.ipcc.ch/report/ar6/wg3/chapter/chapter-5/ (accessed 2025-09-23).
(127) Creutzig, F.; Niamir, L.; Bai, X.; Callaghan, M.; Cullen, J.; Díaz-José, J.; Figueroa, M.; Grubler, A.; Lamb, W. F.; Leip, A.; Masanet, E.; Mata, É.; Mattauch, L.; Minx, J. C.; Mirasgedis, S.; Mulugetta, Y.; Nugroho, S. B.; Pathak, M.; Perkins, P.; Roy, J.; de la Rue du Can, S.; Saheb, Y.; Some, S.; Steg, L.; Steinberger, J.; Ürge-Vorsatz, D. Demand-Side Solutions to Climate Change Mitigation Consistent with High Levels of Well-Being. *Nat. Clim. Change* **2022**, *12* (1), 36–46. https://doi.org/10.1038/s41558-021-01219-y.
(128) Low Indoor Temperatures and Insulation. In *WHO Housing and Health Guidelines*; World Health Organization, 2018.
(129) *California AB209 | 2021-2022 | Regular Session*. LegiScan. https://legiscan.com/CA/text/AB209/id/2606026 (accessed 2025-09-29).
(130) van Vuuren, D. P.; Edmonds, J.; Kainuma, M.; Riahi, K.; Thomson, A.; Hibbard, K.; Hurtt, G. C.; Kram, T.; Krey, V.; Lamarque, J.-F.; Masui, T.; Meinshausen, M.; Nakicenovic, N.; Smith, S. J.; Rose, S. K. The Representative Concentration Pathways: An Overview. *Clim. Change* **2011**, *109* (1), 5. https://doi.org/10.1007/s10584-011-0148-z.
(131) Thomson, A. M.; Calvin, K. V.; Smith, S. J.; Kyle, G. P.; Volke, A.; Patel, P.; Delgado-Arias, S.; Bond-Lamberty, B.; Wise, M. A.; Clarke, L. E.; Edmonds, J. A. RCP4.5: A Pathway for Stabilization of Radiative Forcing by 2100. *Clim. Change* **2011**, *109* (1), 77. https://doi.org/10.1007/s10584-011-0151-4.
(132) Riahi, K.; Grübler, A.; Nakicenovic, N. Scenarios of Long-Term Socio-Economic and Environmental Development under Climate Stabilization. *Technol. Forecast. Soc. Change* **2007**, *74* (7), 887–935. https://doi.org/10.1016/j.techfore.2006.05.026.
(133) Bureau, U. C. *CHARS - Historical Characteristics Tables*. https://www.census.gov/construction/chars/historical/tables.html (accessed 2025-09-30).

(134) *MCL - Act 230 of 1972 - Michigan Legislature*. https://www.legislature.mi.gov/Laws/MCL?objectName=MCL-ACT-230-OF-1972 (accessed 2025-09-30).
(135) Glaeser, E.; Gyourko, J. The Economic Implications of Housing Supply. *J. Econ. Perspect.* **2018**, *32* (1), 3–30. https://doi.org/10.1257/jep.32.1.3.
(136) *Full article: Supply Skepticism: Housing Supply and Affordability*. https://www.tandfonline.com/doi/full/10.1080/10511482.2018.1476899?scroll=top&needAccess=true#abstract (accessed 2025-09-30).
(137) Orders, E. *Unleashing American Energy*. The White House. https://www.whitehouse.gov/presidential-actions/2025/01/unleashing-american-energy/ (accessed 2025-09-30).
(138) Wilson, E. J. H.; Munankarmi, P.; Less, B. D.; Reyna, J. L.; Rothgeb, S. Heat Pumps for All? Distributions of the Costs and Benefits of Residential Air-Source Heat Pumps in the United States. *Joule* **2024**, *8* (4), 1000–1035. https://doi.org/10.1016/j.joule.2024.01.022.
(139) JGCRI/Gcam-Core, 2026. https://github.com/JGCRI/gcam-core (accessed 2026-02-04).
(140) *GCAM v8.2 Documentation: GCAM-USA*. https://jgcri.github.io/gcam-doc/gcam-usa.html (accessed 2026-02-04).